Theses and Dissertations

2017

Advances in Metal-Catalyzed Difluoromethylation and Polydifluoromethylenation Reactions

Long Xu
Lehigh University

Recommended Citation

Xu, Long, "Advances in Metal-Catalyzed Difluoromethylation and Polydifluoromethylenation Reactions" (2017). *Theses and Dissertations*. 2891.
http://preserve.lehigh.edu/etd/2891

Advances in Metal-Catalyzed Difluoromethylation and Polydifluoromethylenation
Reactions

by

Long Xu

A Dissertation

Presented to the Graduate and Research Committee

of Lehigh University

in Candidacy for the Degree of

Doctor of Philosophy

in

Department of Chemistry

Lehigh University

May 22, 2017

Approved and recommended for acceptance as a dissertation in partial fulfillment of the requirements for the degree of Doctor of Philosophy

Long Xu
Advances in Metal-Catalyzed Difluoromethylation and Polydifluoromethylenation Reactions

April 10th, 2017

—————————————————

Defense Date

—————————————————
David Vicic

Dissertation Director

—————————————————

Approved Date

Committee Members:

—————————————————
David Vicic

—————————————————
Robert Flowers

—————————————————
Robert Syvret

—————————————————
Kai Landskron

iii

Acknowledgement

First and foremost, I would like to express my sincere gratitude to my PhD advisor, Dr. David Vicic for his support,guidance and personal example throughout my time at Lehigh University. He teaches me many laboratory tips and tricks and helps me improve my writing and oral-presentation skills which will be very important throughout my career. More importantly, I am thankful to David for giving me the intellectual freedom to work on problems that interested me, which develops my abilities to educate myself and learn how to approach problems.

I would also like to thank my undergraduate advisor, Dr Jianjun Zhang for being an inspirational, knowledgeable, and patient mentor. He encouraged me to pursue a PhD in chemistry, and gave me the foundation for becoming a chemist.

I am, of course, grateful to my family for their kind support and the sacrifices they made throughout the years. I always look forward to and cherish the time with my family.

I'm also blessed to be surrounded by extraordinary lab mates and friends who provide valuable help during my PhD study. I also thank my department for giving me the opportunity to study at an amazing place.

I would like to thank my other committee members Dr. Robert Flowers, Dr. Kai Landskron and Dr. Robert Syvret. Your service is sincerely appreciated.

Last but never the least, I cannot express how thankful and lucky I am to have my wife, Jingjing, in my life. She is the most caring, helpful, and supportive person I have ever met.

Table of Contents

List of Tables

List of Figures

List of Schemes

List of Symbols and Abbreviations

°C	degrees Celsius
Å	Angstrom
%	percent
^{1}H	proton
^{13}C	carbon-13
^{19}F	fluorine-19
acac	acetylacetonate
Ar	aryl
ArX	aryl halide
Br	bromine
Bu	butyl
bpy	2,2′-bipyridine
C	carbon
C_6D_6	benzene-d_6
$CDCl_3$	chloroform-d
CI	chemical ionization
Cl	chlorine
cm	centimeter
cod	1,5-cyclooctadiene
Cu	copper
DCM	dichloromethane
DMA	*N,N*-dimethylacetamide
DMF	*N,N*-dimethylformamide
DMI	1,3-dimethyl-2-imidazolidinone
DMPU	1,3-dimethyl-3,4,5,6-tetrahydro-2-(*1H*)-pyrimidinone
dppm	1,1-bis(diphenylphosphino)methane
dppe	1,2-bis(diphenylphosphino)ethane
dppp	1,3-bis(diphenylphosphino)propane
dppf	1,1'-bis(diphenylphosphino)ferrocene

dippf	1,1′-bis(di-isopropylphosphino)ferrocene
dtbpy	4,4′-di-*tert*-butyl-2,2′-dipyridyl
dmbpy	4,4′-dimethyl-2,2′-dipyridyl
dmobpy	4-4′-Dimethoxy-2-2′-bipyridine
EDG	electron donating group
equiv	equivalent(s)
Et	ethyl
EWG	electron withdrawing group
F	fluorine
Fe	iron
FID	flame ionization detector
g	gram
GC	gas chromatography
GCMS	gas chromatography-mass spectrometry
h	hour(s)
HCl	hydrochloric acid
Hz	hertz
I	iodine
KI	potassium iodide
Ni	nickel
NMP	N-methyl-2-pyrolidinone
NMR	nuclear magnetic resonance
NR	no reaction
me	methyl
OAc	acetate
OR	alkoxy
OTf	triflate
P	phosphors
Pd	palladium
Ph	phenyl

phen	1,10-phenanthroline
ppm	parts per million
py	pyridine
qphos	1,2,3,4,5-pentaphenyl-1′-(di-*tert*-butylphosphino)ferrocene
R	alkyl
segphos	(*R*)-(+)-5,5′-bis(diphenylphosphino)-4,4′-bi-1,3-benzodioxole
Si	silicon
Sn	tin
T	temperature
*t*Bu	*tert*-butyl
TDAE	1,1,2,2-tetrakis(dimethylamino)ethylene
TLC	thin layer chromatography
THF	tetrahydrofuran
TMSCl	chloro trimethylsilane
tmeda	tetramethylethylenediamine
tpy	2,2′:6′,2″-terpyridine
tpy'	4,4′,4″-tri-*tert*-butyl-2,2′:6′,2″-terpyridine
X or Y	halogen
xantphos	4,5-bis(diphenylphosphino)-9,9-dimethylxanthene

Abstract

This thesis details the author's contributions to the fields of difluoromethylation and polydifluoromethylation chemistries. State-of-the-art methodology in difluoromethylation is achieved in our lab either by nickel-catalyzed conventional cross-coupling between electrophiles and the nucleophile $(DMPU)_2Zn(CF_2H)_2$ or by reductive cross-coupling to join HCF_2Cl and aryl halides with a nickel catalyst.

Chapter 1 introduces the benefits of incorporating fluorinated moieties in drug candidates and general methods to install CF_3, $(CF_2)_n$ and CF_2H moieties into arenes and heteroarenes.

Chapter 2 details the first nickel-catalyzed difluoromethylation of aryl halides with a novel difluoromethyl zinc reagent. The new method displays broad substrate scope (aryl iodide, bromide and triflate are well-tolerated) and operational simplicity (reaction is performed at room temperature). Preliminary mechanistic studies reveal that the oxidative addition of alkylated aryl iodides is not taking place under reaction conditions, shutting down the reactivity of this type of substrate.

Chapter 3 presents our attempts to construct a proposed intermediate in fluorinated olefin metathesis, namely a perfluorometallacyclobutane. After several failures, the first example of a platinum perfluorometallacyclobutane is successfully synthesized via halogen exchange between $[(COD)Pt(Me)_2]$ and 1,3-diiodoperfluoropropane. The ligand substitution reaction enabled the preparation of a family of platinum perfluorometallacyclobutanes, which could be systematically characterized by single crystal X-ray diffraction, as well as ^1H, ^{19}F and ^{195}Pt NMR spectroscopies.

Chapter 4 discusses the discovery of a halogen-bonded adduct from the reaction of 1,4-diiodooctafluorobutane with potassium *tert*-butoxide in dioxane. Crystallography reveals an extended two-dimensional network held together by strong iodine-oxygen interactions, which display the shortest iodine-oxygen distance and the longest iodine-carbon distance thus far reported for any perfluoroalkyl iodide substrate. An iron-mediated perfluoroalkylation of benzene is developed using α,ω-diiodoperfluoroalkanes and t-BuOK in DMF at room temperature.

Chapter 5 describes our development of preliminary catalyst and reaction conditions for the nickel-catalyzed reductive cross-coupling of aryl iodides and bromides with HCF_2Cl. Early investigations into the mechanism of this new method were undertaken, and we proposed that a radical process is likely taking place during reaction. The new protocol provides a much cheaper way to difluoromethylate aryl halides compared with the strategy outlined in Chapter 2.

1. Chapter 1: Introduction

1.1. Fluorine Chemistry in Pharmaceuticals

The introduction of fluorine or fluorinated group into a drug candidate plays a key role in life-science oriented research. It imparts drastic effects on a variety of physical and biological properties of drug molecules.[1] For instance, the electron-withdrawing fluoroalkyl group will decrease the basicity of neighboring functionality and this impact on pK_a can modulate the hydrogen-bonding and other binding interactions between the drug molecule and target. Fluorinated or fluoroalkylated arenes often have an increase in hydrophobicity, resulting in enhanced membrane permeability and absorption.[2] Fluorinated molecules tend to gain more resistance against common enzymatic degradation that leads to metabolism of a drug. By impeding this metabolic process, fluorine incorporation often leads to an increased half-life and enhanced bioavailability of a drug candidate. Some examples of this are illustrated in Figure 1a. In Zetia (Ezetimibe), a drug used to inhibit intestinal absorption of cholesterol, the replacement of a hydrogen atom by fluorine prevented oxidative arene degradation.[3] In Emend (Aprepitant), a drug used to treat nausea, the two trifluoromethyl groups provided a significant increase in CNS permeability, and the incorporation of a fluorine atom on the other arene led to a further 2-fold increase in potency.[4]
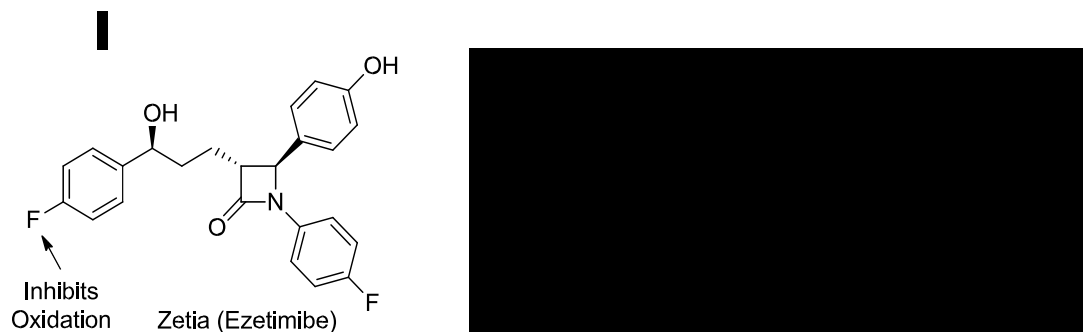
Figure 1a. Examples demonstrating the impact of fluorine on biological activity.

As mentioned above, with the growing importance of fluorinated compounds, organofluorine chemistry has become an integral part of pharmaceutical research. Roughly 20% of all pharmaceuticals are fluorinated.[5] Two more examples of drugs containing fluorine are shown in Figure 1b: Isentress (Reltegravir) is a first-in-class integrase inhibitor used to treat HIV infection, and Januvia (Sitagliptin) is a DPP-4 inhibitor used in the treatment of diabetes mellitus Type 2.
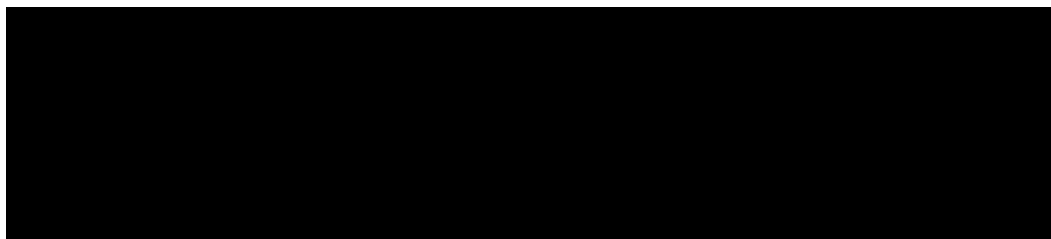
Figure 1b. Examples of fluorine-containing pharmaceutical compounds.

1.2. Methods for Trifluoromethylation

Methods for trifluoromethylation have been developed for decades, as trifluoromethylarenes are among the most common fluorinated compounds and are found in many top-selling drugs (Prozac, Celebrex) and agrochemicals (Lariam, Fipronil). For late stage trifluoromethylation, most research has employed copper catalysts to couple aryl

electrophiles with a CF$_3$ anion. Palladium has also been tested as a catalyst, and a generic catalytic cycle between an aryl halide and a CF$_3$ nucleophile is shown in Scheme 1a.[6-14]

Ar-CF$_3$

L−M^n

Ar-X

Reductive elimination

Oxidative addition

L−M^{n+2} with Ar and CF$_3$

L−M^{n+2} with Ar and X

X$^-$

"$^-$CF$_3$"
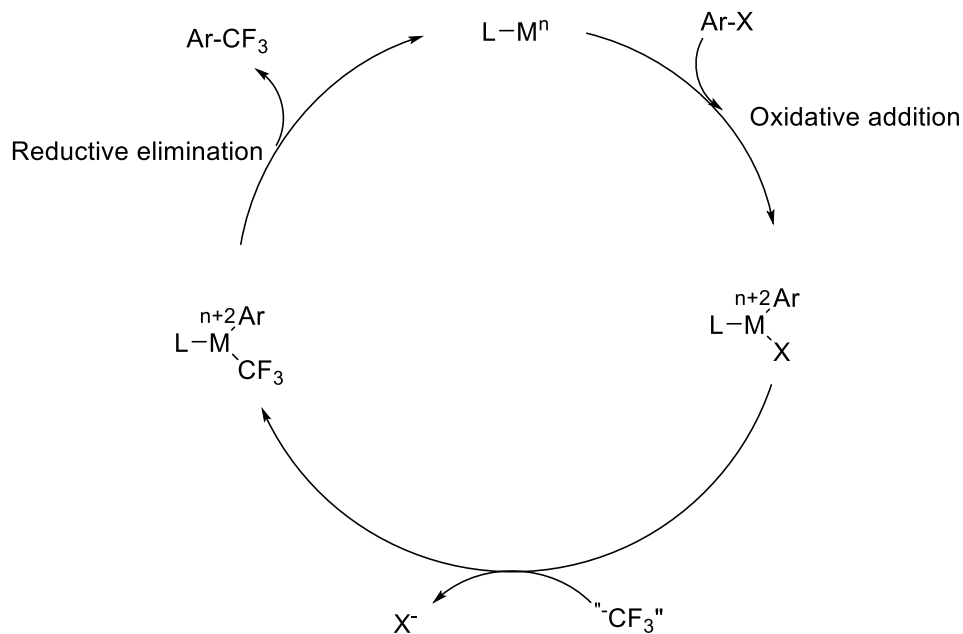
Scheme 1a. Catalytic cycle for the trifluoromethylation of an aryl electrophile.

All cross-coupling reactions with CF$_3$ have been developed with copper with the exception of one Pd/phosphine catalyst. In 2010, Buchwald published the first example of a palladium catalyzed method to trifluoromethylate aryl chlorides.[15] This chemistry involved the use of a precious metal and an expensive phosphine ligand, and only worked for aryl chlorides at temperatures ranging from 120-140 °C. Since that work, there has been no other examples of a trifluoromethylation reaction that is catalytic in a group 10 metal. To make a stronger statement, there still exists no practical late-stage method that is catalytic in metal for preparing the most important fluorinated functional group (trifluoromethyl) from the diverse aryl halide substrate pool.

5

The problems inherent to catalysis are two-fold. First, a convenient nucleophilic source of CF_3 has not yet been employed in reactions with high turnover. Most trifluoromethylations of aryl halides employ various forms of the R_3SiCF_3 reagent that is activated by metal fluorides or t-butoxide. This is troublesome in catalysis because the generation of the CF_3 anion has to be kinetically compatible with all the other steps in a catalytic cycle. If not, a build-up of the CF_3 anion occurs, and decomposition into difluorocarbene and fluoride becomes the dominant reaction pathway. A second problem is the high temperatures needed to reductively eliminate Ar-CF_3 product due to the strength of the metal-CF_3 bond.

It is likely that the future of trifluoromethylation chemistry will focus on the development of nickel catalysts. The motivation for having nickel-catalyzed methods is that nickel is much cheaper than palladium and is well-known to activate aryl chlorides, bromides, iodides, and triflates under mild conditions. Therefore, if nickel-catalyzed methods could indeed be developed, then the substrate scope and the utility of the methodologies would be high. In 2008, our group published the first proof-in-principle that well-defined [Ni(aryl)(CF_3)] complexes could be prepared and then decomposed to form aryl-CF_3 products.[16] Others have sought to identify ligands for nickel computationally in order to more predictably mediate trifluoromethylation reactions.[17] Moreover, it has recently been shown that the high-valent state of nickel can also mediate the important C_{aryl}-$C_{trifluoromethyl}$ bond forming step.[18] Sanford showed that the nickel(II) aryl trifluoromethyl complex **A** (Scheme 1b) reacts with a two-electron oxidant to form the nickel(IV) species **B**, which then eliminates aryl-CF_3 product under extremely mild conditions.
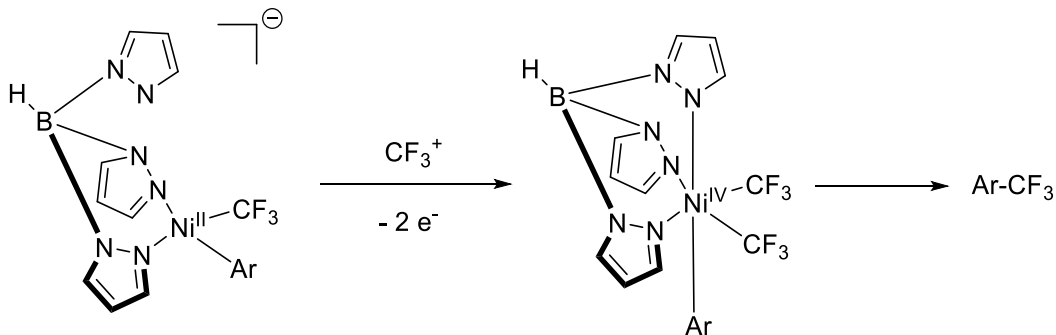
Scheme 1b. Facile reductive elimination of Ar-CF$_3$ from Ni(IV).

The challenges in developing Ni-catalysts for trifluoromethylation are similar to those faced for Pd-catalysts, in that the reductive elimination from Ni(II) intermediate is slow. Preliminary work in this area has been done by our group, showing that the well-defined [(dippe)Ni(Ar)(CF$_3$)] produced Ar$_2$ and [(dippe)Ni(CF$_3$)$_2$] but not ArCF$_3$ upon heating.[16] The formation of [(dippe)Ni(CF$_3$)$_2$] and biaryl product is believed to result from the redistribution reaction where [(dippe)Ni(Ar)(CF$_3$)] generated [(dippe)Ni(CF$_3$)$_2$] and [(dippe)Ni(Ar)$_2$]. The latter one led to the formation of biaryl product. It is noted that only a single bisphosphine ligand (dippe) was examined in this study. The investigation of other ligands will certainly increase the likelihood of finding reaction conditions that can mediate Ar-CF$_3$ bond formation from Ni(II) instead of undergoing bimolecular redistribution process. For instance, ligands bearing bulky substituent might prevent two nickel centers from getting in close proximity to each other. Another strategy is the oxidation of Ar-Ni(II)-CF$_3$ species to Ni(III) or Ni(IV) by which the reductive elimination of Ar-CF$_3$ is facilitated. However, to make the reaction catalytic, regeneration of Ni(0) will be a challenge that needs to be addressed.

1.3. Methods for (CF$_2$)$_n$ Transfer

It has been noted that the CF$_2$ fragment is isosteric to ethereal oxygen and, in some cases, even to carbonyl or gem-dimethylmethylene groups[19] (Scheme 1c).
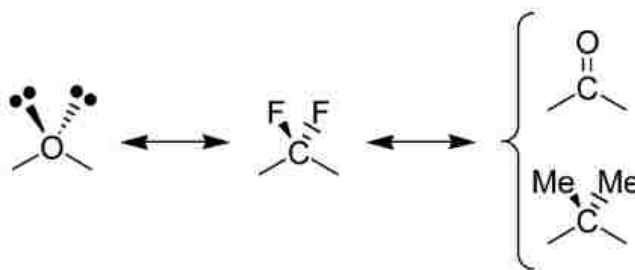
Scheme 1c. Bioisosterism of CF$_2$ Fragment.

Repeating difluoromethylene groups (CF$_2$)$_4$ are present on a derivative of Fulvestrant (fluorinated isomer in Figure 1c) which showed strong antiproliferative activity on MCF-7 cells and unlike the original Fulvestrant and isomer, suppressed the capacity to downregulate ERα in breast carcinoma.[20]

fluorinated isomer of Fulvestrant   isomer of Fulvestrant   Fulvestrant
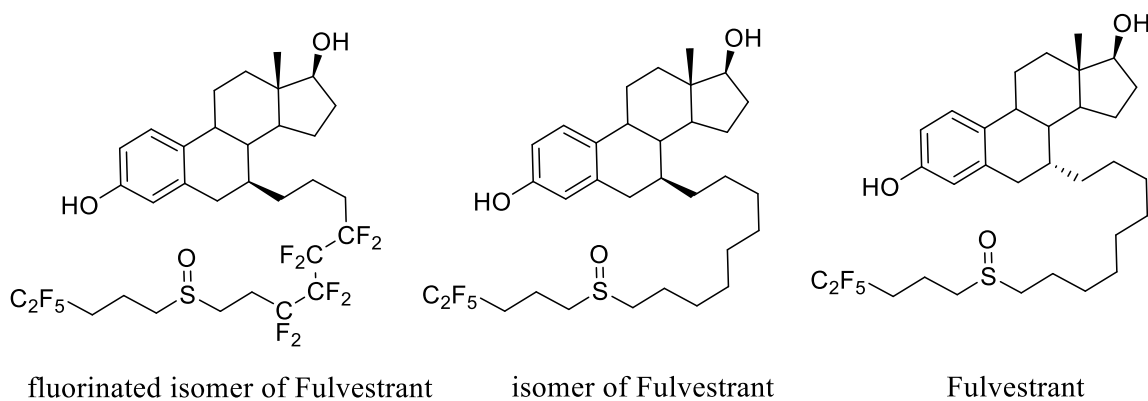
Figure 1c. Structures of Fulvestrant, isomer and fluorinated isomer.

However, the methodologies for the incorporation of repeating difluoromethylene groups have been slow to develop. In a synthesis of fluoroine-containing annulated corannulene,

the 1,4-diiodoperfluorobutane and corannulene were heated at 300 ℃ to afford a pale-yellow complex containing $(CF_2)_4$ (Scheme 1d). This derivative of corannulene was proved to have higher electron affinity than the fullerene electron-acceptor C_{60}.[21]
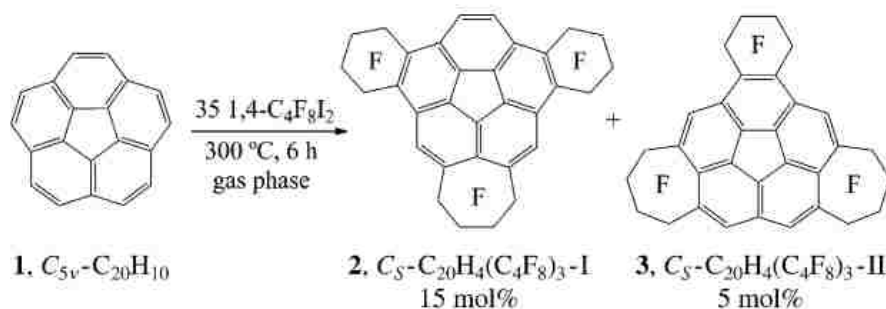
Scheme 1d. Perfluoroalkyl annulation of corannulenen.

Our previous work showed a facile, one-pot synthesis of a metallacyclic dizinc reagent using diethylzinc and 1,3-diiodoperfluoropropane (Scheme 1e)[22]:
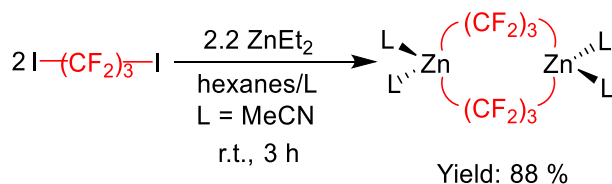
Scheme 1e. Synthesis of perfluorometallacyclic dizinc reagent.

With the zinc reagent in hand, we have provided preliminary results for functionalizing organic diiodides to build up novel organofluorine ring systems. Perfluoroalkyl zinc reagents are known to be able to transmetalate with copper to afford active perfluoroalkyl copper complex, but there have been no reports of ring forming reactions using this methodology. To our delight, the C_3 zinc derivative reacted cleanly with aryl diiodides in the presence of CuCl/1,10-phenanthroline to afford the fluoroalkyl ring-containing structures (Scheme 1f).

9
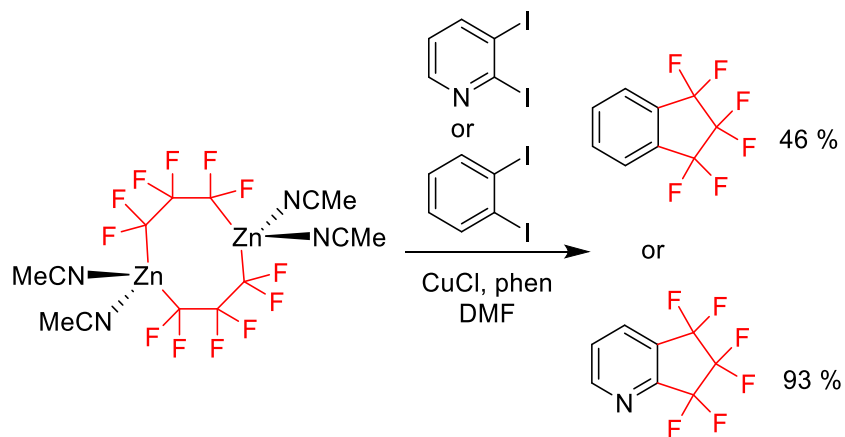
Scheme 1f. Copper-mediated cross-coupling reaction.

1.4. Methods for Difluoromethylation

Similar to arenes bearing a trifluoromethyl group, those bearing a difluoromethyl group are also prevalent in biologically active small molecules. Unlike the CF_3 group, the CF_2H group can participate as a hydrogen-bond donor,[23] and is often invoked as a lipophilic bioisostere of alcohols and thiols.[19] Despite the importance of difluoromethylarenes, methods for their synthesis are significantly less developed than methods to prepare trifluoromethylarenes. Before our studies, most cross-coupling studies focused on using Me_3SiCF_2H as the difluoromethyl delivery agent. Hartwig reported an example of direct difluoromethylations using Me_3SiCF_2H as the difluoromethyl source and a stoichiometric amount of copper catalyst at temperatures greater than 100 °C (Scheme 1g).[24] This reaction was not tolerant to substrates containing aldehydes, ketones, or electron withdrawing groups. Shen reported a method that was catalytic in metal for directly incorporating a difluoromethyl group into aryl halide substrates. As shown in Scheme 1g, this method

10

involved the use of expensive palladium and silver co-catalysts that each required their own supporting ligand.[25] Moreover, the method used Me_3SiCF_2H as the difluoromethyl source in combination with the exogenous base sodium tert-butoxide as the activator. Such conditions made the palladium-catalyzed method in Scheme 1g also incompatible with aldehydes and ketones.
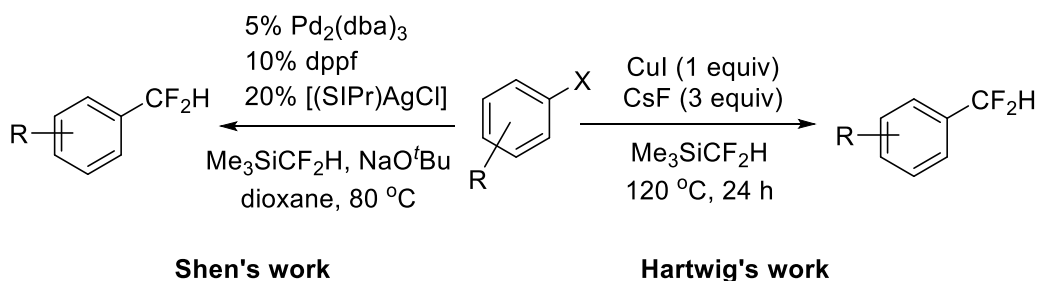
Scheme 1g. Utilization of Me_3SiCF_2H as nucleophilic source of CF_2H

The use of $M\text{-}CF_2H$ reagents ($M = SiR_3$, SnR_3) as CF_2H sources can present several challenges when compared to analogous $M\text{-}CF_3$ reagents. Me_3SiCF_2H is more electron rich than Me_3SiCF_3, which has a number of important implications. First, the CF_2H anion is a poorer leaving group than the CF_3 anion, so more forcing conditions are required to release it in order to perform nucleophilic difluoromethylation chemistry. For example, much higher temperatures have historically been required to perform difluoromethylation reactions than trifluoromethylation reactions under similar conditions. Secondly, the CF_2H anion that is generated from $Me_3Si\text{-}CF_2H$ is a much "hotter" that the CF_3 anion, and consequently a severe limitation of the Me_3SiCF_2H reagent in cross-coupling chemistry is that aldehyde and ketone functionalities are not tolerated. Ketones and aldehydes in the Hartwig and Shen examples, for instance, had to be protected in order for the cross-

couplings to occur. The ability of our difluoromethylzinc reagent to tolerate carbonyl-containing functionalities bodes extremely well for its continued use in emerging difluoromethylation methodologies.

In February 2016, we published a *JACS* communication to report the preparation of a new difluoromethyl nucleophile [(DMPU)$_2$Zn(CF$_2$H)$_2$] that can be used in combination with nickel to directly and catalytically difluoromethylate aryl iodides, bromides, and triflates (Scheme 1h).[26] The substrate scope was unprecedented, and successful couplings were observed with aryl halide substrates bearing electron withdrawing groups, aldehydes, ketones, and esters.
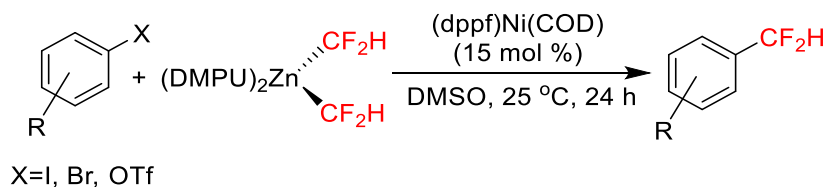
Scheme 1h. First example of nickel-catalyzed difluoromethylation of aryl electrophiles

Several months later, the Mikami group published two articles demonstrating the utilization of [(DMPU)$_2$Zn(CF$_2$H)$_2$][27] and its derivative [(TMEDA)Zn(CF$_2$H)$_2$][28] using catalytic amount of copper or palladium catalyst to diluoromethylate aryl iodides (Scheme 1i). Combined with the nickel chemistry in our lab, these works depict a promising future for the application of [(DMPU)$_2$Zn(CF$_2$H)$_2$], such that its use will be broader and more methods will be developed based on this reagent and transition-metal catalysts.
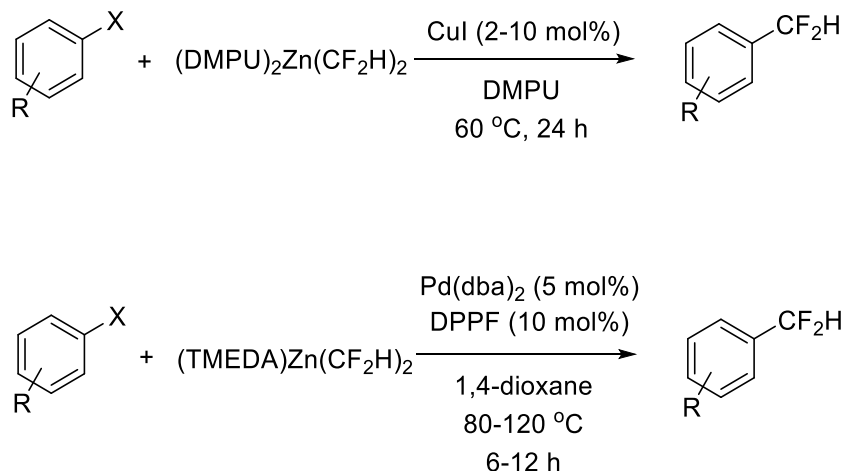
Scheme 1i. More examples of applications using difluomethyl zinc reagents

In the future, with the expected increase of commercial drugs containing CF_2H on the market, more convenient and economical protocols for difluoromethylation are needed in the pharmaceutical industry as well as in lab scale research. Growing interests in this area will promote more development of difluoromethyl reagents to facilitate nucleophilic, electrophilic or radical difluoromethylation.

1.5. Overview of Thesis

The subsequent chapters (2-5) detail our pioneering efforts in developing synthetically useful methods for taming the transfer of $(CF_2)_n$ and CF_2H using α,ω-diiodoperfluoroalkanes and difluoromethyl halides. Chapters 2 and 5 document our exploration in nickel-catalyzed difluoromethylation of arenes using two different stragegies: electrophile-nucleophile coupling and electrophile-electrophile coupling. Chapter 3 and 4 describe the utilization α,ω-diiodoperfluoroalkanes to construct platinum

perfluorometallacyclobutanes and halogen-bonded adduct of 1,4-diiodooctafluorobutane

and potassium *tert*-butoxide with an extended two-dimensional network.

1.6. Reference

1. Wang, H.; Vicic, D. A. *Synlett* **2013**, *24*, 1887.
2. (a) Bégué, J.-P.; Bonnet-Delpon, D. *Bioorganic and Medicinal Chemistry of Fluorine*; John Wiley & Sons: Hoboken, N.J., 2008; (b) Hiyama, T. *Organofluorine Compounds : Chemistry and Applications*; Springer: Berlin ; New York, 2000; (c) Kirsch, P. *Modern Fluoroorganic Chemistry : Synthesis, Reactivity, Applications*; Wiley-VCH ;: Weinheim ; Great Britain, 2004.
3. Vaccaro, W. D.; Sher, R.; Davis, H. R. *Bioorg. Med. Chem. Lett.* **1998**, *8*, 319.
4. Hale, J. J.; Mills, S. G.; MacCoss, M.; Finke, P. E.; Cascieri, M. A.; Sadowski, S.; Ber, E.; Chicchi, G. G.; Kurtz, M.; Metzger, J.; Eiermann, G.; Tsou, N. N.; Tattersall, F. D.; Rupniak, N. M. J.; Williams, A. R.; Rycroft, W.; Hargreaves, R.; MacIntyre, D. E. *J. Med. Chem.* **1998**, *41*, 4607.
5. http://www.fda.gov/downloads/Drugs/DevelopmentApprovalProcess/ DrugInnovation/UCM381803.pdf
6. McLoughlin, V. C.; Thrower, J. *Tetrahedron* **1969**, *25*, 5921.
7. Zanardi, A.; Novikov, M. A.; Martin, E.; Benet-Buchholz, J.; Grushin, V. V. *J. Am. Chem. Soc.* **2011**, *133*, 20901.
8. Oishi, M.; Kondo, H.; Amii, H. *Chem. Commun.* **2009**, 1909.
9. Kondo, H.; Oishi, M.; Fujikawa, K.; Amii, H. *Adv. Synth. Catal.* **2011**, *353*, 1247.
10. Knauber, T.; Arikan, F.; Roschenthaler, G. V.; Goossen, L. J. *Chem. Eur. J.* **2011**, *17*, 2689.
11. Morimoto, H.; Tsubogo, T.; Litvinas, N. D.; Hartwig, J. F. *Angew. Chem. Int. Ed.* **2011**, *50*, 3793.
12. Tomashenko, O. A.; Escudero-Adan, E. C.; Belmonte, M. M.; Grushin, V. V. *Angew. Chem. Int. Ed.* **2011**, *50*, 7655.
13. Dubinina, G. G.; Furutachi, H.; Vicic, D. A. *J. Am. Chem. Soc.* **2008**, *130*, 8600.
14. Dubinina, G. G.; Ogikubo, J.; Vicic, D. A. *Organometallics* **2008**, *27*, 6233.
15. Cho, E. J.; Senecal, T. D.; Kinzel, T.; Zhang, Y.; Watson, D. A.; Buchwald, S. L. *Science* **2010**, *328*, 1679.
16. Dubinina G.G, Brennessel W.W, Miller J.L, Vicic D.A. *Organometallics* **2008**, *27*, 3933.
17. Jover J, Miloserdov F.M, Benet-Buchholz J, Grushin V.V, Maseras F. *Organometallics* **2014**, *33*, 6531.
18. Bour J.R, Camasso N.M, Sanford M.S. *J. Am. Chem. Soc.* **2015**, *137*, 8034.
19. Meanwell, N. A. *J. Med. Chem.* **2011**, *54*, 2529.
20. Agouridas, V.; Magnier, E.; Blazejewski, J. C.; Laios, I.; Anny Cleeren, A.; Denis Nonclercq, D.; Laurent, G.; Leclercq, G. *J. Med. Chem.* **2009**, *52*, 883.

21. Kuvychko, I. V.; Dubceac, C.; Deng, S.; Wang, X.; Granovsky, A. A.; Popov, A. A.; Petrukhina, M. A.; Strauss, S. H.; Boltalina, O. V. *Angew. Chem. Int. Ed.* **2013**, *52*, 7505.

22. Kaplan, P. T.; Xu, L.; Chen, B.; McGarry, K. R.; Yu, S.; Wang, H.; Vicic, D. A. *Organometallics* **2013**, *32*, 7552.

23. Erickson, J. A.; Mcloughlin, J. I. *J. Org. Chem.* **1995**, *60*, 1626.

24. Fier, P. S.; Hartwig, J. F. *J. Am. Chem. Soc.* **2012**, *134*, 5524.

25. Gu, Y.; Leng, X.; Shen, Q. *Nat. Commun.* **2014**, *5*, 5405.

26. Xu, L.; Vicic, D. A. *J. Am. Chem. Soc.* **2016**, *138*, 2536.

27. Serizawa H, Ishii K, Aikawa K, Mikami K. *Org. Lett.* **2016**, *18*, 3686.

28. Aikawa K, Serizawa H, Ishii K, Mikami K. *Org. Lett.* **2016**, *18*, 3690.

2. Chapter 2: Nickel-Catalyzed Cross-Coupling of Aryl Iodides, Bromides, and Triflates with a Difluoromethyl Zinc Reagent

2.1. Introduction

The difluoromethyl group (CF$_2$H) is an important structural motif that has great potential in the area of life science.[1-4] The CF$_2$H unit is also of special interest for its use in drug design as it is a bioisostere of a hydroxyl or thiol group and can act as lipophilic hydrogen bond donor to improve the binding selectivity, membrane permeability and metabolic stability relative to the non-fluorinated parent molecules.[5-10]

While methods for introducing trifluoromethyl and perfluoroalkyl groups have advanced significantly, only few methodologies have been developed to incorporate the CF$_2$H onto organic substrates (Scheme 2a). Baran and coworkers invented a new reagent (Zn(SO$_2$CF$_2$H)$_2$, DFMS) for the difluoromethylation of organic substrates via a radical process.[11] For the nucleophilic direct difluoromethylation, the combination of stoichiometric amount of copper halide catalyst and Me$_3$SiCF$_2$H as the nucleophilic source of CF$_2$H was first reported by Hartwig *et al*, and electron-rich aryl iodides were successfully functionalized.[12] Qing and coworkers later found that the temperature of such a reaction could be lowered to room temperature if sodium *tert*-butoxide was used in place of CsF.[13] Tin reagents could also be used for copper mediated difluoromethylations, and Prakash has reported a complementary protocol outlined in Scheme 2a.[14]

The first example of catalytic difluoromethylation mediated by transition metal was achieved by Shen's group, using DPPF/Pd$_2$(dba)$_3$ as the catalyst and the combination of (NHC)AgCl/ Me$_3$SiCF$_2$H/*t*-BuOK to serve as a CF$_2$H anion source to difluoromethylate

aryl bromides and iodides.[15] An obvious disadvantage of these methods is the use of Me$_3$SiCF$_2$H which must undergo reactions at elevated temperatures or with strong nucleophiles in order to cleave the silicon–CF$_2$H bond. Moreover, the CF$_2$H anion which is generated from Me$_3$SiCF$_2$H will react with aldehydes and ketones as described in the previous chapter.
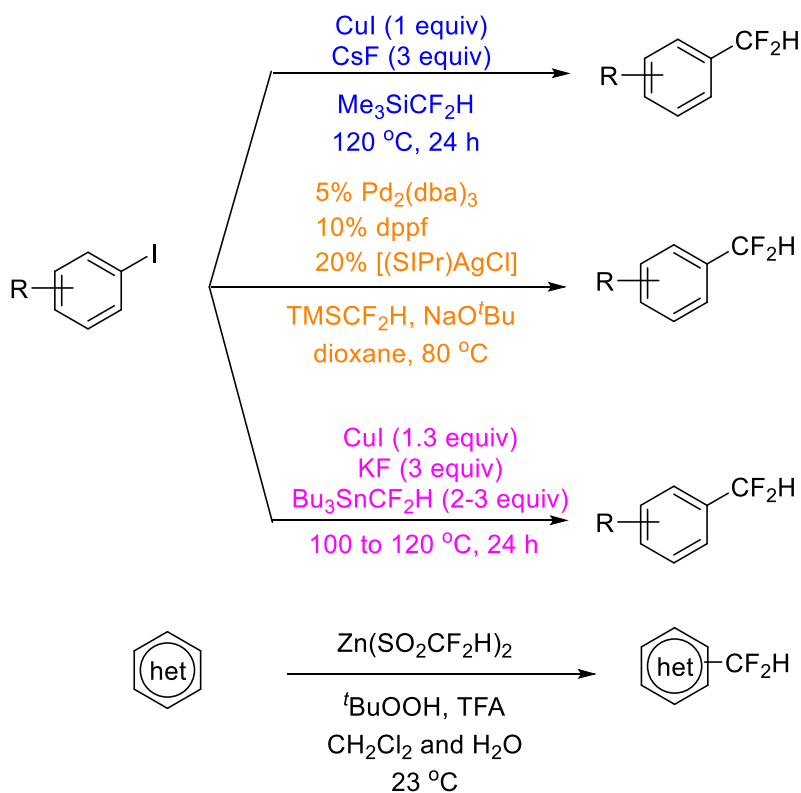
Scheme 2a. Summary of current methodologies for direct difluoromethylation.

2.2. Results and Discussions

2.2.1. Preparation of [(DMPU)$_2$Zn(CF$_2$H)$_2$]

We sought to prepare an easy-to-access and user-friendly zinc difluoromethyl reagent that can be used as a nucleophile in metal-mediated cross-coupling reactions. Halogen exchange was utilized to prepare various organolithium regents, and it also worked for the preparation of perfluoroalkyl zinc regents.[16] These reactions are normally carried out at lower temperature which would be beneficial for isolating the final product. After screening several alkyl zinc regents, diethyl zinc was selected in the reaction with ICF$_2$H to yield L$_n$Zn(CF$_2$H)$_2$. L here was the ligand to stabilize the zinc regent, and it could be some coordinated solvents such as DMF, DMPU, MeCN or some ligands with nitrogen donor atoms, such as TMEDA. We preferred to use simple organic solvents as the stabilizing ligands to make the reaction more practical and at the same time, to avoid the possibility of catalyst deactivation due to the ligands on the zinc reagent.

After the screening of solvent and temperature, [(DMPU)$_2$Zn(CF$_2$H)$_2$] was formed in high isolated yields as a free-flowing solid (Scheme 2b) in the mixture of DMPU and hexane at room temperature. Complex **2.1** is stable in the solid state in the glovebox at room temperature for months, and single crystals were grown to take the first snapshot of a solid state structure of a zinc difluoromethyl complex (Figure 2a).

$$2 \ I-CF_2H \ + \ ZnEt_2 \quad \xrightarrow[94\ \%]{DMPU} \quad (DMPU)_2Zn\overset{\displaystyle ,,,,CF_2H}{\underset{\displaystyle CF_2H}{}}$$

2.1
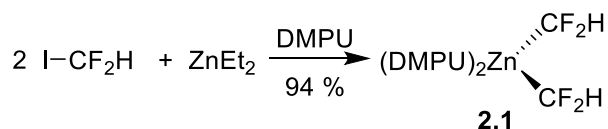
Scheme 2b. Synthesis of [(DMPU)$_2$Zn(CF$_2$H)$_2$].
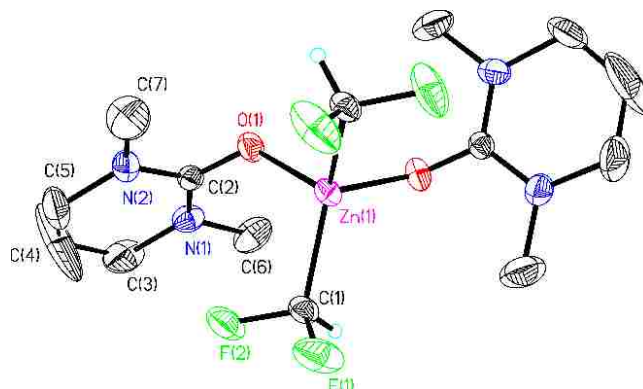
Figure 2a. ORTEP diagrams of [(DMPU)$_2$Zn(CF$_2$H)$_2$]. Selected bond lengths (Å) for **2.1**: Zn1-C1 2.045(2); Zn1-O1 2.0647(19). Selected bond angles (°) for **2.1**: C1-Zn1-C1 134.49(16); C1-Zn1-O1 103.53(9).

Realizing that ICF$_2$H is pricey (5 g for \$285 from SynQuest Labs), the zinc reagent **2.1** would be much better derived from a CF$_3$I source, which is over 37 times cheaper on a per mol basis (25 g for \$50 from SynQuest Labs). Inspired by the synthesis of Me$_3$SiCF$_2$H from Me$_3$SiCF$_3$ and sodium borohydride,[17] we attempted to react the known [Zn(CF$_3$)$_2$] with sodium borohydride to yield [Zn(CF$_2$H)$_2$]. A series of [Zn(CF$_3$)$_2$] was synthesized via diethyl zinc and CF$_3$I with various stabilizing ligands on (DMPU, DME, MeCN). After several screens of reaction conditions, [(DMPU)$_2$Zn(CF$_3$)$_2$] was chosen to react with 10 equivalents of sodium borohydride in diglyme at room temperature (later we found that DME also worked for this transformation). After the reaction mixture was stirred overnight, ^{19}F NMR spectroscopy showed a full conversion of [(DMPU)$_2$Zn(CF$_3$)$_2$] to a doublet at -128 ppm, which might be [(DMPU)$_2$Zn(CF$_2$H)$_2$]. All the volatiles were evaporated on high-vac line, and benzene was used to extract the desired product. Crystals were grown in the mixture of benzene and Et$_2$O at room temperature. X-ray crystallography data was

collected but no reliable solution was given. Further characterization of crystals showed a clean spectrum with only one doublet for CF_2H at -128 ppm in ^{19}F NMR and no over-reduction products were observed. In ^1H NMR, besides the characteristic triplet for CF_2H and peaks from DMPU, a quartet presented at around 0 ppm, which was representative for BH_4^-. Purification of speculative $[(DMPU)_2Zn(CF_2H)_2]$ is still problematic as BH_4^- always shows up in ^1H NMR after various attempts of purification.

After the extraction of putative $[(DMPU)_2Zn(CF_2H)_2]$ using benzene, TMEDA was added in the trial of growing crystal of $[(TMEDA)Zn(CF_2H)_2]$. One piece of crystal was picked and X-ray crystallography revealed a structure of dizinc complex **2.2** bearing two CF_2H ligands, bridged by two fluorides (Scheme 2c, a).

Based on previous observations, we propose that the $[Zn(CF_3)_2]$ reagent is in equilibrium with the α-elimination product (Scheme 2c, b), and that this species exchanges its fluoride with a hydride to produce a zinc hydride complex. That hydride then becomes incorporated onto the carbon of difluorocarbene to afford the CF_2H ligand. Repeating this α-elimination process and reacting with a second hydride source would then furnish a $[Zn(CF_2H)_2]$ reagent. The reaction of $[Zn(CF_3)_2]$ with sodium borohydride to generate $[Zn(CF_2H)_2]$ is interesting in the context of developing related difluoromethylenation reactions. If the mechanism shown in (Scheme 2c, b) is true, the use of other nucleophiles should enable a whole series of $[Zn(CF_2-Nu)_2]$ reagents to be used for coupling reactions. For instance, if $[RO^-]$ was used instead of $[H^-]$, then $[Zn(CF_2OR)_2]$ might be generated, which could be screened for $[CF_2OR]$ transfer activity.
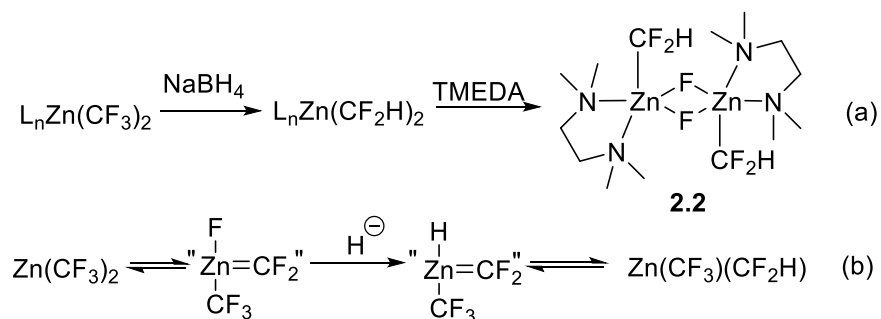
Scheme 2c. (a) Possible pathway for the formation of **2.2**; (b) Proposed mechanism for the reduction of [Zn(CF$_3$)$_2$] by NaBH$_4$

2.2.2. Optimization of the Nickel Catalyzed Difluoromethylation Reaction

Ligand effect. With the new zinc reagent [(DMPU)$_2$Zn(CF$_2$H)$_2$] in hand, we started to test its ability to serve as nucleophilic source of difluoromethyl in metal-mediated cross-coupling reactions. We first tried the combination of bipyridyl ligand and nickel catalyst as a starting point (Table 2a, entry 1).[17] Unfortunately, no product was observed by ^{19}F NMR spectroscopy when dtbpy was the ligand. In contrast, we did observe a new species which was confirmed to be [(dtbpy)Ni(CF$_2$H)$_2$] (**2.3**) by ^{19}F NMR spectgroscopy and single X-ray crystallography (Figure 2b). [(Bipyridyl)Ni(Ar)(X)] intermediates are known to undergo redistribution reactions to afford [(bipyridyl)NiAr$_2$] and [(bipyridyl)NiX$_2$],[18] and further transmetalation of the latter may be the origin of **2.3**. To confirm this hypothesis, we directly react [(dtbpy)NiBr$_2$] with [(DMPU)$_2$Zn(CF$_2$H)$_2$] in MeCN and to our delight, [(dtbpy)Ni(CF$_2$H)$_2$] was observed by ^{19}F NMR. Another diimine ligand, phen was also ineffective for the coupling reaction (Table 2a, entries 2). We then switched to screen phosphine ligands and quantitate yield of desired product was given when dppf was used as the ligand (Table 2a, entries 11). The other phosphine ligands were also tested but did not perform well. The screen result was summarized in Table 2a.
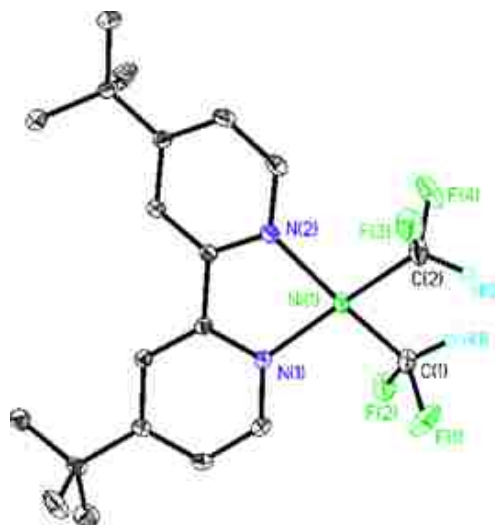
Figure 2b. ORTEP diagram of [(dtbpy)Ni(CF$_2$H)$_2$]. Selected bond lengths (Å) for **2.3**: Ni1-C1 1.8845(16); Ni1-C2 1.8867(16); Ni1-N1 1.9495(13); Ni1-N2 1.9671(13). Selected bond angles (°) for **2.3**: C1-Ni1-C2 85.26(7); C1-Ni1-N1 97.16(6); C2-Ni1-N1 170.58(6); C1-Ni1-N2 165.95(6); C2-Ni1-N2 97.64(6); N1-Ni1-N2 82.22(5).

Solvent effect. With the optimized ligand in hand, a screen of solvent was carried out (Table 2b). The screen revealed that the choice of solvent was also crucial. In non-polar solvent like benzene and toluene, there was only trace amounts of product formed. With the increase of solvent polarity, such as in the case of THF, the yield increased to about 10%. The use of DMSO promoted the yield dramatically to 81% with 15% catalyst loading. The solvent screen is summarized in Table 2b.
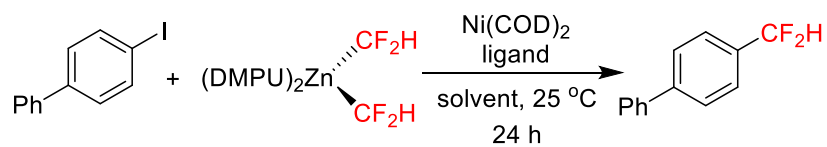
Entry	Ni(COD)$_2$ (mol %)	Ligand (mol %)	Solvent	Yield (%)
1	15	dtbpy (15)	DMSO	0
2	15	phen (15)	DMSO	0
3	15	PPh$_3$ (30)	DMSO	0
4	15	P(n-Bu)$_3$ (30)	DMSO	0
5	15	dppm (15)	DMSO	0
6	15	dppe (15)	DMSO	0
7	15	dppp (15)	DMSO	0
8	15	Xantphos (15)	DMSO	10
9	15	Qphos (15)	DMSO	0
10	15	dippf (15)	DMSO	0
11	**15**	**dppf (15)**	**DMSO**	**80**

Table 2a. Ligand effect. All of the reactions were run on a 0.1 mmol scale in 0.5 mL of solvent for 24 h. 1.2 equiv [(DMPU)$_2$Zn(CF$_2$H)$_2$] was used. The yields of ArCF$_2$H were determined by ^{19}F NMR analysis using α, α , α -trifluorotoluene as an internal standard.
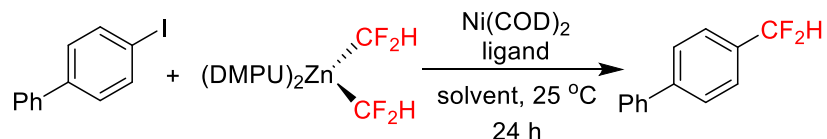
Entry	mol % Ni(COD)$_2$	Ligand (mol %)	Solvent	% Yield
1	15	dtbpy (15)	DMSO	0
2	15	phen (15)	DMSO	0
3	10	dppf (10)	toluene	trace
4	10	dppf (10)	dioxane	trace
5	10	dppf (10)	DMPU	trace
6	10	dppf (10)	THF	10
7	10	dppf (10)	MeCN	15
8	10	dppf (10)	DMF	16
9	10	dppf (10)	DMSO	51
10	**15**	**dppf (15)**	**DMSO**	**80**
11	15	xantphos (15)	DMSO	10

Table 2b. Solvent effect. All of the reactions were run on a 0.1 mmol scale in 0.5 mL of solvent for 24 h. 1.2 equiv [(DMPU)$_2$Zn(CF$_2$H)$_2$] was used. The yields of ArCF$_2$H were determined by ^{19}F NMR analysis using α, α , α -trifluorotoluene as an internal standard.

2.2.3. Scope of the Reaction

After the optimal conditions were identified, we started to test the substrate scope with a variety of aryl iodides. As shown in Table 2c, good to excellent yields of desired products were achieved for those electron deficient aryl iodides, such as 4-iodobenzonitrile. Carbonyl groups (aldehyde, ketone, ester) were also well-tolerated in the system which would be beneficial for the further molecule modification. However, for the substrates with

electron donating groups such as alkyl and methoxy, the yield dramatically decreased, giving little to no product. The explanation for this trend was preliminarily explored by mechanistic studies (see below). In addition, oxygen-, nitrogen-, and sulfur-containing heteroaryl iodides were tolerated as well, showing that the system we developed here has a good compatibility for various aryl and heteroaryl iodides.

To further expand the substrate scope, we tested aryl bromides and triflates as well and to our delight, these substrates were also well-tolerated. To the best of my knowledge, the only other known method for catalytically difluoromethylating aryl bromides operates at 80 °C,[15] whereas the method reported herein operates at room temperature. This shows a great potential for the further application of our coupling system. As shown in Table 2d, similar trend was observed by which aryl bromides with electron withdrawing groups gave better performance that those with the electron donating groups. Aryl triflates also gave good yield for desired products which represents the first example of catalytic difluoromethylation of this class of substrates.

Reaction scheme:

2.3 + (DMPU)$_2$Zn(CF$_2$H)(CF$_2$H) 2.1 → (dppf)Ni(COD) (15 mol %), DMSO, 25 °C, 24 h → product

2.3a
82%

2.3b
80(74)%

2.3c
81%

2.3d
78(71)%

2.3e
91%

2.3f
81(67)%

2.3g
81(75)%

2.3h
61(51)%

2.3i
10%

2.3j
0%

2.3k
28%

2.3l
52(48)%

2.3p
78(65)%

2.3q
82%

2.3r
60%

2.3m
43%

2.3n
51%

2.3o
70%
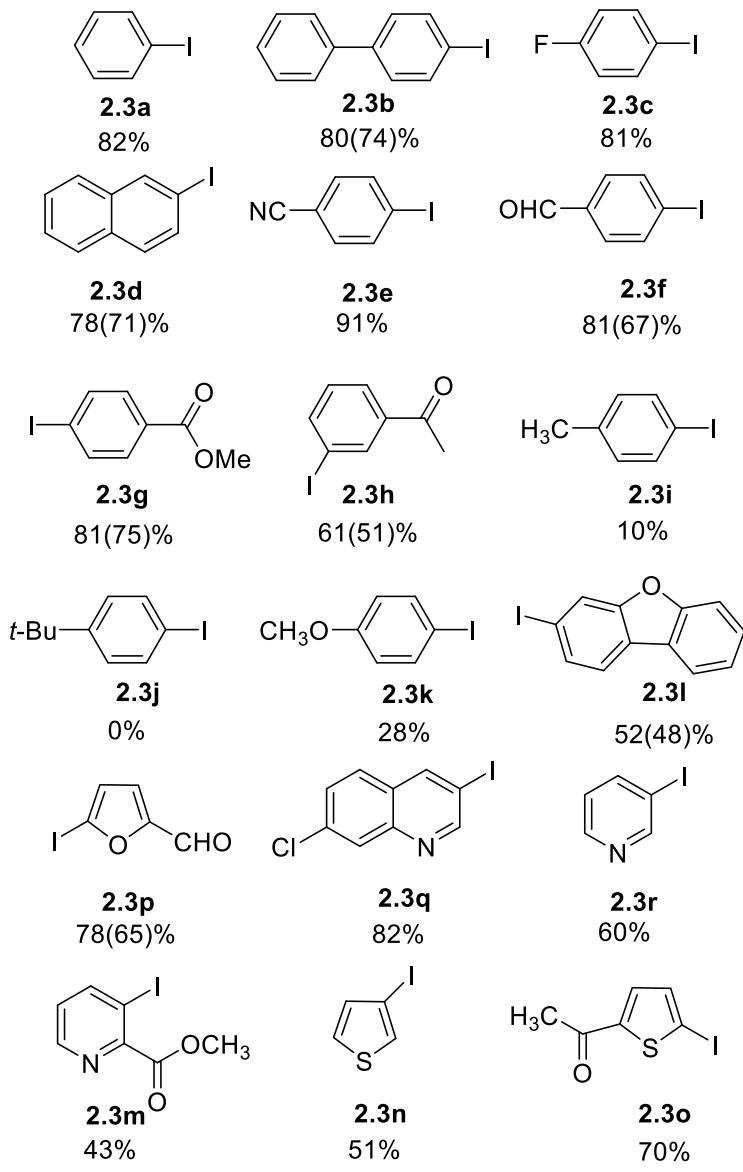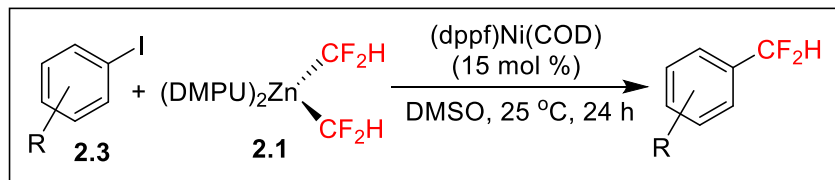
Table 2c. Nickel-catalyzed difluoromethylation of aryl and heteroaryl iodides.

The reaction scheme shows:

Ar–X (2.4) + (DMPU)$_2$Zn(CF$_2$H)$_2$ (2.1) → Ar–CF$_2$H, with conditions (dppf)Ni(COD) (15 mol %), DMSO, 25 °C, 24 h.

2.4a
75%

2.4b
85(78)%

2.4c
78%

2.4d
71(66)%

2.4e
79%

2.4f
71(60)%

2.4g
0%

2.4h
75% di

2.4i
18% mono
10% di

2.4j
65%

2.4k
53%

2.4l
88%

2.4m
58%

2.4n
85%(71%)

2.4o
77(73)%

2.4p
72%
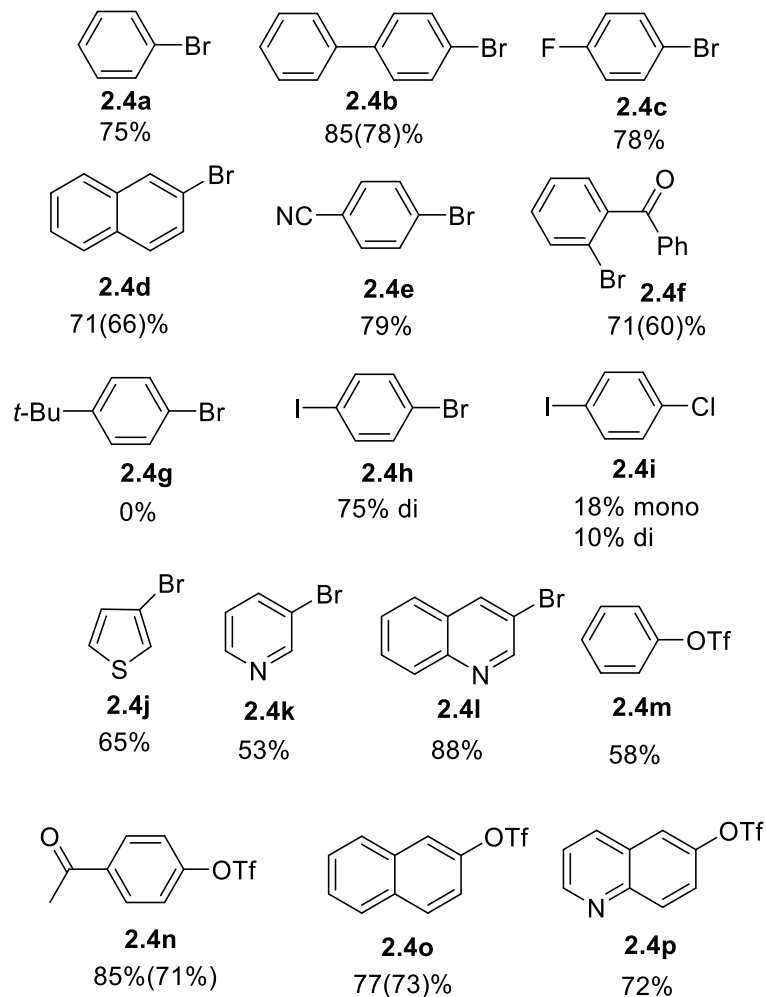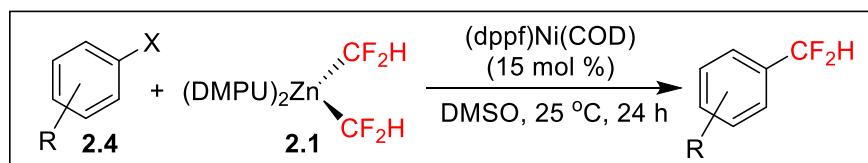
Table 2d. Nickel-catalyzed difluoromethylation of aryl bromides and triflates.

27

2.3. Preliminary Mechanistic Investigation of the Difluoromethylation Reaction

As described above, alkylated aryl substrates were not well-tolerated in the reaction system. We are also puzzled by the fact that the choice of dppf as ligand and DMSO as solvent was essential to the reaction system. One speculative mechanism is shown in Scheme 2d. Several experiments were performed to investigate key steps in the preliminary mechanism.
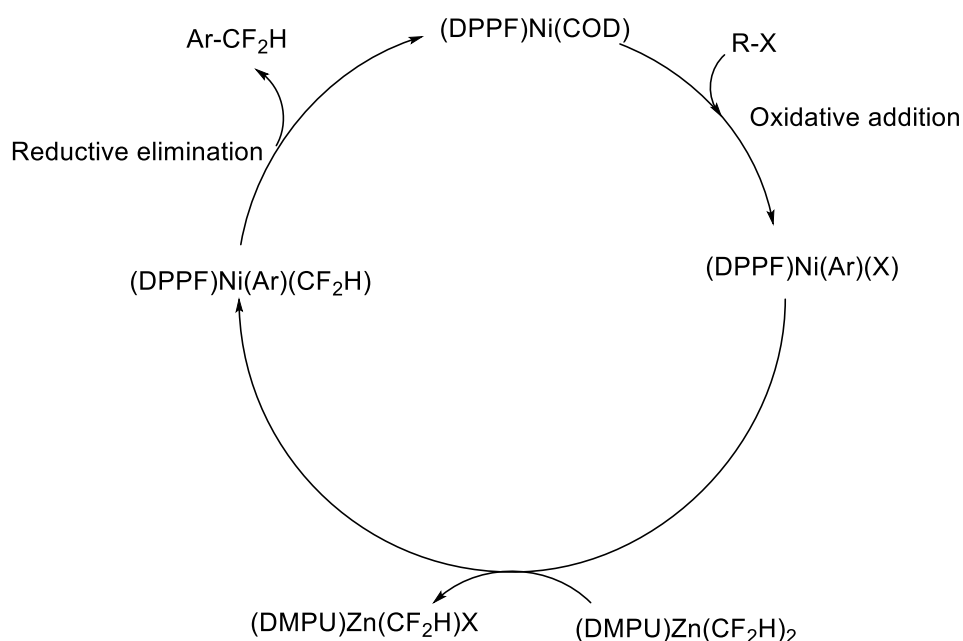
Scheme 2d. Proposed mechanism.

First, we stirred a stoichiometric amount of [(dppf)Ni(COD)] with 4-tert-butyl iodobenzene for 24 hours at room temperature. ^{31}P NMR spectroscopy and GC-MS analysis of the reaction mixture indicated that the nickel catalyst does not activate substrate under these conditions (Figures 2c and 2d). Reaction of [(dppf)Ni(COD)] with 4-iodobenzonitrile under similar conditions led to a new species, which upon addition of **2.1** produced 4-cyano-1-difluoromethylbenzene. Reaction of [(dppf)Ni(COD)] and phenyl iodide produced biphenyl in the absence of the difluoromethyl zinc reagent.
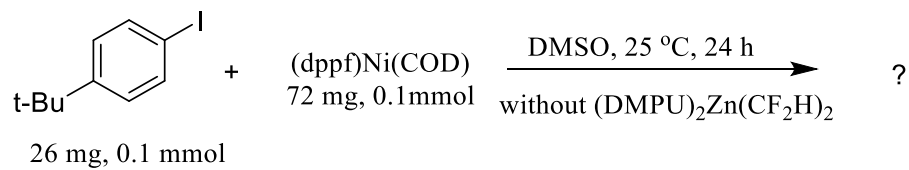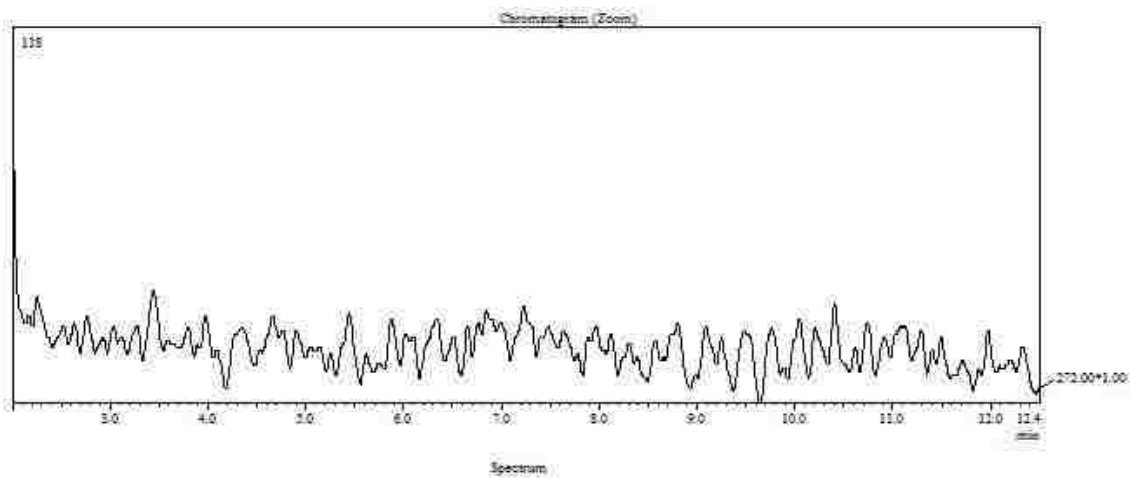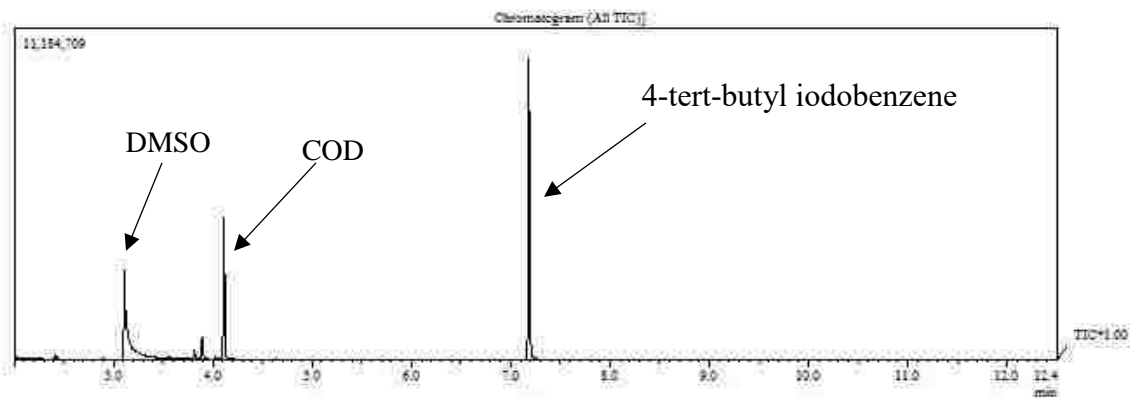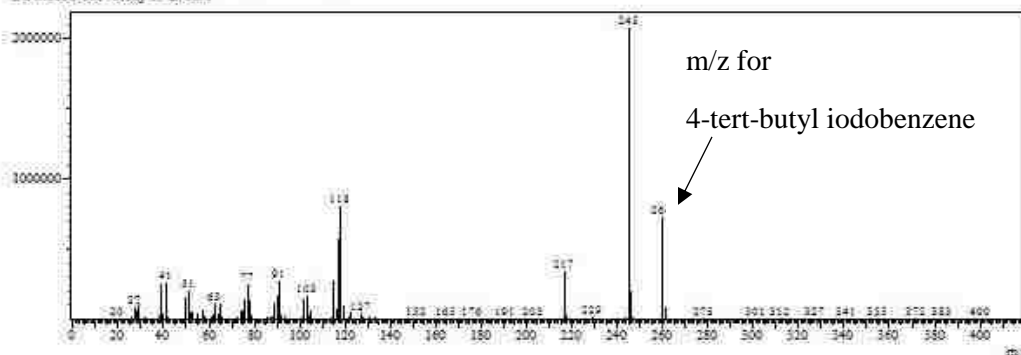
Figure 2c. GC-MS analysis of the monitored reaction.
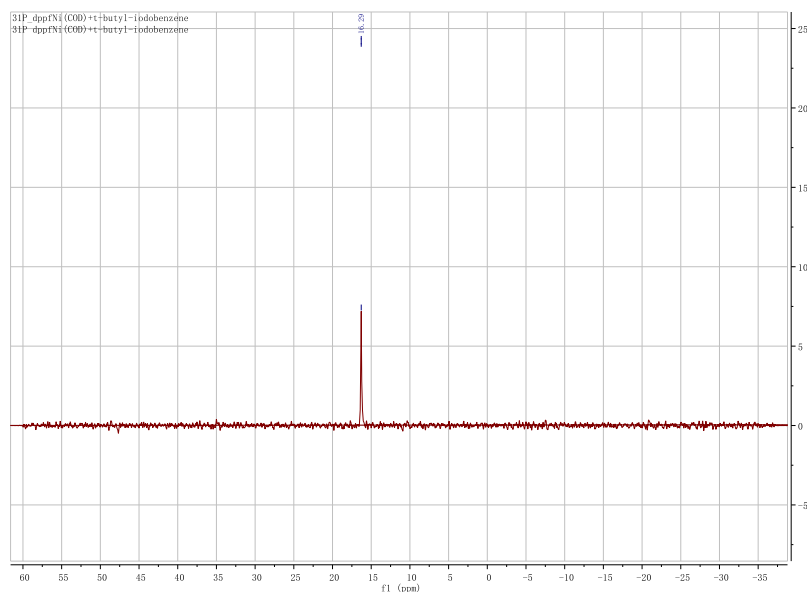
Figure 2d. ^{31}P NMR (151 MHz, DMSO-d_6) spectrum of the monitored reaction, indicating that the catalyst was unreacted and it failed to activate the 4-*tert*-butyliodobenzene under the reaction conditions. The peak at -16 ppm represents starting (dppf)Ni(COD).

These experiments showed under optimized condition, the oxidative addition was not happening in the case of alkylated aryl substrates, and the catalytic cycle could not proceed. Once the aryl iodide substrate could be activated by the Ni(0) to form Ni(Ar)(X), such as in the case of 4-iodobenzonitrile, the addition of difluoromethyl zinc reagent would trigger the transmetalation to give the Ni(Ar)(CF$_2$H). The following reductive elimination would give the desired difluoromethylated aryl product. However, a competing pathway existed where the Ni(Ar)(X) could redistributed to Ni(Ar)$_2$ and NiX$_2$. This pathway was supported by the isolation of (dtbpy)Ni(CF$_2$H)$_2$ after GC-analysis of the reaction mixture of (dppf)Ni(COD) and phenyl iodide in the absence of (DMPU)$_2$Zn(CF$_2$H)$_2$ showed that biphenyl was generated.

2.4. Summary

In this chapter, a novel difluoromethyl reagent [(DMPU)$_2$Zn(CF$_2$H)$_2$] was synthesized and characterized systematically. This reagent was utilized as a nucleophilic source of CF$_2$H to difluoromethylate aryl iodides, bromides and triflates in combination with catalytic amount of [(dppf)Ni(COD)] at room temperature. Preliminary mechanistic studies revealed that the oxidative addition of aryl electrophile was essential for the reaction to proceed. Further studies are currently being carried out in our lab to disclose the reason why dppf held such a special role in this catalytic reaction.

2.5. Experimental

2.5.1. General Information

All manipulations were performed in a nitrogen filled glovebox. Anhydrous solvents were purified by passing through activated alumina and/or copper in a solvent purification system supplied by Pure Process Technology or were purchased from Aldrich. Iododifluoromethane was purchased from SynQuest Labs. Ni(COD)$_2$, ligands, aryl iodides, aryl bromides and aryl triflates were purchased from Aldrich or Strem. All the purchased reagents were used without further purification. [(dppf)Ni(COD)] was synthesized according to the literature.[19] Solution ^{1}H NMR spectra were recorded at ambient temperature on a Bruker DRX 400 MHz spectrometer and referenced to residual proton solvent signals: CDCl$_3$ 7.26 ppm for ^{1}H and CD$_2$Cl$_2$ 5.30 ppm for [1]H. [19]F spectra were recorded on the Bruker NMR spectrometer operating at 470 MHz and referenced to α,α,α-trifluorotoluene as an internal standard (δ = -63.7). Coupling constants (*J*) are reported in

Hz and coupling patterns are described as br = broad, s = singlet, d = doublet, t = triplet, q = quartet, m = multiplet. A Bruker D8 Quest diffractometer was used for X-ray crystal structure determinations. GC-MS were recorded with positive ion mode.

2.5.2. Preparation of (DMPU)$_2$Zn(CF$_2$H)$_2$
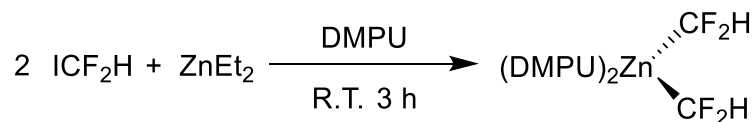
0.5 ml (4.14 mmol) DMPU was cooled to -20 °C. To this, 716 mg (4 mmol) HCF$_2$I was added, followed by the addition of two mL hexane solution of ZnEt$_2$(1 M, 2 mmol) and 10 ml pentane. After the mixture was stirred at room temperature for one hour, white solid precipitated and was collected by filtration. The solid was washed by pentane three times and dried under high-vac line, to give 795 mg (DMPU)$_2$Zn(CF$_2$H)$_2$ (94% yield).
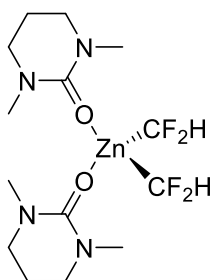
^{1}H NMR (500 MHz, CD$_2$Cl$_2$): δ 6.11 (t, J = 43.3 Hz, 2H), 3.26 (t, J = 5.9 Hz, 8H), 2.95 (s, 12H), 1.97 (quint, J = 6.0 Hz, 4H); ^{19}F NMR (470 MHz, CD$_2$Cl$_2$): δ -128.83 (d, J = 39.4 Hz); ^{13}C NMR (126 MHz, CD$_2$Cl$_2$): δ 21.58, 35.74, 47.70, 145.39 (t, J = 261.2 Hz), 158.29 ppm. Anal.Calcd (found) for C$_{14}$H$_{26}$F$_4$N$_4$O$_2$Zn: C, 39.68 (39.65); H, 6.18 (6.09).

2.5.3. General Procedure for the Difluoromethylation of ArI, ArBr, and ArOTf
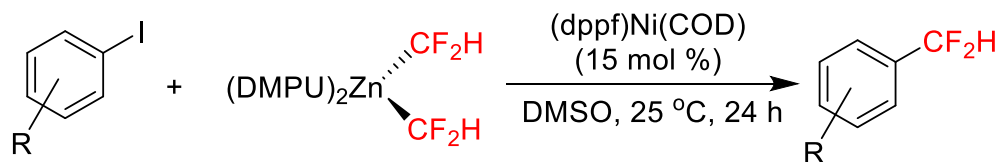
In a nitrogen-filled glove box, ArX (0.2 mmol, 1.0 equiv) and (dppf)Ni(cod) (21.6 mg, 0.03 mmol, 0.15 equiv) were combined in a 20 mL vial. To this vial was added one mL of anhydrous DMSO, followed by $(DMPU)_2Zn(CF_2H)_2$ (52 mg, 0.12 mmol, 1.2 equiv). The vial was sealed and stirred at room temperature for 24 hours. The solution was diluted with CH_2Cl_2 (15 mL). The mixture was filtered through a short plug of Celite, washed with H_2O (20 mL). The organic layer was combined, dried over $NaSO_4$, filtered, and concentrated under vacuum. The crude product was purified by column chromatography on silica gel with hexane or hexane/Et_2O mixture as the eluent to give the product.

2.5.4. Stoichiometric Reaction between 4-*tert*-Butyliodobenzene and Ni(0)
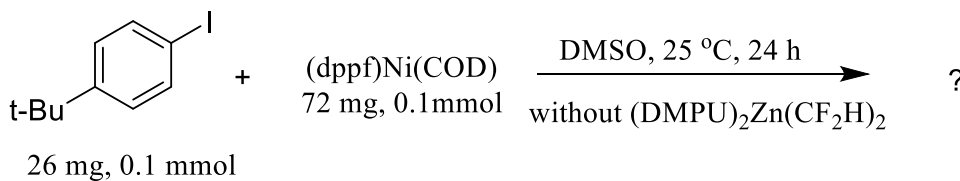
In a nitrogen-filled glove box, 4-*tert*-butyliodobenzene (26 mg, 0.1 mmol) and (dppf)Ni(cod) (72 mg, 0.1 mmol) were combined in a 20 mL vial. To this vial was added one mL of anhydrous DMSO. The vial was sealed and stirred at room temperature for 24 hours. ^{31}P NMR spectroscopy was used to analyze the change of catalyst and GC-MS was used to monitor the organic compounds after reaction.

2.5.5. Analytical Data for the Isolated Organic Products
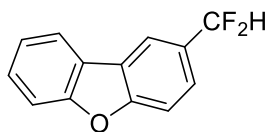
2-(difluoromethyl)dibenzofuran: The title compound was prepared following the standard procedure. After purification, it was isolated as white solid (21 mg, 0.096 mmol, 48% yield). ^{1}H NMR (500 MHz, CDCl$_3$): δ= 8.14 (s, 1H), 8.06 – 7.91 (m, 1H), 7.63 (m, 3H), 7.56 – 7.48 (m, 1H), 7.40 (m, 1H), 6.83 ppm (t, J = 56.7 Hz, 1H); ^{19}F NMR (470 MHz, CDCl$_3$): δ= -108.74 ppm (d, J = 56.5 Hz); ^{13}C NMR (126 MHz, CDCl$_3$): δ= 157.3, 156.5, 129.3, 127.9,124.7, 124.5, 123.6, 123.2, 120.8, 118.5 (t, J = 6.3 Hz),115.02 (t, J = 238.6 Hz, CF$_2$H), 112.0, 111.9 ppm. GC-MS (EI, m/z): 218 (M[+]).
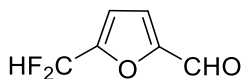
5-(difluoromethyl)-2-furaldehyde: The title compound was prepared following the standard procedure. After purification, it was isolated as yellow oil (19 mg, 0.13 mmol, 65% yield). ^{1}H NMR (500 MHz, CDCl$_3$): δ= 9.74 (s, 1H), 7.29-7.27 (s, 1H), 6.96 – 6.83 (m, 1H), 6.69 ppm (t, J = 53.9 Hz, 1H); ^{19}F NMR (470 MHz, CDCl$_3$): δ= -118.71 ppm (d, J = 53.8 Hz); ^{13}C NMR (126 MHz, CDCl$_3$): δ= 178.1, 153.3, 151.1, 120.0, 111.91 (t, J = 3.6 Hz), 107.9 ppm (t, J = 237.4 Hz, CF$_2$H); GC-MS (EI, m/z):146 (M[+]).
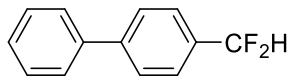
4-(difluoromethyl)-1,1'-biphenyl: The title compound was prepared following the standard procedure. After purification, it was isolated as white solid (30 mg, 74% yield on ArI; 32 mg, 78% yield on ArBr).. ^{1}H NMR (500 MHz, CDCl$_3$): δ= 7.69 (d, J = 8.0 Hz, 2H), 7.63 – 7.55 (m, 4H), 7.52 – 7.45 (m,

2H), 7.43 – 7.37 (m, 1H), 6.71 ppm(t, *J* = 56.5 Hz, 1H); ^{19}F NMR (470 MHz, CDCl$_3$): δ= -111.47 ppm (d, *J* = 56.1 Hz); ^{13}C NMR (126 MHz, CDCl$_3$) δ= 143.82 (t, *J* = 2.5 Hz)), 140.30, 133.34 (t, *J* = 22.7 Hz), 129.04, 128.03, 127.55, 127.37, 126.15 (t, *J* = 5.0 Hz), 114.89 ppm (t, *J* =239.4 Hz, CF$_2$H); GC-MS (EI, m/z): 204.0 (M$^+$).

2-(difluoromethyl)naphthalene: The title compound was prepared following the standard procedure. After purification, it was isolated as white solid (25 mg, 71% yield on ArI; 23 mg, 66% yield on ArBr; 26 mg, 73% yield on ArOTf).. ^{1}H NMR (500 MHz, CDCl3): δ= 8.10 – 7.80 (m, 4H), 7.77 – 7.40 (m, 3H), 6.82 ppm (t, *J* = 56.4 Hz, 1H); ^{19}F NMR (470 MHz, CDCl$_3$): δ= -111.66 ppm (d, *J* = 56.4 Hz). ^{13}C NMR (126 MHz, CDCl$_3$): δ= 134.33 (t, *J* = 1.4 Hz), 132.57, 131.64 (t, *J* = 22.3 Hz), 128.91, 128.54, 127.98, 127.50, 126.91,126.00 (t, *J* = 7.6 Hz), 122.12 (t, *J* = 4.8 Hz), 115.20 ppm (t, *J* = 238.5 Hz, CF$_2$H); GC-MS (EI, m/z): 178 (M$^+$).

(2-(difluoromethyl)phenyl)(phenyl)methanone: The title compound was prepared following the standard procedure. After purification, it was isolated as yellow oil (28 mg, 0.12 mmol, 60% yield).. ^{1}H NMR (500 MHz, CDCl$_3$): δ= 7.91 – 7.77 (m, 3H), 7.72 – 7.60 (m, 2H), 7.55 (t, *J* = 7.5 Hz, 1H), 7.52 – 7.42 (m, 3H), 7.07 ppm (t, *J* = 55.8 Hz, 1H); ^{19}F NMR (470 MHz, CDCl$_3$): δ= -112.90 ppm (d, *J* = 55.9 Hz); ^{13}C NMR (126 MHz, CDCl$_3$): δ= 196.6, 137.3 (t, *J* = 5.3 Hz), 137.0, 134.0 (t, *J*= 22.5 Hz), 133.6, 131.0, 130.4 , 129.7, 129.5, 128.5, 126.2 (t, *J*= 7.2 Hz), 112.3 ppm (t, *J*= 238.6 Hz, CF$_2$H); GC-MS (EI, m/z): 232 (M$^+$).
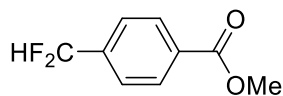
methyl 4-(difluoromethyl)benzoate: The title compound was prepared following the standard procedure. After purification, it was isolated as white solid (28 mg, 0.15 mmol, 75% yield).. ^{1}H NMR (500 MHz, CDCl$_3$): δ= 8.14 (d, J = 8.0 Hz, 2H), 7.60 (d, J = 7.8 Hz, 2H), 6.70 (t, J = 56.1 Hz, 1H), 3.95 ppm (s, 3H); ^{19}F NMR (470 MHz, CDCl$_3$): δ= -113.41 ppm (d, J = 56.9 Hz); ^{13}C NMR (126 MHz, CDCl$_3$): δ= 166.2, 138.3 (t, J = 21.8 Hz), 132.1, 130.0, 125.5 (t, J= 5.8 Hz), 114.0 (t, J = 239.8 Hz, CF2H), 52.4 ppm; GC-MS (EI, m/z): 186 (M[+]).
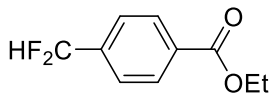
ethyl 4-(difluoromethyl)benzoate: The title compound was prepared following the standard procedure. After purification, it was isolated as colorless oil (27 mg, 0.13 mmol, 68% yield). ^{1}H NMR (500 MHz, CDCl$_3$): δ= 8.14 (d, J = 8.0 Hz, 2H), 7.59 (d, J = 7.9 Hz, 2H), 6.70 (t, J = 56.1 Hz, 1H), 4.41 (q, J = 7.1 Hz, 2H), 1.42 ppm (t, J = 7.1 Hz, 3H); ^{19}F NMR (470 MHz, CDCl$_3$): δ= -113.31 ppm (d, J = 56.3 Hz); ^{13}C NMR (126 MHz, CDCl$_3$): δ= 166.6, 138.3 (t, J = 21.7 Hz), 132.7, 130.0, 125.7 (t, J= 5.6 Hz), 114.0 (t, J = 239.9 Hz, CF2H), 61.2, 14.2 ppm; GC-MS (EI, m/z): 200 (M[+]).
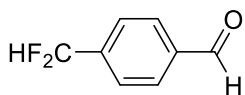
4-(Difluoromethyl)benzaldehyde: The title compound was prepared following the standard procedure. After purification, it was isolated as colorless oil (21 mg, 0.13 mmol, 67% yield). ^{1}H NMR (500 MHz, CDCl$_3$): δ= 10.09 (s, 1H), 7.99 (d, J = 7.8 Hz, 2H), 7.70 (d, J = 7.7 Hz, 2H), 6.72 ppm (t, J = 56.0 Hz, 1H); ^{19}F NMR (470 MHz, CDCl$_3$): δ= -114.03 ppm (d, J = 56.2 Hz); ^{13}C NMR (126 MHz,

CDCl$_3$): δ= 191.4, 140.0 (t, $J = 21.5$ Hz), 137.7, 129.9, 126.3 (t, $J = 6.1$ Hz), 114.0 ppm (t,
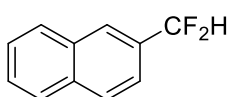
$J = 240.1$ Hz, CF$_2$H); GC-MS (EI, m/z): 156 (M$^+$).
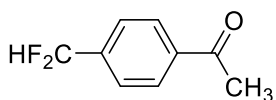
1-(4-(Difluoromethyl)phenyl)ethanone: The title compound was prepared following the standard procedure. After purification, it was isolated as colorless oil (24 mg, 0.14 mmol, 71% yield). ^{1}H NMR (500 MHz, CDCl$_3$): δ= 8.05 (d, $J = 8.4$ Hz, 2H), 7.63 (d, $J = 8.1$ Hz, 2H), 6.71 (t, $J = 56.1$ Hz, 1H), 2.65 ppm(s, 3H); ^{19}F NMR (470 MHz, CDCl$_3$): δ= -113.15 ppm (d, $J = 56.1$ Hz); ^{13}C NMR (126 MHz, CDCl$_3$): δ= 197.4, 138.8, 138.5 (t, $J = 22.4$ Hz), 128.6, 125.9 (t, $J = 6.2$Hz), 113.9 (t, $J = 238.1$ Hz, CF$_2$H), 26.8 ppm; GC-MS (EI, m/z): 170 (M$^+$).
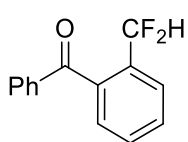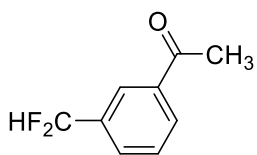
1-(3-(Difluoromethyl)phenyl)ethanone: The title compound was prepared following the standard procedure. After purification, it was isolated as colorless oil (18 mg, 0.1 mmol, 51% yield. ^{1}H NMR (500 MHz, CDCl$_3$): δ= 8.24 – 7.98 (m, 2H), 7.81 – 7.67 (m, 1H), 7.67 – 7.52 (m, 1H), 6.71 (t, $J = 56.2$ Hz, 1H), 2.65 ppm (s, 3H); ^{19}F NMR (470 MHz, CDCl$_3$): δ= -114.03 ppm (d, $J = 56.1$ Hz); ^{13}C NMR (126 MHz, CDCl$_3$): δ= 197.1, 137.5, 134.9 (t, $J = 22.8$ Hz), 130.5, 129.9 (t, $J = 5.9$ Hz), 129.2, 125.5 (t, $J = 6.5$ Hz), 114.1 (t, $J= 238.3$ Hz, CF$_2$H), 26.7 ppm; GC-MS (EI, m/z): 170 (M$^+$).

2.6. Reference

1. Wang, H.; Vicic, D. A. *Synlett* **2013**, *24*, 1887.
2. Hu, J. B.; Zhang, W.; Wang, F. *Chem. Commun.* **2009**, 7465.
3. Singh, R. P.; Shreeve, J. M. *Synthesis* **2002**, 2561.
4. Eujen, R.; Hoge, B.; Brauer, D. J. *J. Organomet. Chem.* **1996**, *519*, 7.
5. Burton, D. J.; Hartgraves, G. A. *J. Fluor. Chem.* **2007**, *128*, 1198.
6. Erickson, J. A.; McLoughlin, J. I. *J. Org. Chem.* **1995**, *60*, 1626.
7. Meanwell, N. A. *J. Med. Chem*. **2011**, *54*, 2529.
8. Narjes, F.; Koehler, K. F.; Koch, U.; Gerlach, B.; Colarusso, S.; Steinkuhler, C.; Brunetti, M.; Altamura, S.; De Francesco, R.; Matassa, V. G. *Bioorg. Med. Chem. Lett*. **2002**, *12*, 701.
9. Chowdhury, M. A.; Abdellatif, K. R. A.; Dong, Y.; Das, D.; Suresh, M. R.; Knaus, E. E. *J. Med. Chem*. **2009**, *52*, 1525.
10. Fujikawa, K.; Kobayashi, A.; Amii, H. *Synthesis* **2012**, *44*, 3015.
11. Fujiwara, Y.; Dixon, J. A.; Rodriguez, R. A.; Baxter, R. D.; Dixon, D. D.; Collins, M. R.; Blackmond, D. G.; Baran, P. S. *J. Am. Chem. Soc.* **2012**, *134*, 1494.
12. Fier, P. S.; Hartwig, J. F. *J. Am. Chem. Soc.* **2012**, *134*, 5524.
13. Jiang, X.-L.; Chen, Z.-H.; Xu, X.-H.; Qing, F.-L. *Org. Chem. Front.* **2014**, *1*, 774.
14. Prakash, G. K. S.; Ganesh, S. K.; Jones, J.-P.; Kulkarni, A.; Masood, K.; Swabeck, J. K.; Olah, G. A. *Angew. Chem., Int. Ed.* **2012**, *51*, 12090.
15. Gu, Y.; Leng, X.; Shen, Q. *Nat. Commun.* **2014**, *5*, 5405.
16. Kaplan, P. T.; Xu, L.; Chen, B.; McGarry, K. R.; Yu, S.; Wang, H.; Vicic, D. A. *Organometallics* **2013**, *32*, 7552.
17. Phapale, V. B.; Guisan-Ceinos, M.; Bunuel, E.; Cardenas, D. J. *Chem. - A Eur. J.* **2009**, *15*, 12681.
18. Everson, D. A.; Jones, B. A.; Weix, D. J. *J. Am. Chem. Soc.* **2012**, *134*, 6146.
19. Yin, G; Kalvet I; Englert, U, Schoenebeck, F. *J. Am. Chem. Soc.* **2015**, *137*, 4164.

3. Chapter 3 Construction and Characterization of Perfluorometallacyclobutanes

3.1. Introduction

It is universally believed that metallacyclobutanes are the key intermediates in olefin metathesis, which entails the redistribution of fragments of olefins by the scission and regeneration of carbon-carbon double bonds.[1-8] Below is a catalytic cycle for the self-metathesis of propene to give 2-butene and ethylene (Scheme 3a).
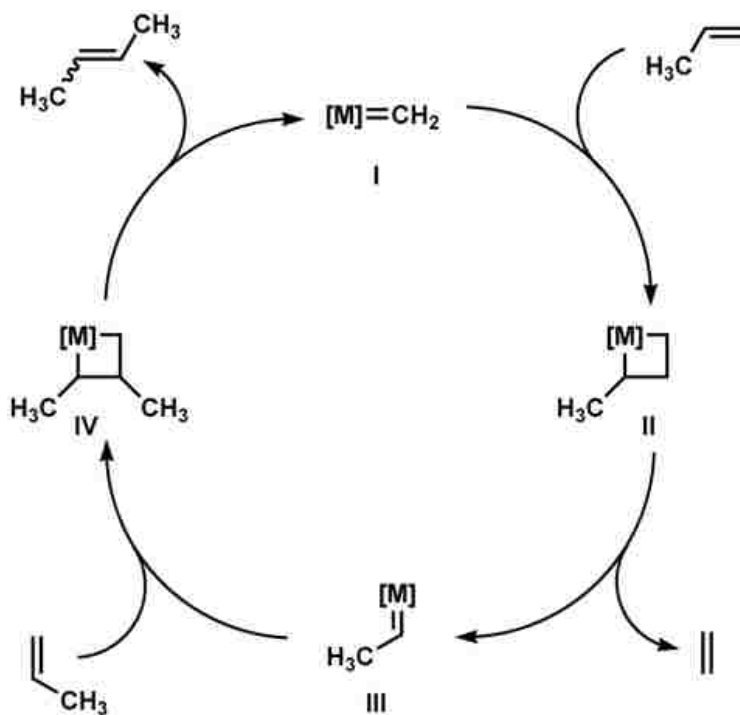
Scheme 3a. Proposed mechanism for olefin metathesis.

However, perfluorometallacyclobutanes have been studied in much less detail compared to metallacyclobutanes, and the analogous metathesis of fluorinated olefins has not been

extensively reported. Grubbs and co-workers demonstrated that, in the presence of difluoroethylene, a ruthenium metathesis precatalyst can stoichiometrically produce the formally cross-metathesized products **3.1** and **3.2** (Scheme 3b).[9] The amount of **3.2** increased to over 98 % when the reaction was carried out at 60 °C, implying that pathway **A** is preferred over pathway **B** at elevated temperatures (Scheme 3b). While the ruthenium complexes **3.1** and **3.2** could be isolated cleanly, the organic products of a second turnover of olefin metathesis (ethylene and tetrafluoroethylene) were not observed. This result indicated that the reaction was not catalytic, and highlights the fact that more studies are needed to understand how to develop catalytic processes with *gem*-difluoroalkenes.
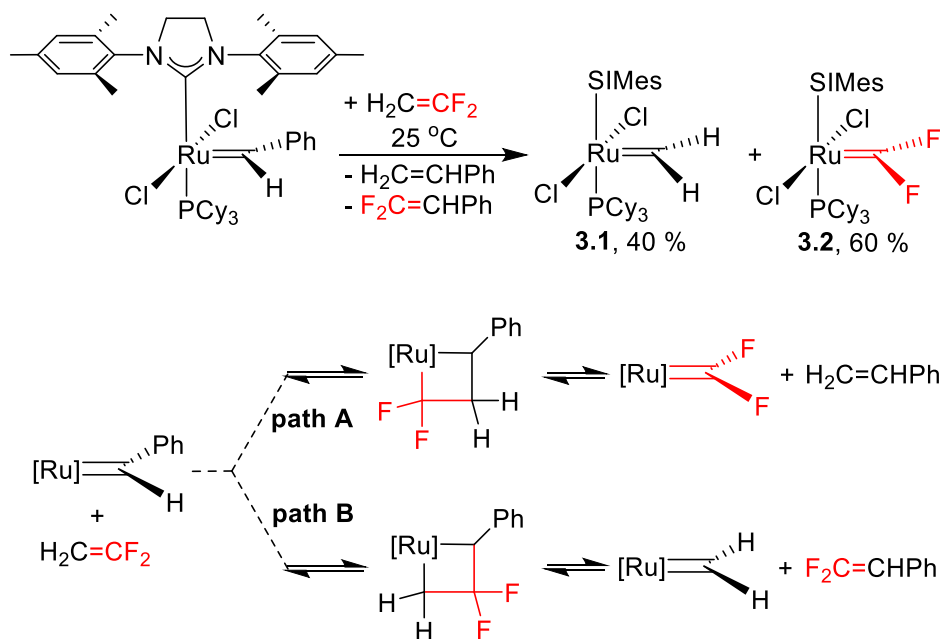
Scheme 3b. Example of a metathesis-like reaction of difluoroethylene.

In 2015, Morizawa group developed the first example of catalytic olefin metathesis with tetrafluoroethylene and analogous fluoroolefins.[10] A series of ruthenium precatalysts (**3.3**, **3.4** and **3.5**) were synthesized. After optimization, TON of this catalytic reaction could reach as high as 13.4 at 60 ^{o}C in benzene within 1 hour (Scheme 3c).
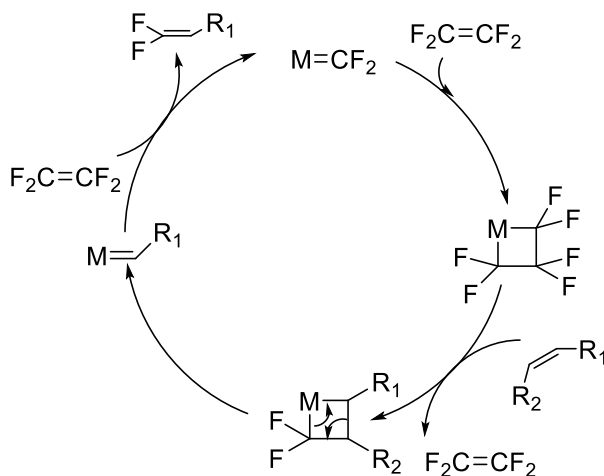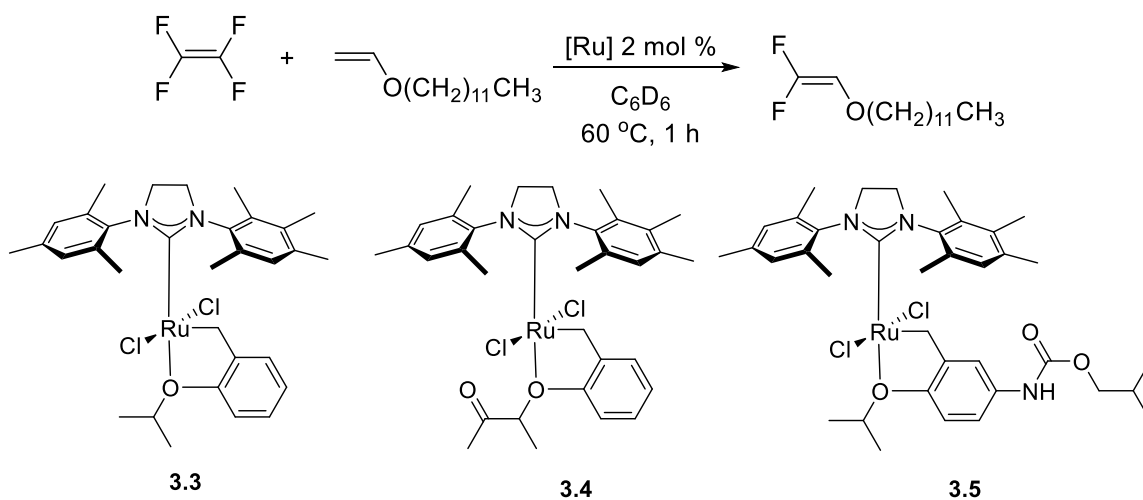
Scheme 3c. Reaction tested (top), catalysts used (middle), and possible mechanism for olefin cross-metathesis fluorinated olefins (bottom).

To the best of my knowledge, there are only three reported transition-metal perfluorometallacyclobutanes, synthesized by decarbonylation of an iron(II) bis(acyl) complex[11] and formal [2+2] cycloaddition[12,13] respectively (Scheme 3d):
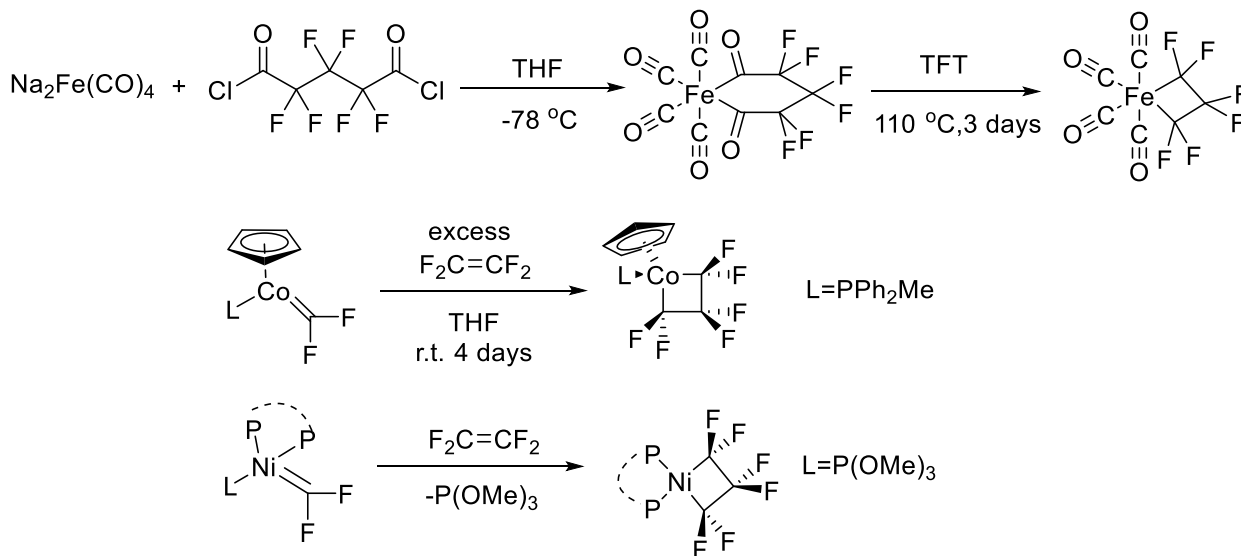
Scheme 3d. Three routes to synthesize perfluorometallacylcobutane complexes.

These three routes require either long reaction time (3-4 days) or use of the gaseous tetrafluoroethylene as a reactant which is not convenient and safe for those small laboratories that are not equipped for generating and handling tetrafluoroethylene. Versatility is another limitation here because the starting material is either $Na_2Fe(CO)_4$ or cobalt fluorocarbene, which have to be pre-synthesized. Therefore, it is highly demanded to design a mild and versatile strategy to construct perfluorometallacylcobutanes from readily available molecules in order to better study the perfluoroalkene metatheses reaction pathway.

3.2. Result and Discussion

3.2.1. Transmetalation of a Nickel (II) Precursor with a Dizinc Reagent.

Our previous work showcased a facile, one-pot synthesis of metallacyclic dizinc reagent using diethylzinc and 1,3-diiodoperfluoropropane (Scheme 3e):[14]
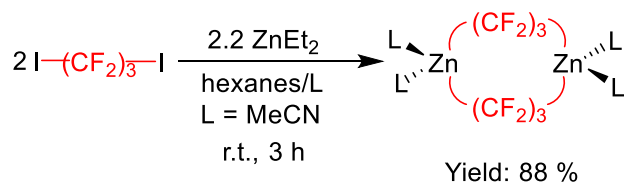
Scheme 3e. Synthesis of perfluorometallacyclic dizinc reagent.

Both diethylzinc (1.0 M in hexanes) and 1,3-diiodoperfluoropropane are in liquid form at room temperature, and the reaction can be finished within 3 hours. After decanting the top hexane layer, dizinc reagent that is analytically pure is obtained by recrystallization from benzene and acetonitrile solution overnight. This dizinc reagent is expected to provide entries to a diverse class of new perfluorometallacyclobutanes through convenient transmetalation approaches, as it has been shown successfully for the C_4 derivative which reacted readily with a nickel(II) precursor [(DME)NiBr$_2$] (Scheme 3f):[14]
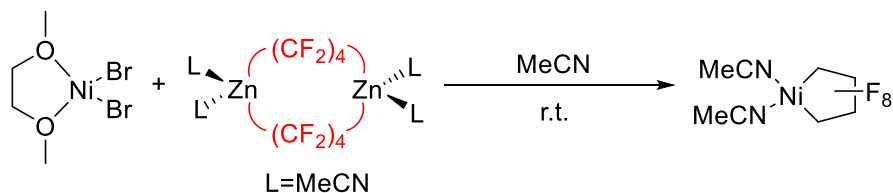
Scheme 3f. Transmetalation of a nickel(II) precursor by the C_4 dizinc reagent.

Unfortunately, preliminary attempts to synthesize the analogous metallacyclic nickel(II) complex from C_3 dizinc reagent was not successful under the same reaction condition for the C_4. ^{19}F NMR spectroscopy showed no fluorine signals for the crude mixture. At first, we reasoned that the nickel(II) perfluorometallacyclobutane complex was not stable and decomposed readily at room temperature. Later, Baker's reported a way to synthesize nickel(II) perfluorometallacyclobutane via the reaction between $[L_nNi=CF_2]$ with tetrafluoroethylene (Scheme 3d). This indicates that our failure to synthesize the similar compound might arise from the choice of ligand to stabilize the final product. In our case, only MeCN and some nitrogen donor ligands like bipyridine and dtbpy were tested. No phosphine ligand were screened in this process.

3.2.2. Transmetalation of a Iron (II) Precursor with a Dizinc reagent.

According to the literature report, $[(CO)_4Fe(CF_2CF_2CF_2)]$ was thermostable even at 110 °C. This promoted us to design a route to synthesize iron(II) perfluorometallacyclobutane complexes through transmetalation by combining varies of iron(II) precursors and C_3 dizinc reagent (Scheme 3g):
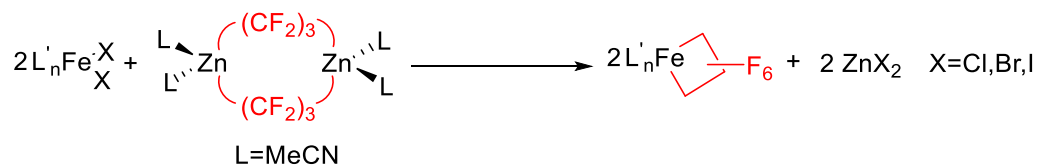
Scheme 3g. Proposed route to synthesize iron(II) perfluorometallacyclobutane.

The first iron(II) precursor that was examined was $[cis\text{-}(CO)_4FeBr_2]$[15] which was expected to give the identical product $[(CO)_4Fe(CF_2CF_2CF_2)]$. The *cis* form of iron(II) dihalides is

necessary here because it could be envisioned that the two α-CF$_2$ are *cis* to each other in the final structure[11] (Figure 3a). We reason that the *cis* precursor would react more easily with dizinc reagent to accomplish the ring closure upon transmetalation.
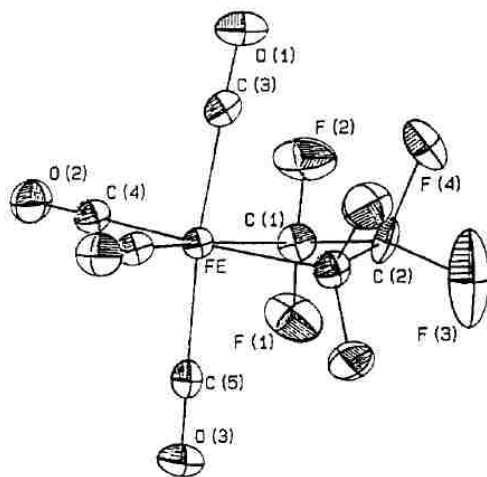
Figure 3a. Structure of [(CO)$_4$Fe(CF$_2$CF$_2$CF$_2$)].

With the freshly made [*cis*-(CO)$_4$FeBr$_2$] in hand, the next step in the progression of this aim was to screen various reaction conditions to construct the perfluorometallacyclobutane. Well-defined structures through transmetalation from zinc reagent to iron(II) were rare, which made this step complicated. One reported case showed the reduction of an iron(II) complex to iron(I) in an iron-catalyzed Negishi cross-coupling reaction (Scheme 3h):[16]

$$[FeX_2(dpbz)_2] \ + \ 1,4\text{-}tol_2Zn \quad \xrightarrow{\text{r.t.}} \quad \cdots \quad + \ ZnX_2 \ + \ 0.5 \ (4\text{-Me-}C_6H_4)_2$$
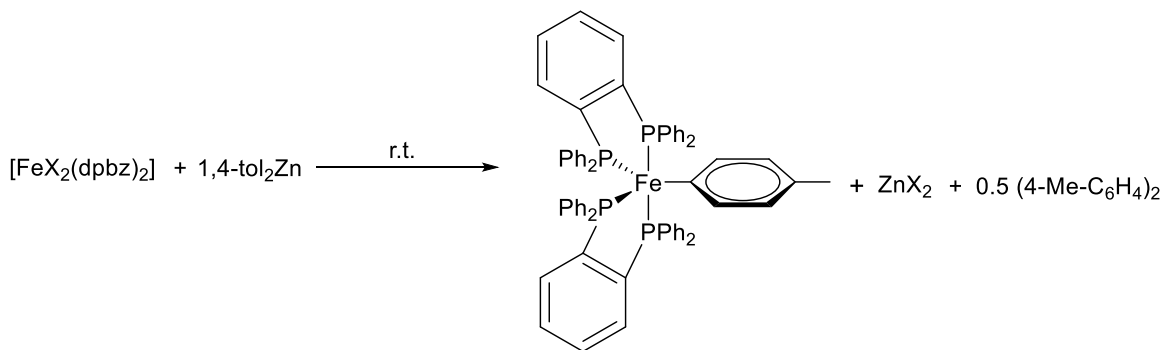
Scheme 3h. Reduction of iron(II) to iron(I) by a diaryl zinc reagent.

45

The iron(II) precursor was reduced by the zinc reagent at room temperature which might indicate a single electron transfer pathway in this process. This undesired pathway should be avoided in order to synthesize the iron(II) perfluorometallacyclobutane complex. We therefore thought that temperature control was essential for this synthetic challenge. Gradually warming up the reaction mixture from -78 ℃ or even lower to room temperature was preferable. Unfortunately, though dozens of attempts have been made, we yet failed to generate the desired iron perfluorometallacyclobutane complex. The final ^{19}F NMR spectrum showed no major peaks for product after each trial.

3.2.3. Stepwise Construction of a Platinum Perfluorometallacyclobutane Derivative from a Platinum Dimethyl Complex and 1,3-Diiodoperfluoropropane

Direct transmetallation from C$_3$ dizinc reagent [(MeCN)$_2$Zn((CF$_2$)$_3$)$_2$Zn(MeCN)$_2$] to the metal center to form the perfluorometallacylcobutane has failed in the previous trials in our lab. We then switched our strategy to synthesize the target product through halogen metathesis. It has been shown by Clark *et al.* that [(COD)PtMe$_2$] reacts with [CF$_3$I] to afford [(COD)Pt(CF$_3$)$_2$] (Scheme 3i).[17]
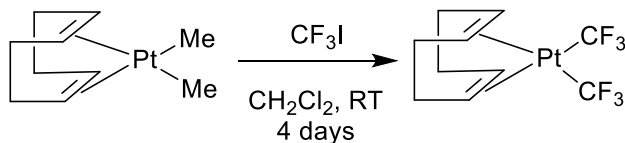
Scheme 3i. Synthesis of [(COD)Pt(CF$_3$)$_2$].

Combined with our previous route to prepare the C$_3$ dizinc regent (Scheme 3e), this work inspired us to synthesize platinum perfluorometallacyclobutanes by reacting [(COD)PtMe$_2$]

with [IC$_3$F$_6$I]. To our surprise, the addition of [IC$_3$F$_6$I] occurred in a stepwise fashion, and the mono-substituted intermediate [(COD)Pt(C$_3$F$_6$I)Me] could be isolated (Scheme 3j) when [(COD)PtMe$_2$] reacted [IC$_3$F$_6$I] in MeCN.

Solvents proved to be essential for this conversion to [(COD)Pt(C$_3$F$_6$I)Me]. We screened MeCN, THF, CH$_2$Cl$_2$, DMF, benzene, toluene, and MeCN gave the best result. In other solvents, the yield was either lower or no product formed in the end. Temperature was also important. The experiments carried out at room temperature worked better than those at elevated temperature which gave a complex mixture of target product along with some unknown species. The reaction finished in one hour, and extended time failed to increase the yield of [(COD)Pt(C$_3$F$_6$I)Me].The optimized condition was shown in Scheme 3j:
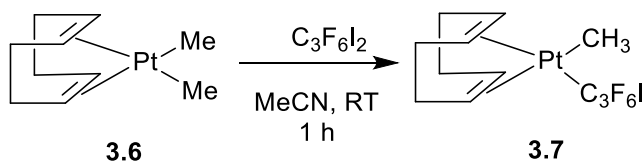
Scheme 3j. Synthesis of [(COD)Pt(C$_3$F$_6$I)Me].

Thanks to the air and moisture-stability of complex **3.7**, the compound could be purified by column chromatography with a 43% isolated yield. It was then characterized by X-ray diffraction and ^{1}H, ^{19}F NMR spectroscopies. An ORTEP diagram of **3.7** is provided in Figure 3b. This mixed methyl/perfluoroalkyl complex provided a direct comparison of bond length between the Pt-C$_{fluoroalkyl}$ (2.060 Å) and Pt-C$_{methyl}$ (2.162 Å). Shorter distances for M-C$_{fluoroalkyl}$ are commonly observed for the late metal perfluoroalkyl complexes and π-back-bonding has been proposed to explain the shortening of the predominantly covalent M−C$_{fluoroalkyl}$ relative to M−C$_{alkyl}$.[18]
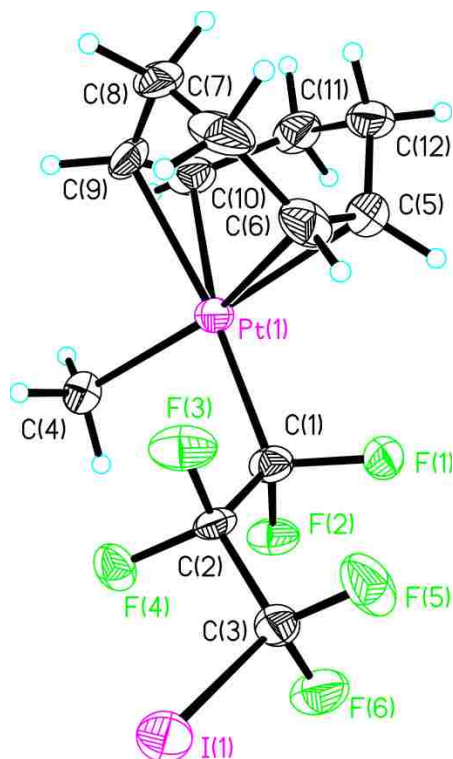
Figure 3b. ORTEP diagram of **3.7**. Selected bond lengths (Å): Pt1-C1 2.060(11); Pt1-C4 2.162(11); Pt1-C10 2.232(12); Pt1-C9 2.240(11); Pt1-C6 2.243(12); Pt1-C5 2.307(13). Selected bond angles (°): C1-Pt1-C4 89.3(5); C1-Pt1-C10 160.6(5); C4-Pt1-C10 91.9(5); C1-Pt1-C9 163.5(5); C4-Pt1-C9 90.1(5); C1-Pt1-C6 92.1(5); C4-Pt1-C6 154.6(5); C9-Pt1-C6 81.6(6); C1-Pt1-C5 97.2(5); C4-Pt1-C5 168.3(5); C9-Pt1-C5 86.4(5); C6-Pt1-C5 35.4(5).

With the isolated $[(COD)Pt(C_3F_6I)Me]$ in hand, we attempted to cyclize it to form the desired platinum perfluorometallacyclobutane complex. Unlike the first substitution of the methyl ligand, the second methyl ligand substitution needed to be performed at higher temperatures. We first heated complex in MeCN (same solvent in which we synthesized complex) at 90 °C but no cyclized product was generated. Heating a dichloromethane solution of **3.7** at 90 °C for 36 hours led to the formation of the targeted **3.8** in 50 % isolated yield. A faster rate could be achieved if the reaction was performed in pyridine with a 49 % isolated yield of **3.9** after only 16 hours (Scheme 3k). Other solvents like DMF, THF, benzene, toluene did not work for this conversion. It also turned out that the isolation of

48

[(COD)Pt(C$_3$F$_6$I)Me] was necessary for the this step as the excess mount of C$_3$F$_6$I$_2$ would interfere with [(COD)Pt(C$_3$F$_6$I)Me] to give some unknown complex according to ^{19}F NMR spectroscopy.

Cyclization to the symmetric targeted metallacycles was evident in the ^{19}F NMR spectra, and the two distinct fluorine resonances of **3.8** and **3.9** exhibited couplings to the ^{195}Pt nuclei. For **3.8**, the resonance for the proximal CF$_2$ groups appeared at δ = -111.5 and displayed a $^2J_{\text{F–Pt}}$ coupling of 525.2 Hz. The distal CF$_2$ group had a resonance at δ = -120.0 with a smaller $^3J_{\text{F–Pt}}$ of 180.6 Hz. The resonances for **3.9** appeared at similar chemical shift values (δ = -111.0 and -126.4) with similar $^2J_{\text{F–Pt}}$ and $^3J_{\text{F–Pt}}$ couplings (525.2 and 176.8 Hz, respectively). Both of the new perfluorometallacyclobutane complexes **3.8** and **3.9** were structurally characterized, and select structural data are provided in Figures 3c and 3d.
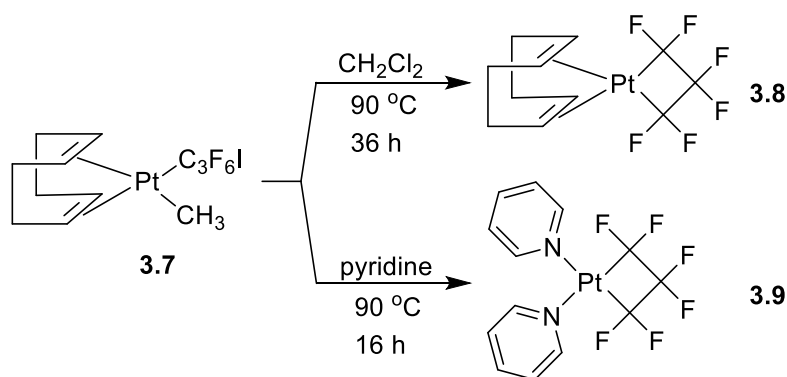
Scheme 3k. Formation of perfluorometallacyclobutanes in CH$_2$Cl$_2$ and pyridine at elevated temperature.
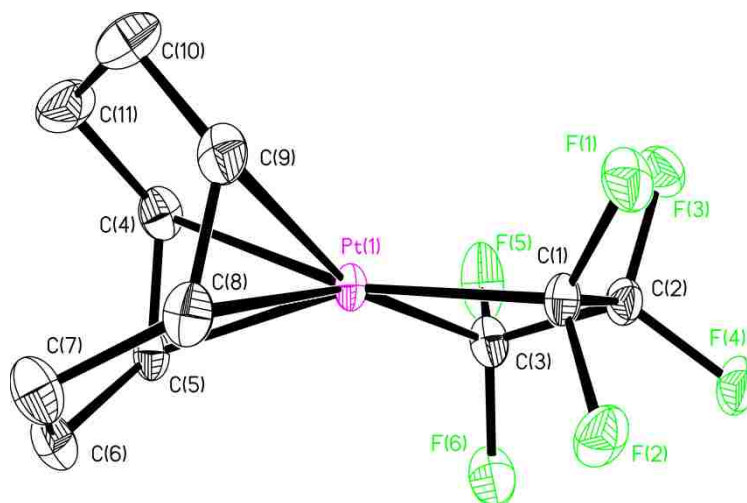
Figure 3c. ORTEP diagram of **3.8**. Hydrogens are removed for clarity. Selected bond lengths (Å): Pt1-C1 2.028(4); Pt1-C3 2.045(4); Pt1-C9 2.251(4); Pt1-C8 2.271(4); Pt1-C5 2.273(4); Pt1-C4 2.285(4). Selected bond angles (°): C1-Pt1-C3 68.93(16); C1-Pt1-C9 100.52(16); C3-Pt1-C9 162.62(16); C1-Pt1-C8 103.22(15); C3-Pt1-C8 157.84(17); C1-Pt1-C5 159.69(16); C3-Pt1-C5 99.94(15); C1-Pt1-C4 162.37(16); C3-Pt1-C4 105.74(16).
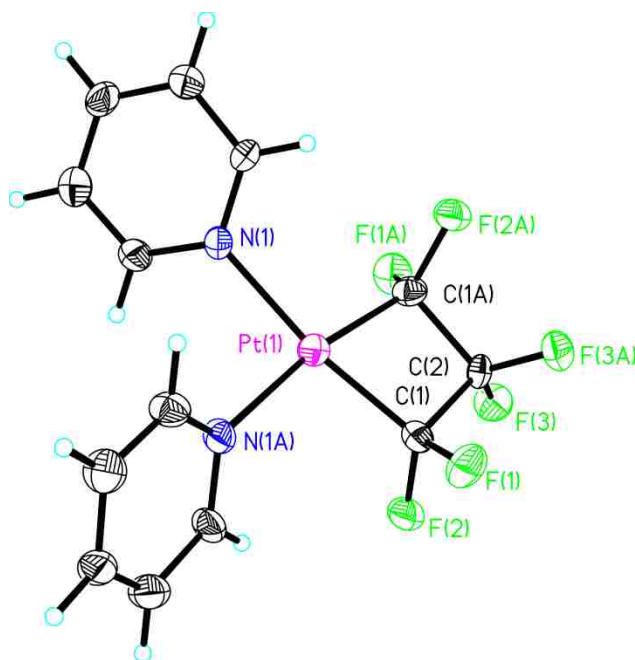
Figure 3d. ORTEP diagram of **3.9**. Selected bond lengths (Å): Pt1-C1 1.987(15); Pt1-N1 2.108(12). Selected bond angles (°): C1-Pt1-C1A 72.6(8); C1-Pt1-N1A 98.0(5); C1-Pt1-N1 170.6(5); N1-Pt1-N1A 91.3(7).

The purification of complexes **3.8** and **3.9** were different. Complex **3.9** was air and moisture-stable, and it could be purified by column chromatography. Complex **3.8** was bench-stable, but it was converted to another compound during column chromatography. This was shown by the ^{19}F NMR spectroscopy when we characterized all the separated compounds. Complex **3.8** was not present (no peak at δ = -111.5 and δ = -120.0 with 2:1 ratio). A new species with two peaks at δ -102.25 (s, $J(^{19}F–^{195}Pt)$ =401.7 Hz, 2F) and δ - 119.59 (s, 2F) showed up, and following recrystallization gave us the opportunity to characterize the new compound structurally. Complex **3.8** underwent a complicated reaction to afford the new fluorinated carboxylate complex **3.10** (Scheme 3l). Complex **3.10** has been structurally characterized and the ORTEP diagram is shown in Figure 3e.
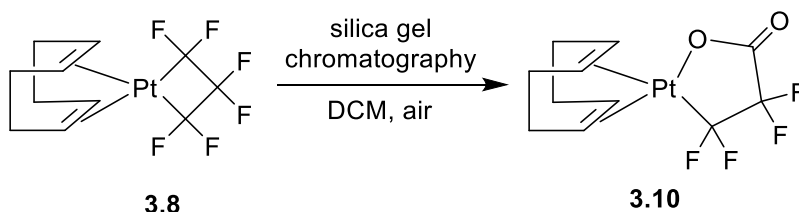
Scheme 3l. Unexpected conversion to form the new fluorinated carboxylate complex.

We found only one other report in the literature that documents the preparation of such fluoroalkyl carboxylate metallacycles. That procedure involved reacting low valent metal centers with cyclic fluorinated anhydrides to afford products similar to **3.10** via a decarbonylation reaction.[19] This work identifies a new synthetic route to such metallacyclic functionalities. Difluoromethylene groups of perfluoroalkyl metallacycles located alpha to a d^8 metal center are known to be reactive towards fluorine substitution reactions.[20] Here, it is noteworthy that clean substitution of both fluorines has occurred near the metal center,

and that the ancillary ligands (COD vs. pyridine) can tune such reactivity. Further mechanistic investigations of the unusual transformation described in Scheme 3l are ongoing in our lab.
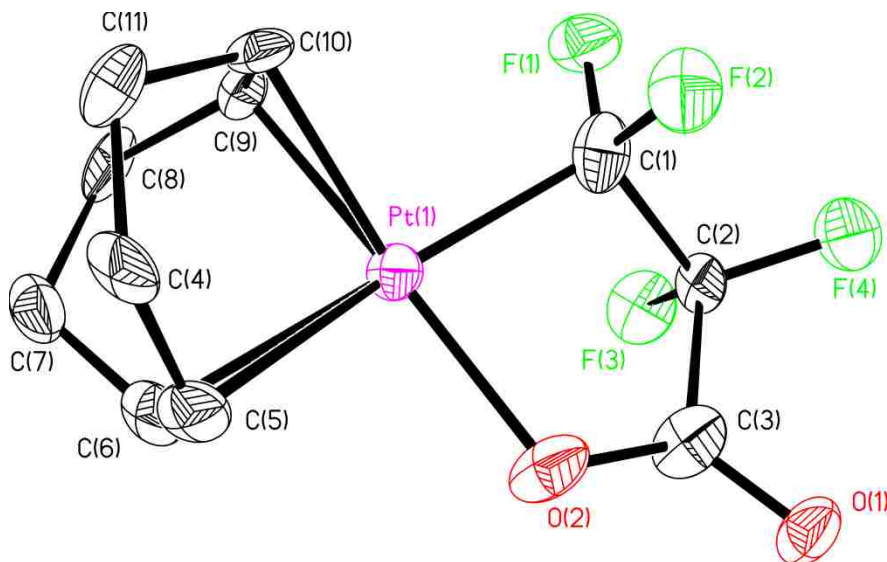
Figure 3e. ORTEP diagram of **3.10**. Hydrogens are removed for clarity. Selected bond lengths (Å): Pt1-O2 2.050(12); Pt1-C1 2.07(2); Pt1-C9 2.141(15); Pt1-C10 2.156(15); Pt1-C5 2.274(16); Pt1-C6 2.301(17); O1-C3 1.23(2); O2-C3 1.27(2). Selected bond angles (°): O2-Pt1-C1 83.2(7); O2-Pt1-C9 164.3(6); O1-C3-O2 127.4(17); C1-Pt1-C10 95.2(7).

For the formation of complex **3.10**, It is possible that the fluorine abstraction was aided by the silicon due to the formation of the strong Si-F bond. An isotope experiment would be necessary to figure out the source of oxygen which might come from H_2O or O_2.

It is known that pyridine is a labile ligand which will be replace by other bidentate ligands very smoothly. We choose complex **3.9** as the precursor to synthesize a series of platinum perfluorometallacyclobutane complex as it could be repeatedly purified by column chromatography. Bipyridine was first installed by the reaction with complex **3.9** in THF at room temperature for 15 minutes to yield complex **3.11**, confirmed by ^{1}H and ^{19}F NMR

spectroscopy. A clean substitution was achieved, and the product was purified by simple filtration with a 91% isolated yield. The addition of dtbpy to complex **3.9** was also performed in THF at room temperature. ^{19}F NMR spectroscopy of the reaction mixture showed a full ligand substitution to form comlex **3.12** after 30 minutes. The enhanced solubility of **3.12** caused more product loss during purification which lowered the isolated yield to 51%. Both complexes **3.11** and **3.12** were structurally characterized, and an ORTEP diagram of complex **3.12** is shown in Figure 3f. As shown in Scheme 3m, ligand substitution afforded a family of platinum perfluorometallacyclobutanes that could be synthesized and systematically characterized. This methodology provides a convenient strategy to generate the perfluorometallacyclobutanes without handling tetrafluoroethylene gas or decarboxylation at high temperature.
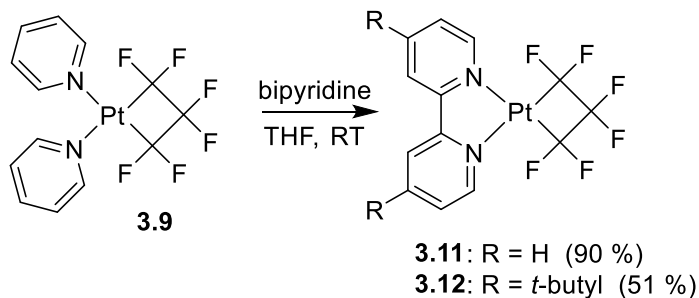
**Scheme 3m.** Ligand substitution to generate more platinum perfluorometallacyclobutanes.
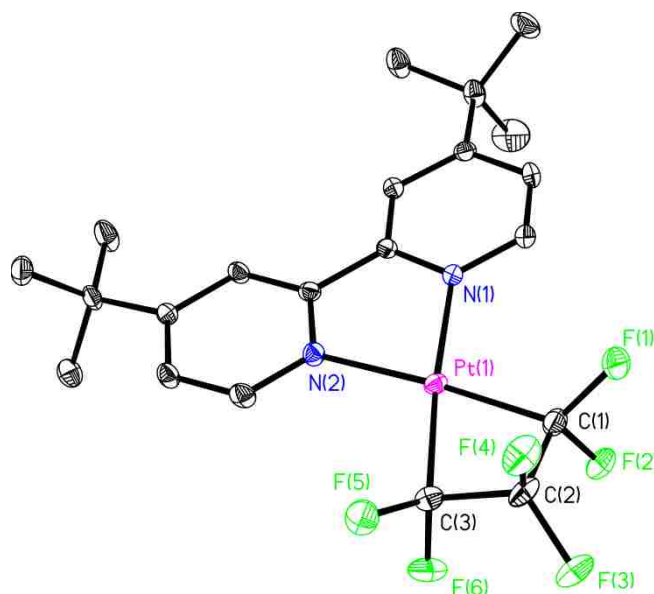
Figure 3f. ORTEP diagram of **3.12**. Hydrogens are removed for clarity. Selected bond lengths (Å): Pt1-C1 1.999(2); Pt1-C3 2.006(3); Pt1-N1 2.077(2); Pt1-N2 2.081(2). Selected bond angles (°): C1-Pt1-C3 69.37(11); C1-Pt1-N1 106.00(10); C3-Pt1-N1 174.99(9); C1-Pt1-N2 175.94(9); C3-Pt1-N2 106.63(10); N1-Pt1-N2 77.97(8); C1-Pt1-C2 35.74(10); C3-Pt1-C2 35.91(10); N1-Pt1-C2 140.11(9); N2-Pt1-C2 140.59(9).

Platinum has one medium sensitivity NMR spin-½ nucleus (^{195}Pt) that yields narrow signals over a very wide chemical shift range with 13000 ppm span, and a change of 100 ppm or more can be observed when varying ligand substituents. ^{195}Platinum NMR spectroscopy is mostly used for studying the structure, conformation, and dynamics of platinum complexes, and investigating platinum binding in biological systems. Because platinum is widely used as a catalyst in industry and medicine, its chemistry and NMR features have been widely studied. There are several difficulties in referencing platinum transition metal complexes. Some key features of platinum NMR referencing have been noted: (a) the relatively large temperature dependence of the chemical shift (several tenths of a ppm per degree is usual), (b) interactions with solvent and/or substance added as internal reference, (c) uncertainties due to isomers.[21] δ^{195}Pt are normally expressed relative to a standard sample, $K_2[PtCl_6]$ or $K_2[PtCl_4]$ in D_2O.

With the series of platinum perfluorometallacyclobutanes in hand, we explored the changes in magnetic environment of the platinum center upon fluoroalkylation and metallacycle formation by ^{195}Pt NMR spectroscopy (Figure 3h). We used [(COD)Pt(Me)$_2$] as the external standard with $\delta = -3593$. It was observed that the chemical shift of the platinum center appeared much more upfield in **3.7** versus the dimethyl complex **3.6** ($\delta = -3815$ vs -3593, respectively). This indicates an increased shielding of ^{195}Pt for complex **3.7** as calculated charge of M-R$_f$ show more negative charge on metal than M-R. The same trend was observed when replacing both methyl ligands and forming the metallacyclic **3.8** which led to an even further upfield shift ($\delta = -3856$ vs -3815). Comparing the dtbpy ligated metallacycle **3.12** with COD analogue **3.8**, its Pt resonance was more downfield ($\delta = -3750$ vs -3856), showing that dtbpy ligand was more deshielding than COD ligand (Figure 3h).
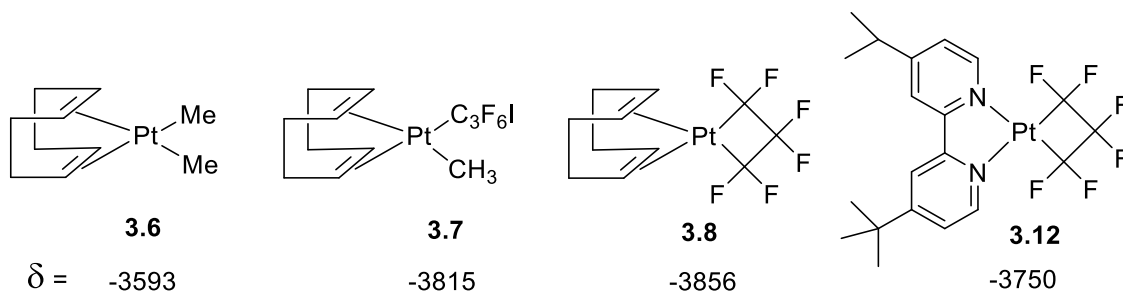
Figure 3h. δ^{195}Pt for different platinum complexes in CD$_2$Cl$_2$

We also attempted to react our platinum perfluorometallacyclobutanes with 4-fluorostyrene to study the possibility that it could mediated a perfluoroalkene metatheses reaction. The reaction between platinum perfluorometallacyclobutane and fluorine-labeled 4-fluorostyrene might occur by the mechanism shown in Scheme 3n. We carried out this reaction in a sealed NMR tube and that was placed into oil bath for heating. Various combinations of temperature and solvents have been tried, but no promising results have

been gained so far. The platinum perfluorometallacyclobutanes are more stable than we expected.
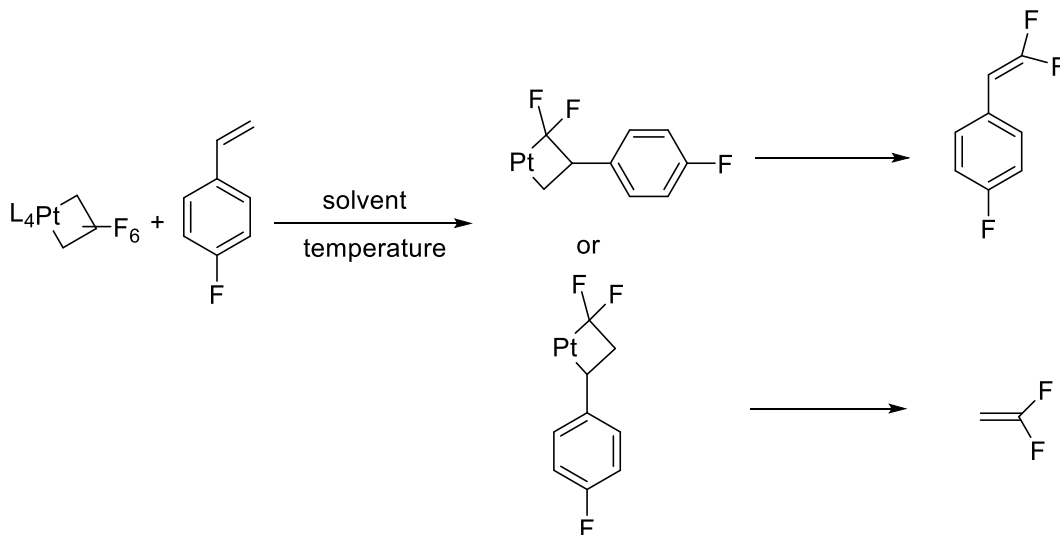
Scheme 3n. Possible pathway for perfluoroalkene metatheses involving platinum metallacyclobutane.

3.3. Summary

In this study, we successfully synthesized a family of platinum perfluorometallacyclobutanes via halogen metathesis of [(COD)Pt(Me)$_2$] and [C$_3$F$_6$I$_2$] followed by ligand substitution. All these organometallic complexes were systematically characterized by single crystal X-ray diffraction, ^{1}H and ^{19}F NMR spectroscopies. This methodology has more than doubled the number of known perfluorometallacyclobutanes in the literature. Though our attempts to investigate the perfluoroalkene metatheses reaction was not successful, this work should be useful towards the preparation of other transition-metal perlfuorometallacyclobutanes. This new methodology to prepare perfluorometallacyclobutanes also avoids the use of tetrafluoroethylene, which is

becoming increasingly difficult to purchase due to the explosion hazards associated with its use. We have also taken a snapshot of a unique transformation whereby one $[Pt(C_3F_6)]$ functionality is converted to $[Pt(C_3F_4O_2)]$. Mechanism of this conversion is being further studied in our lab.

3.4. Experimental Procedures.

General Considerations: All manipulations were performed using standard Schlenk and high vacuum techniques or in a nitrogen filled glovebox. Solvents were purified by passing through activated alumina and/or copper in a solvent purification system supplied by Pure Process Technology. 1,3-diiodohexafluoropropane was prepared according to a previously published procedure.[93] Solution ^1H NMR spectra were recorded at ambient temperature on a Bruker DRX 500 MHz spectrometer and referenced to residual proton solvent signals. ^{19}F spectra were recorded on the Bruker NMR spectrometer operating at 470 MHz and referenced to α,α,α-trifluorotoluene as an internal standard (δ = -63.7). ^{195}Pt spectra were recorded on a Bruker NMR spectrometer operating at 108 MHz and referenced to $[(COD)PtMe_2]$ as an external standard (δ = –3593). Coupling constants (J) are reported in Hz and coupling patterns are described as br = broad, s = singlet, d = doublet, t = triplet, q = quartet, m = multiplet. A Bruker D8 Quest diffractometer was used for X-ray crystal structure determinations.

Preparation of [(COD)Pt(C₃F₆I)(CH₃)] (3.7): $[(COD)Pt(CH_3)_2]$ (792 mg, 2.38 mmol) was suspended in 6 mL of acetonitrile. A solution of 1,3-diiodohexafluoropropane $[C_3F_6I_2]$ (959 mg, 2.38 mmol) in 4 mL of acetonitrile was then added drop wise to the suspension,

almost immediately forming a clear yellow solution. The solution was left to stir at room temperature for one hour. Excess MeCN and [$C_3F_6I_2$] were removed via high-vacuum line. The dried solid was redissolved in a solution of 2 mL diethyl ether and 2 mL hexanes and was purified via column chromatography (1/1 Et_2O/hexanes) to afford [(COD)Pt(C_3F_6I)(CH$_3$)] (647 mg, 43%). Crystals suitable for X-ray diffraction were grown from a slow evaporation of ether. ^{1}H NMR (CDCl$_3$, 500 MHz): δ 5.40-5.35 (m, 2H), 5.16-5.10 (m, 2H), 2.52-2.37 (m, 8H), 0.88 (s, $^2J(^1H–^{195}Pt)$ =78.8 Hz, 3H). ^{19}F NMR (CDCl$_3$, 470 MHz): δ -55.64 (s, 2F), -93.55 (s, $^2J(^{19}F–^{195}Pt)$ =401.4 Hz), -107.35 (s, 2F). ^{195}Pt (CD$_2$Cl$_2$, 107 MHz): δ -3815 (t, ^2J ($^{195}Pt–^{19}F$) =380.9 Hz). Anal. Calcd (found) for $C_{12}H_{15}F_6IPt$: C, 24.21 (24.58) ; H, 2.54 (2.65). Crystal Data for $C_{11}H_{12}F_6Pt$ (M =453.30 g/mol): monoclinic, space group P21/c (no. 14), a = 6.7555(7) Å, b = 16.2492(16) Å, c = 10.9159(11) Å, β = 102.770(2)°, V = 1168.6(2) Å3, Z = 4, T = 140(2) K, μ(MoKα) = 12.063 mm-1, Dcalc = 2.576 g/cm3, 20803 reflections measured (6.308° ≤ 2Θ ≤ 61.094°), 3316 unique (Rint = 0.0376, Rsigma = 0.0219) which were used in all calculations. The final R1 was 0.0260 (I > 2σ(I)) and wR2 was 0.0550 (all data).

Preparation of [(COD)Pt(C_3F_6)] (3.8): [(COD)Pt(C_3F_6I)(CH$_3$)] (125 mg, 0.20 mmol) was dissolved in 2 mL of methylene chloride. The solution was transferred to a resealable high-pressure vial and stirred for 36 hours at 90 °C. A slight color change from light yellow to yellow was seen after ~1 day. The solution was then dried using a high-vacuum line. The solution was recrystallized in Et_2O/pentane to yield clear crystals that were washed with *n*-pentane to yield [(COD)Pt(C_3F_6)] (48 mg, 50%). ^{1}H NMR (THF-d_8, 500 MHz): δ 5.78 (br s, $^2J(^1H–^{195}Pt)$ = 21.5 Hz, 4H), 2.61 (d, J=9.1 Hz, 4H), 2.48-2.40 (m, 4H).^{19}F NMR (THF-d_8, 470 MHz): δ -111.5 (s, ^2J ($^{19}F–^{195}Pt$) =525.2 Hz, 4F), -125.0 (s, $^3J(^{19}F–^{195}Pt)$ =180.6 Hz,

2F). Anal. Calcd (found) for $C_{11}H_{12}F_6Pt$: C, 29.15 (29.36); H, 2.67 (2.74). Crystal Data for

$C_{11}H_{12}F_6Pt$ ($M =453.30$ g/mol): monoclinic, space group P2$_1$/c (no. 14), $a =$
6.7555(7) Å, $b =$ 16.2492(16) Å, $c =$ 10.9159(11) Å, $\beta =$ 102.770(2)°, $V =$
1168.6(2) Å^3, $Z = 4$, $T = 140(2)$ K, μ(MoKα) = 12.063 mm^{-1}, $Dcalc = 2.576$ g/cm^3, 20803
reflections measured (6.308° $\leq 2\Theta \leq$ 61.094°), 3316 unique ($R_{int} = 0.0376$, R$_{sigma} = 0.0219$)
which were used in all calculations. The final R_1 was 0.0260 (I > 2σ(I)) and wR_2 was
0.0550 (all data).

Preparation of [(pyr)₂Pt(C₃F₆)] (3.9): [(COD)Pt(C₃F₆I)(CH₃)] (294 mg, 0.47 mmol) was
dissolved in 8 mL of pyridine. The clear solution was transferred to a resealable high-
pressure vial, then heated to 90 °C for 16 h. The solution was dried using a high vacuum
line, and redissolved in 5 mL of methylene chloride. The product was purified via column
chromatography (methylene chloride) to produce [(pyr)₂Pt(C₃F₆)] (115 mg, 49%). ^{1}H
NMR (CDCl₃, 500 MHz): δ 8.54 (d, J=6.6 Hz 4H), 7.89 (t, J=7.7Hz, 2H), 7.44 (t, J=7.1Hz,
4H).^{19}F NMR (CDCl₃, 470 MHz): δ -111.0 (s, $^2J(^{19}F–^{195}Pt)$ =525.2 Hz, 4F), -126.4 (s, ^3J
$(^{195}Pt–^{19}F)$=176.8 Hz, 2F). Anal. Calcd (found) for $C_{13}H_{10}F_6N_2Pt$: C, 31.02 (31.56) ; H,
2.00 (2.58). Crystal Data for $C_{13}H_{10}F_6N_2Pt$ ($M =503.32$ g/mol): monoclinic, space group
C2/c (no. 15), $a =$ 17.6565(19) Å, $b =$ 8.8261(9) Å, $c =$ 10.6223(11) Å, $\beta =$
121.743(2)°, $V =$ 1407.7(3) Å^3, $Z = 4$, $T = 140(2)$ K, μ(MoKα) = 10.031 mm^{-1}, $Dcalc =$
2.375 g/cm^3, 8367 reflections measured (7.704° $\leq 2\Theta \leq$ 54.776°), 1559 unique ($R_{int} =$
0.0484, R$_{sigma} = 0.0345$) which were used in all calculations. The final R_1 was 0.0773 (I >
2σ(I)) and wR_2 was 0.1691 (all data).

Preparation of [(COD)Pt(O₂C₃F₄)] (3.10): [(COD)Pt(C3F6)] (23 mg, 0.051 mmol) was
suspended in 2 mL of diethyl ether. The solution was filtered, and the solute was transferred

to a glass vial. The vial was taken out of the nitrogen-filled glovebox, and the cap was removed from the vial. The solution was left to undergo a slow evaporation of solvent. After all diethyl ether was removed, the remaining clear crystals were washed with 1 mL of hexanes and dried on a high-vacuum line to afford $[(COD)Pt(O_2C_3F_4)]$ (13 mg, 53%). ^1H NMR (CDCl$_3$, 500 MHz): δ 5.87−5.83 (m, 2H), 5.03−5.00 (m, 2H), 2.70−2.35 (m, 8H). ^{19}F NMR (CDCl$_3$, 470 MHz): δ −102.3 (s, ^2J(19F−195Pt) = 402 Hz 2F), −120 (s, 2F). Anal. Calcd (found) for $C_{11}H_{12}F_4O_2Pt$: C, 29.54 (30.27); H, 2.70 (2.92). Crystal Data for $C_{11}H_{12}F_4O_2Pt$ (M =447.30 g/mol): triclinic, space group P-1 (no. 2), $a = 6.3410(14)$ Å, $b = 8.327(2)$ Å, $c = 11.491(3)$ Å, $\alpha = 102.145(6)°$, $\beta = 93.505(5)°$, $\gamma = 100.070(5)°$, $V = 581.0(2)$ Å^3, $Z = 2$, $T = 142(2)$ K, μ(MoKα) = 12.119 mm^{-1}, $Dcalc$ = 2.557 g/cm^3, 1772 reflections measured ($6.56° \leq 2\Theta \leq 47.566°$), 1772 unique ($R_{int}$ = N/A, R_{sigma} = 0.0454) which were used in all calculations. The final R_1 was 0.0488 (I > 2σ(I)) and wR_2 was 0.1280 (all data).

Preparation of [(bpy)Pt(C$_3$F$_6$)] (3.11): $[(pyr)_2Pt(C_3F_6)]$ (50 mg; 0.1 mmol) and 2,2'-bipyridine (30 mg; 0.2 mmol) were dissolved in 2 ml THF and the mixture was stirred at room temperature for 15 h. After this, the cloudy mixture was filtrated. The yellow solid was washed with Et$_2$O (10 ml) three times and then was collect to give 45 mg title compound (90% yield). ^1H NMR (500 MHz, DMSO-d_6) δ 8.80 (d, J=4.9 Hz, 2H), 8.66 (d, J=7.6 Hz, 2H), 8.39 (t, J=8.5 Hz, 2H), 7.87 (t, J=6.7 Hz 2H). ^{19}F NMR (CDCl$_3$, 470 MHz): δ -110.33 (s, ^2J(^{19}F–^{195}Pt) =561.6 Hz, 4F), -127.09 (s, ^3J(^{195}Pt–^{19}F)=149.2 Hz, 2F). Anal. Calcd (found) for $C_{13}H_8F_6N_2Pt$: C, 31.22 (31.15) ; H, 1.81 (1.61).

Preparation of [(tbpy)Pt(C$_3$F$_6$)] (3.12): $[(pyr)_2Pt(C_3F_6)]$ (70 mg, 0.14 mmol) was dissolved in 1 mL of THF. A solution of 4,4'-Di-tert-butyl-2,2'-dipyridyl (74.8 mg, 0.28

mmol) in 1 mL THF was added drop wise to the platinum solution. The mixture was left to stir overnight. Solvent was then removed via high-vacuum line. Five milliliters of diethyl ether were added to the dried solid, and the solution was filtered using a filter frit. The solid was dried using high vacuum line to yield a yellow solid, $[(tbpy)Pt(C_3F_6)]$ (44 mg, 51%). X-ray quality crystals were grown from a slow evaporation of CH_2Cl_2. ^{1}H NMR (CD_2Cl_2, 500 MHz): δ 8.93 (d, J=5.7 Hz, 2H), 7.95 (s, 2H), 7.58 (d, J=5.7 Hz, 2H), 1.44 (s, 18H).^{19}F NMR (CD_2Cl_2, 470 MHz): δ -110.04 (s, $^2J(^{19}F-^{195}Pt)$ =555.0 Hz, 4F), -127.27 (s, 2F). ^{195}Pt (CD_2Cl_2, 108 MHz): δ -3750 (quint, $^2J(^{195}Pt-^{19}F)$ =560.8 Hz). Anal. Calcd (found) for $C_{21}H_{24}F_6N_2Pt$: C, 41.11 (29.63); H 3.94 (2.81). Crystal Data for $C_{21}H_{24}F_6N_2Pt$ (M =613.51 g/mol): monoclinic, space group P2$_1$/c (no. 14), a = 9.8403(11) Å, b = 16.1420(18) Å, c = 13.3723(15) Å, β = 96.328(2)°, V = 2111.1(4) Å^3, Z = 4, T = 140(2) K, μ(MoKα) = 6.708 mm^{-1}, $Dcalc$ = 1.930 g/cm^3, 37182 reflections measured (5.906° $\leq$ 2Θ $\leq$ 61.238°), 5945 unique (R_{int} = 0.0220, R$_{sigma}$= 0.0127) which were used in all calculations. The final R_1 was 0.0206 (I > 2σ(I)) and wR_2 was 0.0500 (all data).

3.5. Reference

1. Grela, K; Harutyunyan, S; Michrowska, A. *Angew. Chem. Int. Ed.*, **2002**, *114*, 4038.
2. Katz, T. J.; McGinnis, J. *J. Am. Chem. Soc.* **1975**, 97, 1592.
3. Grubbs, R. H.; Burk, P. L.; Carr, D. D. *J. Am. Chem. Soc.* **1975**, *97*, 3265.
4. Katz, T. J.; Rothchild, R. *J. Am. Chem. Soc.* **1976**, *98*, 2519.
5. Grubbs, R. H.; Carr, D. D.; Hoppin, C.; Burk, P. L. *J. Am. Chem. Soc.* **1976**, *98*, 3478.
6. Katz, T. J.; McGinnis, J. *J. Am. Chem. Soc.* **1977**, *99*, 1903.
7. Grubbs, R. H. Handbook of Metathesis; Wiley-VCH: Weinheim, Germany, 2003
8. Herisson, J.-L.; Chauvin, Y. *Makromol. Chem. 1971*, **141**, 161.
9. Trnka, T. M.; Day, M. W.; Grubbs, R. H. *Angew. Chem., Int. Ed.* **2001**, *40*, 3441.
10. Takahira, Y; Morizawa, Y. *J. Am. Chem. Soc.*, **2015**, *137*, 7031.
11. Karel, K. J.; Tulip, T. H.; Ittel, S. D. *Organometallics* **1990**, *9*, 1276.
12. Harrison, D. J.; Lee, G. M.; Leclerc, M. C.; Korobkov, I.; Baker, R. T. *J. Am. Chem. Soc.* **2013**, *135*, 18296.
13. Harrison, D. J.; Daniels, A. L.; Korobkov, I; Baker, R. T. *Organometallics*, **2015**, *34*, 5683.
14. Kaplan, P. T.; Xu, L.; Chen, B.; McGarry, K. R.; Yu, S.; Wang, H.; Vicic, D. A.; *Organometallics* **2013**, *32*, 7552.
15. Turrell, P. J.; Wright, J. A.; Peck, J. N. T.; Oganesyan, V. S.; Pickett, C. J.; *Angew. Chem. Int. Ed.* **2010**, *49*, 7508.
16. Adams, C. J.; Bedford, R. B.; Carter, E.; Gower, N. J.; Haddow, M. F.; Harvey, J. N.; Huwe, M.; Cartes, M. A.; Mansell, S. M.; Mendoza, C.; Murphy, D. M.; Neeve, E. C.; Nunn, J. *J. Am. Chem. Soc.* **2012**, *134*, 10333.
17. Clark, H. C.; Manzer, L. E. *J. Organometal. Chem.* **1973**, *59*, 411.
18. Taw, F. L.; Clark, A. E.; Mueller, A. H.; Janicke, M. T.; Cantat, T.; Scott, B. L.; Hay, P. J.; Hughes, R. P.; Kiplinger, J. L. *Organometallics* **2012**, *31*, 1484.
19. Maleckis, A.; Sanford, M. S. *Organometallics* **2014**, *33*, 3831.
20. Giffin, K. A.; Harrison, D. J.; Korobkov, I.; Baker, R. T. *Organometallics* **2013**, *32*, 7424.
21. Still, B. M; Kumar, P. G.; Aldrich-Wright, J. R.; Price, W. S. *Chem. Soc. Rev.* **2007**, *36*, 665.

4. Chapter 4. New Perfluoroalkyl Iodide Reagents and Their Applications

4.1. Introduction

Perfluoroalkyl iodides are known to be very resistant to normal S_N2 or S_N1 nucleophilic attack because steric effects and lone-pair repulsive forces associated with the fluorine substituents shield the carbons from nucleophiles.[1] However, reactions of the perfluoroalkyl iodides with some kind of nucleophiles like enamine, thiolate, phenoxide, sulfinates, enolates, and nitronates result in displacement of iodide by the nucleophiles. Some of the reactions have been shown to proceed via anionic chain processes initiated by different types of halophilic attacks,[2] although different and competitive pathways, e.g., $S_{RN}1$ mechanism, have been found in some other cases[3] (Scheme 4a).
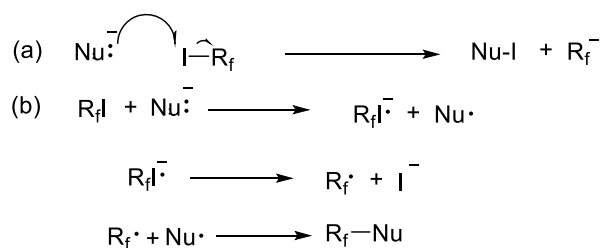
Scheme 4a. (a) Halophilic attack. (b) $S_{RN}1$ pathway

The ability of halogen atoms in certain molecules to interact with electron donors has been exploited in such fields as crystal engineering, anion recognition, and self-assembly processes.[4-13] Halogen-bonding interactions between perfluoroalkyl iodides and nucleophiles have also been universally observed.[14-16] Through halogen bonding (XB), which is the non-covalent interaction that occurs between a halogen atom (Lewis acid) and a Lewis base, donor-acceptor complexes can be formed between perfluoroalkyl iodides and

amines, given that fluorine atoms inductively boost the electron acceptor ability of the terminal iodine substituents. For instance, the N→I-R$_f$ intermolecular interaction is specific, directional, and strong enough to drive the self-assembly of diiodo-perfluoroalkanes and dinitrogen-hydrocarbons into 1-D infinite networks which are stable, solid, and crystalline at room temperature and in aerobic conditions (Figure 4a).[17]
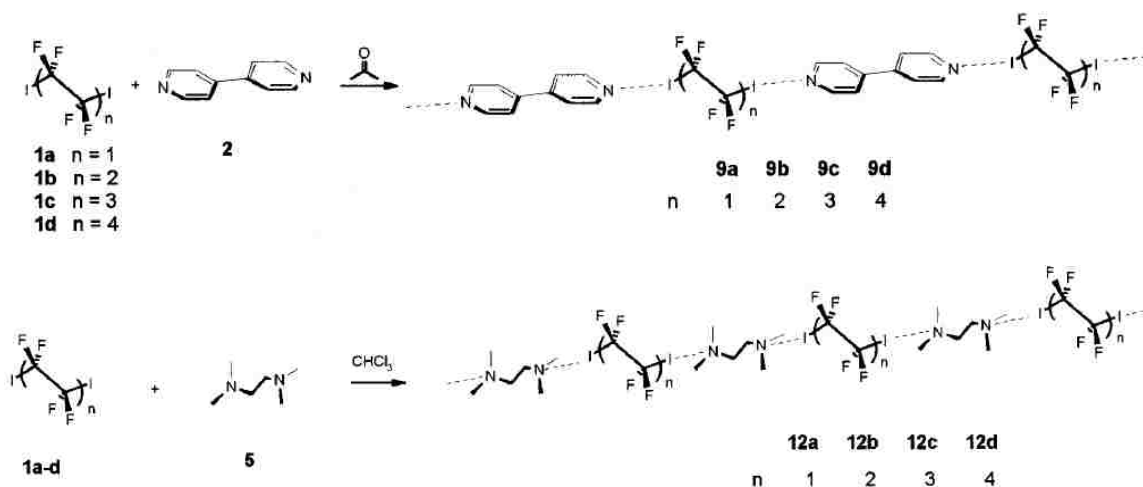
Figure 4a. 1-D infinite chain through halogen bonding between diiodo-perfluoroalkanes and dinitrogen-hydrocarbons

Oxygen is a weaker electron donor in this kind of interaction than nitrogen. Well-defined complexes of O→I-R$_f$ have been reported rarely. One example in CCDC database showed an endless 1-D chain of alternating α,ω-diiodoperfluoroalkane and 1,4-dioxane based on oxygen---iodine interactions (Figure 4b).[18] In this case, the distance between O and I is 2.814 Å which was considerably longer than the average covalent bond between O and I (2.14 Å), but shorter than the sum of the corresponding van der Waals radii of O (1.52 Å) and I (1.98 Å). These complexes were isolated as colorless crystals and it was found that the chemical shifts of α-CF$_2$ observed in ^{19}F resonances of α,ω-diiodoperfluoroalkanes in

1,4 dioxane solvents are apparently shifted upfield (up to 5.6 ppm) compared with that of pure α,ω-diiodoperfluoroalkanes.

3a-c
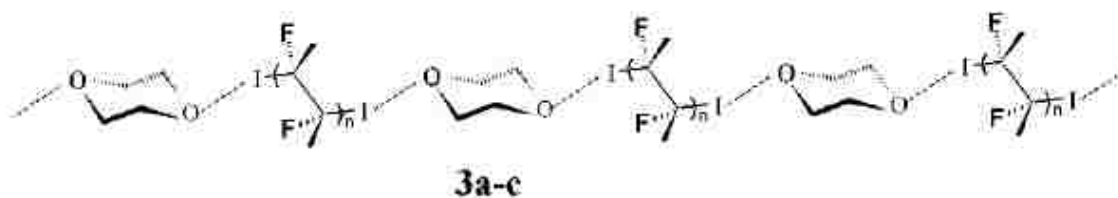
Figure 4b. 1-D infinite chain of α,ω-diiodoperfluoroalkane and 1,4-dioxane.

This example showed clearly the nature and the degree of the halogen bonding with neutral oxygen -donor molecules. However, there have been no examples of halogen bonding of perfluoroalkyl iodides with *anionic* oxygen donor molecules that have been structurally characterized.   An infrared and NMR study has detected a halogen bonding interaction between CF_3I and $[Me_4N][OCF_3]$, but that species was stable only at low temperatures.[19] Herein, we describe in detail the strong and stable halogen bond that forms between 1,4-diiodooctafluorobutane and potassium *tert*-butoxide.

4.2. Result and Discussion

4.2.1. Unique Discovery of a Novel Halogen-Bonded Adduct

It was discovered in our group that a novel 2-D polymeric structure could be synthesized by mixing 1,4-diiodooctafluorobutane and four equivalents of potassium *tert*-butoxide at room temperature. White solid precipitated from solution instantly upon the addition of 1,4 diiodofluorobutane to the 1,4-dioxane solution of potassium *tert*-butoxide. After filtration,

a fine white powder was collected and an ^{19}F NMR spectrum of this white powder in DMF showed two singlets at -88 and -114 ppm with 1:1 ratio, which indicated a symmetric structure. The white solid is air and moisture-sensitive and should be stored at inert atmosphere. The ^{19}F NMR chemical shifts for pure 1,4 diiodofluorobutane in DMF are -61 and -113 ppm, meaning that the chemical shift of α-CF$_2$ in this complex were significantly shifted upfield (27 ppm). We reasoned that such a huge change in ^{19}F NMR might indicate some unique properties of this unknown reagent and following attempt to grow crystals for the characterization by single crystal X-ray allowed us to take a snapshot of the complex **4.1** below (Figure 4c). The qualified crystal was grown in the mixture of DMF and trifluorotoluene while the attempts using other solvent combinations failed.
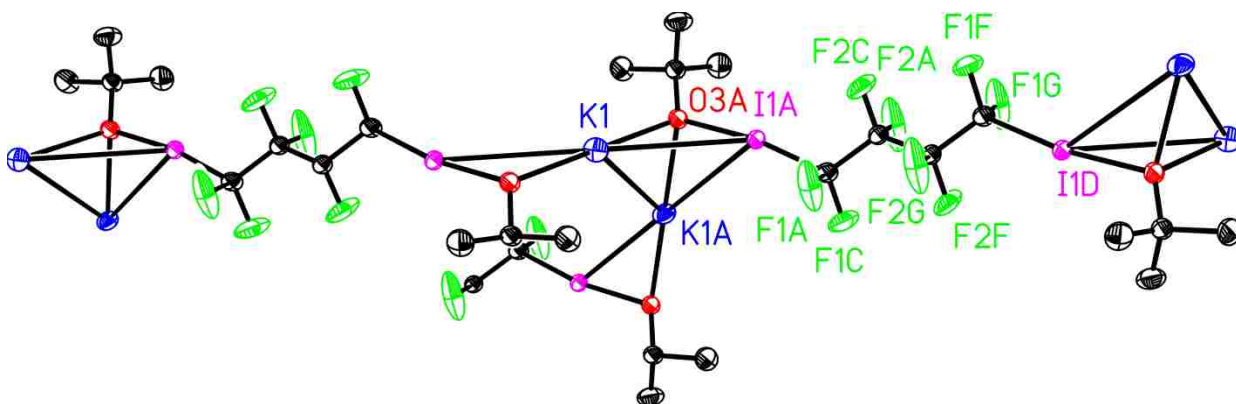
Figure 4c. ORTEP diagrams showing the unit cell of new halogen bonding complex **4.1**. The disordered potassium-bound DMF solvent molecules have been omitted for clarity. Selected bond lengths (Å): iodine-carbon 2.281(8); iodine-oxygen 2.391(6).
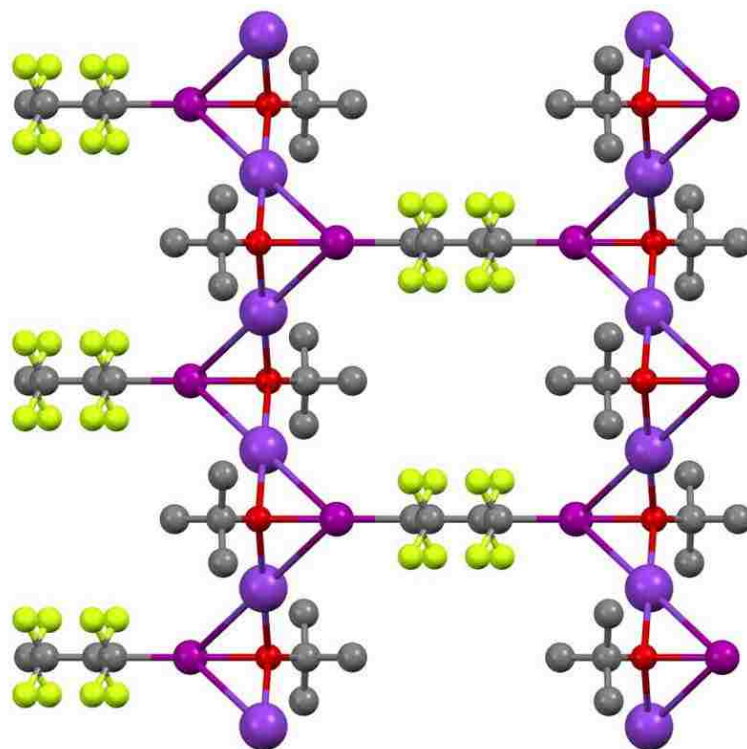
Figure 4d. Solid-state structure depicting the networked arrangement of **4.1**. Color scheme: O red, C grey, F yellow, I magenta, K purple.

First of all, complex **4.1** is structurally unique. To our surprise, the distance of O3A and I1A in Figure 4c was 2.340 Å, which was extremely short and only 66.8% of the sum of the van der Waals radii of O and I (3.5 Å). If this O→I interaction is regarded as halogen bonding, to our best of knowledge, it is the shortest O-I distance ever found, almost comparable to the bond length of covalent O-I bond in the hypervalent iodine compound of Togni's reagent (Scheme 4b).
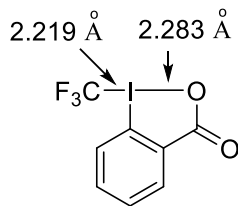
Scheme 4b. Selected bond length in Togni's reagent.

With regards to the supramolecular architecture that is observed, the X-ray analysis reveals that the use of anionic instead of neutral oxygen donors has introduced another dimensionality to the extended molecular network (Figure 4d). The network is not an infinite chain, as has previously been observed with neutral oxygen donors, but rather infinite sheets by virtue of the fact that the potassium counter-ions can chelate to multiple iodine atoms. This data raises the intriguing possibility that the use of other different counter-cations might lead to more complex architectures, including those possessing three-dimensionality.

Considering such a strong interaction between oxygen and iodine, we reasoned that this complex might be an intermediate during the halophilic attack reaction as shown in Scheme 4a, which ought to be very reactive. The bond length of C1A and I1A was elongated to 2.239 Å which was very close to the C-I bond length in the above Togni's reagent, whereas the average bond length of C-I bond of 1,4-diiodooctafluorobutane which was cocrystalized with different nitrogen and oxygen donors was 2.138 Å, calculated from the CCDC database. This indicated an obvious weakening of the C-I bond, further supported by the reaction between the reagent and acetonitrile which instantly generated $H(CF_2)_4H$ and led to a black mixture at room temperature. The formation of $H(CF_2)_4H$ was also observed in THF and Et_2O. However, in some solvents which didn't have active hydrogen atoms, like DMF and benzonitrile, ^{19}F NMR spectroscopy showed no signal for $H(CF_2)_4H$. So in terms of reactivity, this super reactive reagent was totally different from those polymeric compounds of α,ω-diiodoperfluoroalkane formed through normal halogen bonding.

We proceeded to synthesize a series of similar compounds from 1,3-diiodoperfluoropropane and 1,6-diiodoperfluorohexane. Similarly, white precipitates were generated after mixing 1,3-diiodoperfluoropropane and 1,6-diiodoperfluorohexane in the 1,4-dioxane solution of potassium *tert*-butoxide (complexes **4.1** and **4.2**). ^{19}F NMR analysis also revealed a significant upfield chemical shift of the α-CF_2 in DMF, indicating a similar polymeric framework as complex **4.1**. Dissolving complex **4.2** and **4.3** in MeCN led to the formation of gas and black mixture as well. Following ^{19}F NMR analysis confirmed that $H(CF_2)_nH$ (n=3, 6) was generated. This indicated that interaction between potassium *t*-butoxide and α,ω-diiodoperfluoroalkane were universal.

With these novel C_3, C_4 and C_6 iodine reagents in hand, it remains necessary to find a route to efficiently transfer $(CF_2)_n$ (n=3,4,6) moieties to other organic or inorganic groups. At this stage, it is still ambiguous that the carbon end in the iodine reagent behaves as a carbanion R_f^- or a carbon radical $R_f\cdot$ because both can abstract hydrogen atom from the solvent to generate $H(CF_2)_4H$. The attempts to react this new compound with electrophiles at room temperature, like $(DME)NiBr_2$, CuCl, TMSCl and $(t\text{-}BuNC)_4FeCl_2$ failed to give the product which has the $-(CF_2)_4-$ transferred to the metal complex, but led to the formation of the $C_4F_8I_2$. The reaction between the compound and $(CO)_5Fe$ at room temperature led to an evolution of large amount of bubbles and obvious color change. However, ^{19}F NMR spectroscopy showed that no fluorine signals were present anymore.

4.2.2. Iron(II)-catalyzed Perfluoroalkylation of Arenes through C-H Transformations Using α,ω-diiodoperfluoroalkanes.

Recent work by Xile Xu and coworkers showed an iron-catalyzed 1,2-addition of perfluoroalkyl iodides to alkynes and alkenes (Scheme 4c).[20] However, the role of iron(II) was ambiguous in this reaction, because it was found that the Cs_2CO_3 itself was able to catalyzed the reaction alone. The authors reasoned that the iron(II) was activating the alkenes and alkynes to broaden the scope of alkene and alkyne substrates which was relatively small if only Cs_2CO_3 was used.
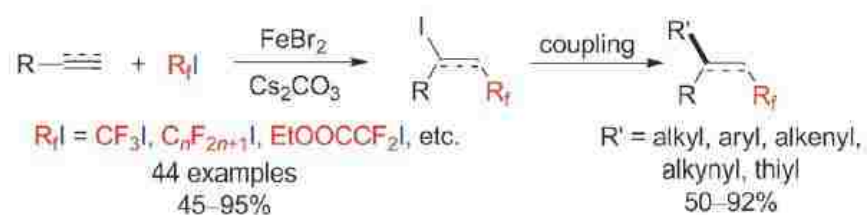
Scheme 4c. 1,2-addition of perfluoroalkyl iodides to alkynes and alkenes

The generation of perfluoroalkyl radical thermally was described in a synthesis of fluoroine-containing annulated corannulene. The 1,4-diiodoperfluorobutane and corannulene were heated at 300°C which led to a pale-yellow crude product (Scheme 4d). This derivative of corannulene was proved to have higher electron affinity than the fullerene electron-acceptor C_{60}.[21]
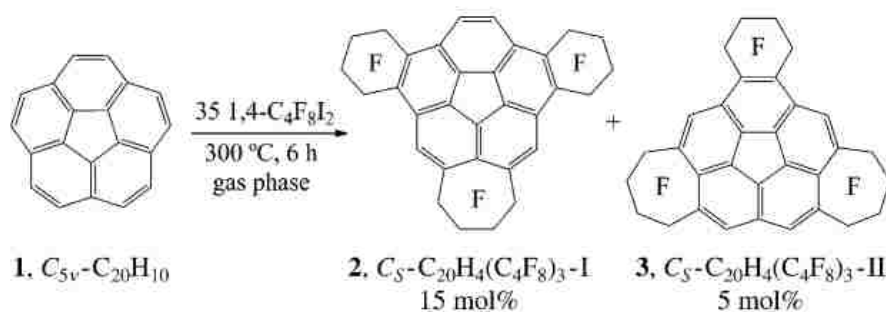
Scheme 4d. Perfluoroalkyl annulation of corannulenen.

Another example involving the thermolysis of α,ω-diiodoperfluoroalkane to generate perfluoroalkyl radicals was described by some USSR scientists who reacted α,ω-diiodoperfluoroalkane with benzene and naphthalene at 250 °C for 8 hours to obtain perfluoroalkylation products (Scheme 4e).[22]
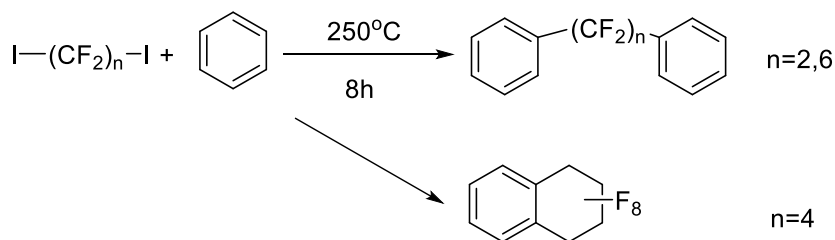
Scheme 4e. Thermal perfluoroalkylation of arenes.

Based on the above work, we proposed that if the halogen-bonded iodine reagent was a source of perfluoroalkyl radical, it would react with benzene to form the perfluoroalkylation products. Reaction of complex **4.1** with benzene at room temperature and 85 °C respectively gave the 1,4-diiodoperfluorobutane in both cases. This indicated that in solvent of benzene, **4.1** collapsed to generate the original 1,4-diiodoperfluorobutane

71

and potassium *tert*-butoxide. Inspired by Xu's work, we then explored the perfluoroalkylation of arenes with the presence of iron catalyst. Our initial iron(II)-catalyzed perfluoroalkylation of aromatics involved benzene as the aromatic substrate and solvent at the same time. For benzene as the solvent, potassium *t*-butoxide is an efficient base to neutralize the pH of the reaction mixture (Table 4a).
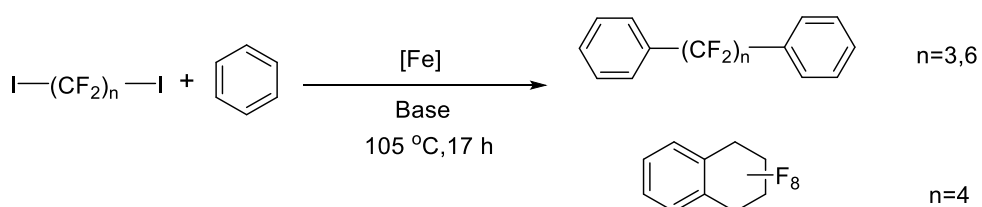
Entry	Catalyst[a]	Ligand[C]	Base	Temperature	Time	Substrate	Yield[b]
1	$FeCl_2$		*t*-BuOK	105 °C	17h	1,3-diiodoperfluoropropane	N.R.
2	$FeBr_2$		*t*-BuOK	105 °C	17h	1,3-diiodoperfluoropropane	N.R.
3	FeI_2		*t*-BuOK	105 °C	17h	1,3-diiodoperfluoropropane	N.R.
4	$FeCl_3$		*t*-BuOK	105 °C	17h	1,3-diiodoperfluoropropane	N.R.
5	$FeBr_3$		*t*-BuOK	105 °C	17h	1,3-diiodoperfluoropropane	N.R.
6	$FeCl_2$	4 *t*-BuNC	*t*-BuOK	105 °C	17h	1,3-diiodoperfluoropropane	40%
7	$FeCl_2$	4 *t*-BuNC	*t*-BuOK	105 °C	17h	1,4-diiodoperfluorobutane	10%
8	$FeCl_2$	4 *t*-BuNC		105 °C	17h	1,4-diiodoperfluorobutane	10%
9		4 *t*-BuNC	*t*-BuOK	105 °C	17h	1,4-diiodoperfluorobutane	0%
10			*t*-BuOK	105 °C	17h	1,4-diiodoperfluorobutane	N.R.

11	FeCl$_2$	4 t-BuNC	DIPEA	105 °C	17h	1,4-diiodoperfluorobutane	trace
12	FeCl$_2$	4 t-BuNC	t-BuOk	105 °C	17h	1,6-diiodoperfluorohexane	45%
13	FeCl$_2$	4 t-BuNC	K$_3$PO$_4$	105 °C	17h	1,6-diiodoperfluorohexane	30%

[a]For the reaction in pure benzene, catalyst (t-BuNC)$_4$FeCl$_2$ was pre-synthesized by reacting 4 equivalent t-butyl isocyanide and 1 equivalent iron(II) dichloride in diethyl ether for 3 days. [b]Yields were determined by ^{19}F NMR spectroscopy. [c]t-BuNC = t-butyl isocyanide.

Table 4a. Preliminary screen of iron catalysts and bases for the perfluoroalkylation of benzene.

The bases are important for this iron catalyzed reaction. Without base, the conversion was slow and the formation of 1,4-dichloroperfluorobutane was observed when 1,4-diiodoperfluorobutane was used as substrate and FeCl$_2$ was used as catalyst. With the increase of basicity, the conversion became faster and potassium t-butoxide gave almost quantitative conversion though yield was not improved significantly. Control experiments were performed to see if it was the iron(II) that catalyzed the reaction. In one recent work by Xu etc., Cs$_2$CO$_3$ itself was able to induce a 1,2 addition of perfluoroalkyl iodides to olefins through a radical process. It was shown that without iron(II) chloride, neither t-BuOK nor the combination of t-BuOK and ligand t-butyl isocyanide catalyezed the reaction, which indicated that this perfluoroalkylation reaction was induced directly by iron(II) catalyst. It was also noteworthy that in benzene, all the iron(II) and iron(III) catalyst without ligand were not able to convert the starting materials to the desired products.

In order to expand the scope of the aromatic substrates, other solvents besides benzene need to be screened. In this process, the hydrolyzed product which was H(CF$_2$)$_n$H showed up for various solvents, including THF, Et$_2$O, CH$_3$CN, DMF,CH$_2$Cl$_2$ and pentane with the formation of trace amount of the desired products when t-BuOK was used as base. This

might be explained by the previous discovery in our lab, that is, α,ω-diiodoperfluoroalkanes and *t*-BuOK will form a 2-D polymeric structure which will precipitate rapidly in 1,4-dioxane and this white solid will react vigorously with various solvents except those which don't have active hydrogens, such as DMF, benzene, benzonitrile. Following this discovery, the solvents were screened again with K_3PO_4 as the base (Table 4b).
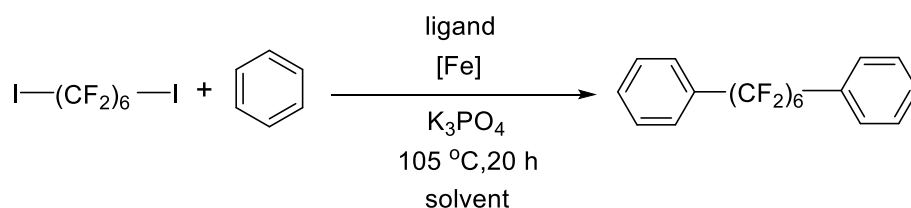
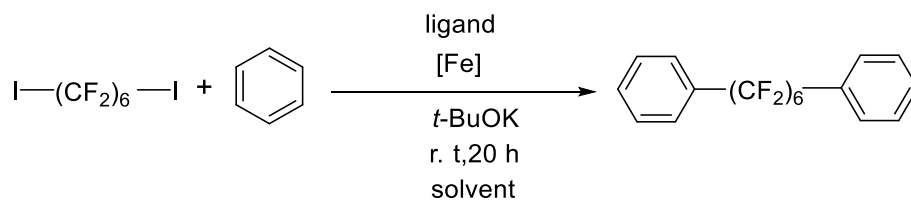| Entry	Catalyst[a]	Ligand[c]	Base	Solvent	Temperature	Time	Yield[b]
1	$FeCl_2$	4 *t*-BuNC	K_3PO_4	THF	105 °C	20h	6%
2	$FeCl_2$	4 *t*-BuNC	K_3PO_4	diglyme	105 °C	20h	trace
3	$FeCl_2$	4 *t*-BuNC	K_3PO_4	DMF	105 °C	20h	24%
4	$FeCl_2$	4 *t*-BuNC	K_3PO_4	DMA	105 °C	20h	18%
5	$FeCl_2$	4 *t*-BuNC	K_3PO_4	DMPU	105 °C	20h	trace
6	$FeCl_2$	4 *t*-BuNC	K_3PO_4	DMI	105 °C	20h	trace
7	$FeCl_2$	4 *t*-BuNC	K_3PO_4	TBME	105 °C	20h	10%
8	$FeCl_2$	4 ArNC	K_3PO_4	TBME	105 °C	20h	25%
9	$FeCl_2$		K_3PO_4	DMSO	105 °C	20h	35%
10	$FeBr_2$		K_3PO_4	DMSO	105 °C	20h	trace
11	$FeCl_3$		K_3PO_4	DMSO	105 °C	20h	N.R.
12	$FeCl_2$	2 PPh_3	K_3PO_4	DMSO	105 °C	20h	60%
13	$FeCl_2$	4 *t*-BuNC	K_3PO_4	DMSO	105 °C	20h	10%
14	$FeCl_2$	4 ArNC	K_3PO_4	DMSO	105 °C	20h	60%
15	$FeCl_2$	TMEDA	K_3PO_4	DMSO	105 °C	20h	25%
16	$FeCl_2$	Bipyridine	K_3PO_4	DMSO	105 °C	20h	trace

[a]For the reaction in DMSO, all the catalysts were synthesized *in-situ*. [b]Yields were determined by ^{19}F NMR. [c]ArNC = 2,6-dimethylphenyl isocyanide. PPh_3=triphenylphosphine.

Table 4b. Solvent screen for the perfluoroalkylation of benzene

The solvent is very important for the efficiency of the aromatic perfluoroalkylation (as shown in Table 4b), because perfluoroalkyl radicals can significantly abstract hydrogen from C-H bonds of the solvent (the rates of abstraction by R_f˙ are $>10^3$ larger than those of the analogue hydrocarbon radicals),[23] which is consistent with our observation. When 1,6-diiodoperfluorohexane was used, for THF, Et_2O, CH_3CN, dichloromethane, DMF, DMA, DMPU, DMI and diglyme, the hydrolyzed product was the major species, whereas TBME and DMSO suppressed the formation of the hydrolyzed product and improved the yield of the desired product. DMSO turned out to be a preferable solvent for the perfluoroalkyl radical addition to aromatic substrates because of both the good solubility for the iron catalysts and the inertness of hydrogens from DMSO which will not be abstracted by the perfluoroalkyl radicals.[10] Unlike in benzene, iron(II) dichloride was able to catalyze the reaction itself in DMSO, which might due to the improved solubility of the iron(II) dichloride or the possible DMSO-iron(II) complex. Ligands also had a significant effect on the yields of reaction. With the ligand 2,6-dimethylphenyl isocyanide or triphenlyphosphine on, it gave the best yield (60% by ^{19}F NMR spectroscopy, see Table 4b, entry 12 and 14). In some previous work, iron(II) bis(triphenylphosphine)dichloride [$FeCl_2(PPh_3)_2$] was known to induce living radical polymerization. When [$FeCl_2(TMEDA)$] was used, yield was lower and hydrolyzed product appeared again which might come from the abstraction of the hydrogens on the ligand. [$FeCl_2(bipy)_2$] was also tested, which gave only trace amount of the product. It should be pointed out that *t*-butyl isocyanide as ligand in DMSO was not as efficient as in pure benzene because starting material was almost recovered with extreme low yield of desired product (10% in DMSO vs 45% in benzene). Other bases, like CsF, CsOH, *t*-BuOK, EtOK were not compatible with this catalytic

system, either lead to the recovery of the starting materials or the extremely low yield of the desired products. Another interesting fact about the reaction described in Table 4b was that in order to get a higher yield, the reaction mixture had to be heated gradually to the desired temperature, otherwise the yield was extremely low with a dark reaction mixture in the end. This might due to the stability of the iron catalyst in the initial stage of the reaction, by which time the dramatic temperature change probably tampered with the iron catalysts.

As mentioned above, α,ω-diiodoperfluoroalkanes will react with t-BuOK in various solvents to generate $H(CF_2)_nH$ at room temperature, which could be suppressed by DMF as the solvent. It was found that iron(II) catalysts could convert 1,6-diiodoperfluorohexane and benzene to the desired product at **room temperature** with t-BuOK (Table 4c).


entry	catalyst	ligand	base	solvent	temperature	time	yield
1	$FeCl_2$	PPh_3	t-BuOK	DMF	R.T.	24h	35%
2	$FeCl_2$	Bipy	t-BuOK	DMF	R.T.	24h	46%
3	$FeCl_2$	2 Bipy	t-BuOK	DMF	R.T.	24h	30%
4	$FeCl_2$	Phen	t-BuOK	DMF	R.T.	24h	12%
5	$FeCl_2$	Terpyridine	t-BuOK	DMF	R.T.	24h	10%
6	$FeCl_2$	Bipy'	t-BuOK	DMF	R.T.	24h	20%
7	$FeCl_2$	TMEDA	t-BuOK	DMF	R.T.	24h	13%

Table 4c. Optimization at room temperature for the perfluoroalkylation of benzene

C_4F_9I and $C_6F_{13}I$ were also tested in the system shown in Table 4c, and a full conversion of C_4F_9I and $C_6F_{13}I$ was achieved. For C_4F_9I, the ^{19}F NMR yield of desired product Ph-C_4F_9 was 78%, and the yield of Ph-C_6F_{13} was 75% for $C_6F_{13}I$. At this point, the reaction requires stoichiometric amount of iron(II) catalyst (1 equivalent), whereas catalytic amount of catalyst could not achieve the transformation efficiently.

Iron is the most abundant transition metal in nature and plays a very important role in life process. This cheap and environmentally benign element has been proved to be catalytically active in various organic transformations. Iron-catalyzed C-H transformations have achieved rapid development in the past several years. Below is an example of iron-catalyzed C-H bond arylation with aryl halides, which was proposed as a radical pathway (Scheme 4f).[24]
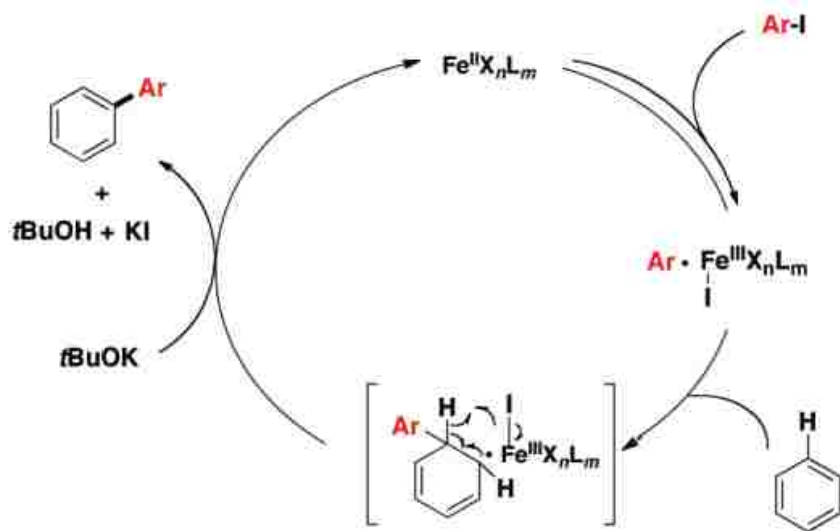
Scheme 4f. Proposed mechanism for the C-H arylation catalyzed by iron(II)

If our reaction adopts a similar pathway as shown in the Scheme 4f, the iron(II) catalyst will be oxidized to iron (III) and then reduced to iron (II) by the conserted radical arylation of benzene to finish the catalytic cycle. We reasoned that in our case, the catalytic cycle stuck at the stage of iron (III) which was not able to be reduced to iron (II). As shown in Table 4b, $FeCl_3$ could not mediate the perfluoroalkylation. The future work is to pursue a strategy to *in situ* reduce iron (III) to iron (II) to make the reaction catalytic. A broader substrate scope of arenes and heteroarenes is desired as well.

4.3. Summary

We have shown that 1,4-diiodooctafluorobutane reacts with potassium *tert*-butoxide in dioxane to afford a halogen-bonded adduct with an extended two-dimensional network held together by strong iodine-oxygen interactions. The new complex represents the first example of a structurally characterized halogen bonding network involving anionic oxygen donor atoms with perfluoroalkyl iodides. The *tert*-butoxide adduct displays the shortest iodine-oxygen distance and the longest iodine-carbon distance thus far reported for any perfluoroalkyl iodide substrate.

Though attempts to utilized the iodine reagents as a hot $(CF_2)_n$ source failed, a Fe-mediated perfluoroalkylation of benzene was developed using α,ω-diiodoperfluoroalkanes and *t*-BuOK in DMF at room temperature. The role of *t*-BuOK is still ambiguous in this system. It either accelerates the perfluoroalkylation process with high basicity and solubility in DMF or activates the α,ω-diiodoperfluoroalkanes by forming the 2-D polymeric structure. A more detailed mechanistic analysis and enlarged synthetic scope of the Fe-mediated reaction will be the next stage of our investigation.

4.4. Experimental Procedures

General Considerations: All manipulations were performed under an inert atmosphere using standard Schlenk and high vacuum techniques or in a nitrogen filled glovebox. Solvents were purified by passing through activated alumina and/or copper in a solvent purification system supplied by Pure Process Technology. 1,4-diiodooctafluorobutane was purchased from SynQuest Labs, Inc. and used without further purification. Solution ^{1}H NMR spectra were recorded at ambient temperature on a Bruker DRX 500 MHz spectrometer and referenced to residual proton solvent signals. ^{13}C NMR spectra were recorded on a Bruker NMR spectrometer operating at 125 MHz and referenced to solvent signals. ^{19}F spectra were recorded on the Bruker NMR spectrometer operating at 470 MHz and referenced to α,α,α-trifluorotoluene at δ -67.3. A Bruker D8 Quest diffractometer was used for X-ray crystal structure determinations.

Synthesis of complex 4.1: 450 mg (4 mmol) of potassium *t*-butoxide was dissolved in 4 mL of 1,4-dioxane. To this was added dropwise 453 mg (1 mmol) of 1,4-diiodooctafluorobutane in 4 mL of 1,4-dioxane. The mixture was stirred at room temperature for 15 min. Then the mixture was filtered through a glass frit and the residue was washed with diethyl ether. The residue was then dried under vacuum to remove all the volatiles. The off-white powder was then dissolved into a 1:5 mixture of DMF:trifluorotoluene and placed in a −35 °C freezer overnight to form colorless crystals. ^{19}F NMR (DMF-d_7, 470 MHz):δ -88 (br s), -114 (br s). The thermal and air-sensitivity of **4.1** precluded elemental analysis.

General procedure for the iron-catalyzed reaction. (a)

Iron (II) dichloride (0.1 mmol, 12.7mg) and triphenylphosphine (0.2mmol, 52mg) were weighted into a pressure vial and dissolved in 0.5ml DMSO. The whole mixture was stirred at room temperature for 15min. To this mixture, 0.5 ml benzene solution of 0.1 mmol (55 mg) 1,6-diiodododecafluorohexane was added, followed by the addition of 0.6 mmol (126 mg) K_3PO_4. The pressure vial was sealed and placed in an oil bath which was gradually warmed up to 105 ^{o}C and then heated for 20h.

General procedure for the iron-catalyzed reaction at room temperature. (b)

Iron (II) dichloride (0.1 mmol, 12.7mg) and bipyridine (0.1mmol, 16mg) were weighted into a 20 ml vial and dissolved in 0.5ml DMF. The mixture was stirred at room temperature for 15min. To this mixture, 0.5 ml benzene solution of 0.1 mmol (55 mg) 1,6-diiodododecafluorohexane was added, followed by the addition of 0.4mmol (45 mg) *t*-BuOK. The whole mixture was stirred at room temperature for 24h.

General procedure for the iron-catalyzed reaction in pure benzene (c)

Tetrakis(*t*-butyl isocyanide) Iron (II) dichloride (0.1 mmol, 46mg) was weighted into a pressure vial. To this mixture, 1 ml benzene solution of 0.1 mmol (55 mg) 1,6-diiodododecafluorohexane was added, followed by the addition of 0.4 mmol (45 mg) *t*-BuOK. The pressure vial was sealed and placed in an oil bath which was gradually warmed up to 105 ^{o}C and then heated for 20h.

4.5. Reference

1. Modern Fluoroorganic Chemistry; Kirsch, P., Ed.; Wiley-VCH: Weinheim, Germany, 2004.
2. Li, X.; Jiang, X.; Pan, H.; Hu J.; Fu, W. *Pure&Appl. Chem.* **1987**, *59*, 1015.
3. Feiring, A. E. *J. Org. Chem.* **1985**, *50*, 3269.
4. Ding, X.; Tuikka, M.; Haukka, M.; InTech: 2012, p 143
5. Erdelyi, M. *Chemical Society Reviews* **2012**, *41*, 3547
6. Legon, A. C. *Phys. Chem. Chem. Phys.* **2010**, *12*, 7736
7. Metrangolo, P.; Meyer, F.; Pilati, T.; Resnati, G.; Terraneo, G. *Angew. Chem., Int. Ed.* **2008**, *47*, 6114
8. Metrangolo, P.; Resnati, G. *Cryst. Growth Des.* **2012**, *12*, 5835
9. Metrangolo, P.; Resnati, G. *Chem. Commun.* **2013**, *49*, 1783.
10. Mukherjee, A.; Tothadi, S.; Desiraju, G. R. *Acc. Chem. Res.* **2014**, *47*, 2514
11. Politzer, P.; Lane, P.; Concha, M. C.; Ma, Y.; Murray, J. S. *J. Mol. Model.* **2007**, *13*, 305
12. Politzer, P.; Murray, J. S.; Clark, T. *Phys. Chem. Chem. Phys.* **2010**, *12*, 7748
13. Priimagi, A.; Cavallo, G.; Metrangolo, P.; Resnati, G. *Acc. Chem. Res.* **2013**, *46*, 2686
14. Minkwitz, R.; Broechler, R.; Berkei, M. *Z. Anorg. Allg. Chem.* **1996**, *622*, 1749
15. Minkwitz, R.; Hertel, T.; Braeutigam, A. *Z. Anorg. Allg. Chem.* **1997**, *623*, 151
16. Minkwitz, R.; Jakob, J. *Z. Anorg. Allg. Chem.* **1997**, *623*, 613
17. Cardillo, P.; Corradi, E.; Lunghi, A.; Valdo Meille, S.; Messina, T. M.; Metrangolo, P.; Resnati, G. *Tetrahedron* **2000**, *56*, 5535
18. Chu, Q.; Wang, Z.; Huang, Q.; Yan, C.; Zhu, S. *J. Am. Chem. Soc.* **2001**, *123*, 11069.
19. Minkwitz, R.; Broechler, R.; Berkei, M. *Z. Anorg. Allg. Chem.* **1996**, *622*, 1749.
20. Xu, T.; Cheung, C. W.; Hu, X. *Angew. Chem. Int. Ed.* **2014**, *126*, 5010.
21. Kuvychko, I. V.; Dubceac, C.; Deng, S.; Wang, X.; Granovsky, A. A.; Popov, A. A.; Petrukhina, M. A.; Strauss, S. H.; Boltalina, O. V. *Angew. Chem. Int. Ed.* **2013**, *52*, 7505.
22. Knunyants, I. L.; Shokins, V. V.; Krasuskaya, P. M.; Khrlakyan, S. P. *Seriya Khimicheskaya* **1967**, *7*, 1520.
23. Bravo, A.; Bjørsvik, H.; Fontana, F.; Liguori, L.; Mele, L.; Minisci, F. *J. Org. Chem.* **1997,** *62,* 7128.
24. Vallee, F.; Mousseau, J. J.; Charette, A. B. *J. Am. Chem. Soc.* **2010**, *132*, 1514.

5. Chapter 5: Nickel-catalyzed reductive coupling of aryl halides and HCF₂Cl

5.1. Introduction

Nickel-catalyzed conventional cross-coupling between aryl halides and $(DMPU)_2Zn(CF_2H)_2$ has been reported by our group recently.[1] The novel difluoromethyl zinc reagent, synthesized from diethyl zinc and HCF_2I, serves as a source of "$^-CF_2H$". However, this synthetic protocol for difluoromethylation is facing following challenges: firstly, the organozinc regent is air-sensitive which has to be stored at inert atmosphere; secondly, the high cost of HCF_2I lowers economy of the reaction.
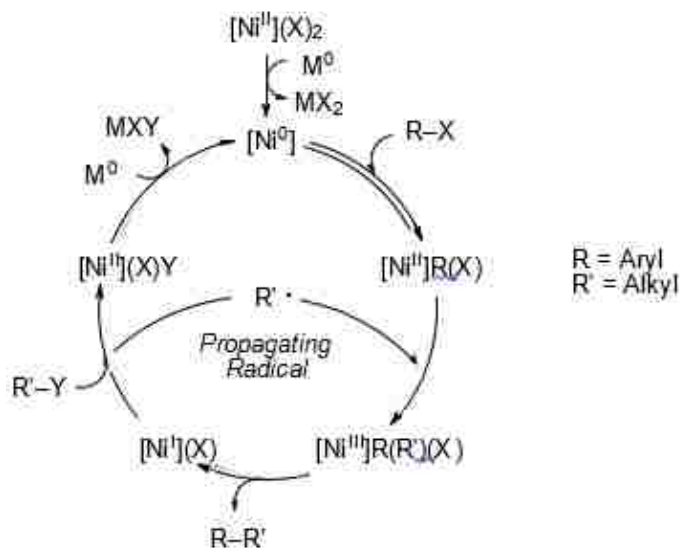
Scheme5a. Radical chain cross-coupling of aryl halides with alkyl halides.

In the last decade, nickel-catalyzed reductive coupling between electrophiles such as aryl halides and alkyl halides has drawn attention from synthetic chemists due to its synthetic

and operational simplicity without preparation of moisture and air-sensitive organometallic reagents. [2-13] The Weix group is one the pioneers in this field and a plausible mechanism has been proposed based on the mechanistic studies as shown in Scheme 5a.[14]

However, reductive coupling between difluoromethyl halides and aryl halides has not been reported yet. This is probably hindered by the fact that HCF_2X (X=I, Br) will react with the reductant such as Zn to generate intermediacy of stoichiometric organometallic reagents $Zn(CF_2H)X$ *in situ* as described in Scheme 5b.[15]

$$Zn + HCF_2Br \xrightarrow[60\,°C]{DMF} Zn(CF_2H)_2 + Zn(CF_2H)Br$$

$$Zn + HCF_2I \xrightarrow[R.T.]{DMF} Zn(CF_2H)I$$
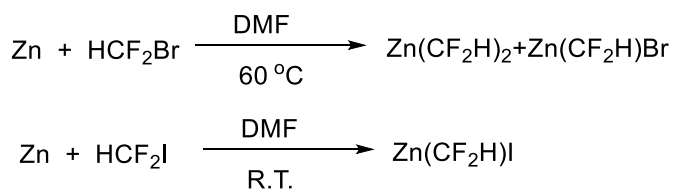
Scheme 5b. Insertion of zinc to HCF_2X (X=I, Br).

Chlorodifluoromethane (HCF_2Cl) is known as HCFC-22, or R-22, and is commonly used as a propellant and refrigerant. Due to the compound's ozone depletion potential (ODP) and high global warming potential (GWP), the use of chlorodifluoromethane is limited worldwide. A strategy to utilize and consume this compound is highly desired to turn it into valuable products. It is known that through dehydrohalogenation, HCF_2Cl yields difluorocarbene upon treatment with strong base, which is used in the laboratory as reactive intermediate. Difluoromethylation of phenols and thiophenol with HCF_2Cl can be readily achieved by this methodology (Scheme 5c).[16,17]

$$\text{Nu}^- \xrightarrow{\quad [\,:\text{CF}_2\,]\quad} \text{Nu-CF}_2^- \xrightarrow{\quad ``\,\text{H}^+\,"\quad} \text{Nu-CF}_2\text{H}$$

with difluorocarbene precursor/reagent above the first arrow.

OH → OCF$_2$H

CHClF$_2$ (excess), NaOH (H$_2$O)

dioxane, 70 °C

65%

SH → SCF$_2$H

CHClF$_2$ (excess), NaOH

TCB, TDA-1, 90 °C

85%
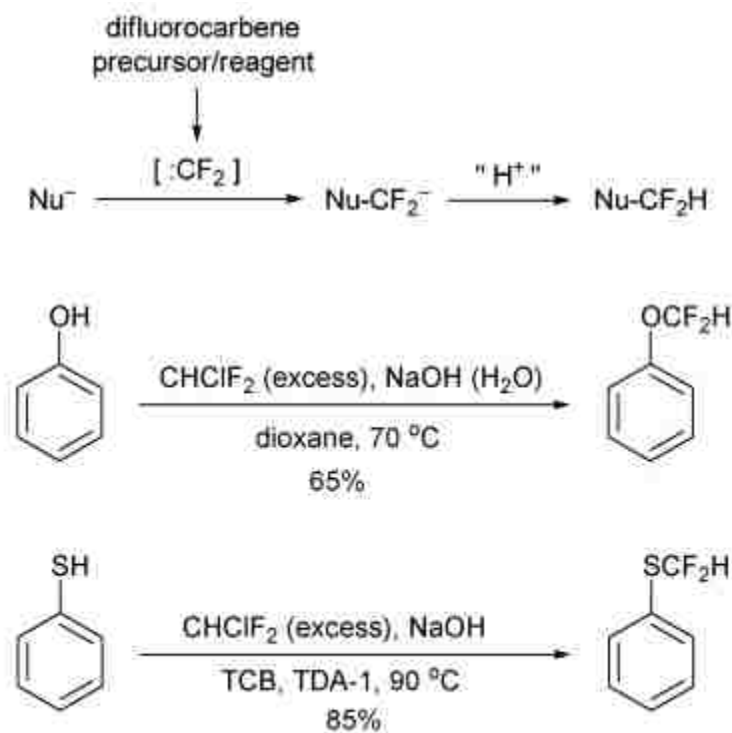
Scheme 5c. Difluorocarbene from HCF$_2$Cl treated with strong bases.

Here we would like to design a reaction system based on the mechanism shown in Scheme 5a. Unlike HCF$_2$I and HCF$_2$Br, the relatively inert C-Cl bond prevents reaction between HCF$_2$Cl and zinc to form Zn(CF$_2$H)Cl even at 100 °C. This provides the possibility to utilize HCF$_2$Cl as the partner in reductive coupling with aryl halides to generate difluoromethylated arenes and heteroarenes.

5.2. Results and Discussion

5.2.1. Preliminary Mechanistic Study

To verify the possibility of proposed catalytic system, a mechanistic study was firstly performed. In a reductive coupling catalytic cycle, it is known that Ni (II) is reduced to Ni(0) by Zn or Mn, followed by oxidative addition of aryl halides to Ni(0). The challenge lies in developing a contructive reaction between in situ generated Ni(Ar)X and HCF_2Cl, which has never been shown before. Another consideration is that Ni(Ar)X might undergo redistribution to form $Ni(Ar)_2$ and NiX_2. We carefully picked (dtbpy)Ni(o-tol)Cl as a model system because it is a stable Ni(II) complex that avoids the side reactions. The gaseous HCF_2Cl was firstly bubbled into solvent, such as DMF, followed by the addition of certain amount of trifluorotoluene to quantify the concentration of HCF_2Cl via ^{19}F NMR spectroscopy. The sealed vial of HCF_2Cl and (dtbpy)Ni(o-tol)Cl was heated at 80 °C in DMF for 16 hours. To our delight, the desired product 1-difluoromethyl-2-methyl-benzene was generated with a NMR yield of 23%, confirmed by ^{19}F NMR spectroscopy and GC-MS analysis (Scheme 5d)
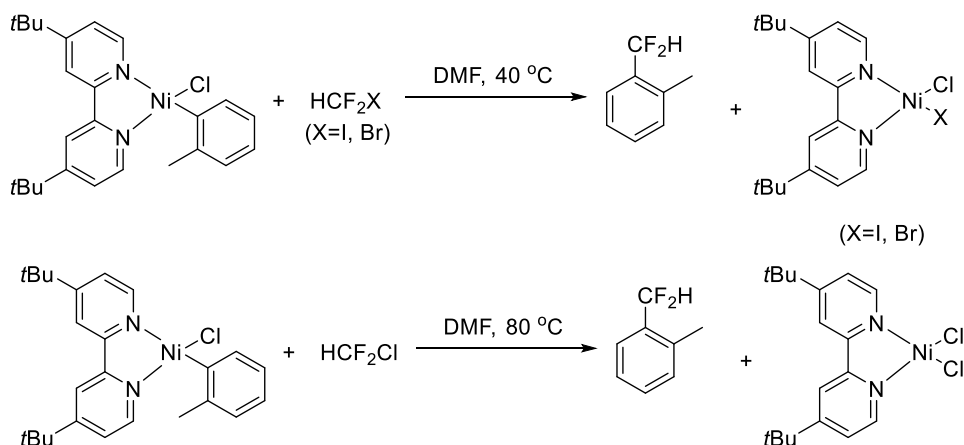
Scheme 5d. Activation of HCF_2X (X=Cl, Br, I) by [Ni(Ar)X].

Two analogous experiments using HCF_2I and HCF_2Br were performed as well, which gave 1-difluoromethyl-2-methyl-benzene in the end (Scheme 5d). It is interesting to notice that besides the same target product 1-difluoromethyl-2-methyl-benzene at -115 ppm, one peak at -104 ppm showed up in ^{19}F NMR spectra for HCF_2I and HCF_2Br whereas it was not the case for HCF_2Cl (Figure 5a). At this point we are still not clear about what it is. The color of solutions for these all three experiments turned to bright green, indicating there might be the byproducts $(dtbpy)NiX_2$ (X=Cl,Br,I). To verify the hypothesis, growing crystal out of the final mixture is at our next stage of investigation.
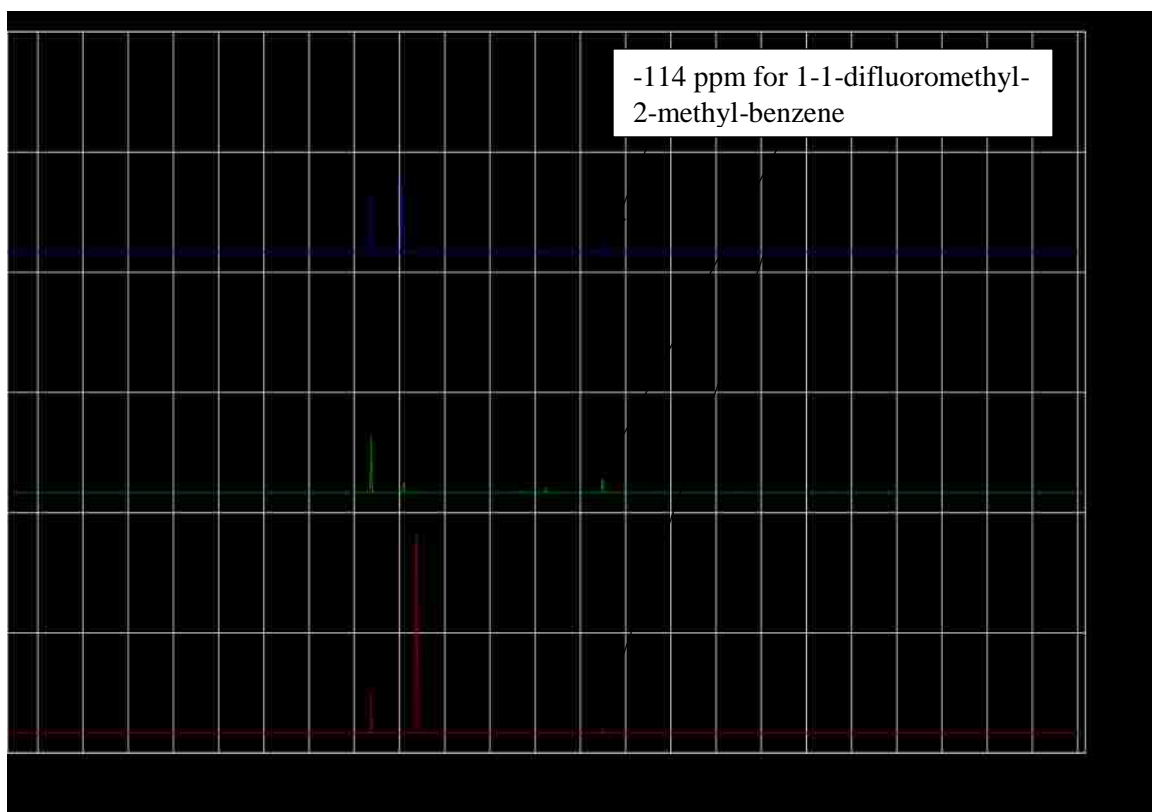
Figure 5a. Spectrums for the comparison of using HCF_2Cl (red), HCF_2Br (blue) and HCF_2I (green)

Monitoring the reaction between $(dtbpy)Ni(o-tol)Cl$ and HCF_2I in DMF gave us more information. At room temperature, the reaction proceeded to give 1-difluoromethyl-2-

86

methyl-benzene with a NMR yield of 53% within one hour. Additionally, a peak at -116 ppm grew in and then decreased with the extension of reaction time to 16 hours. The yield of desired product increased to 67% during this process. Heating the resulted mixture at 40 °C eliminated the peak at -116 ppm and promoted the yield of 1-difluoromethyl-2-methyl-benzene to 72% (Figure 5b). We reasoned that the peak at -116 ppm might represent a nickel intermediate prior to the formation of 1-difluoromethyl-2-methyl-benzene. Attempts of getting a qualified crystal for single X-ray is undergoing to take a snapshot of the proposed intermediate. Reacting (dtbpy)Ni(o-tol)Cl with HCF_2Cl at room temperature failed to give the desired product which was coincident with the fact that C-Cl bond is much more inert than C-I bond.
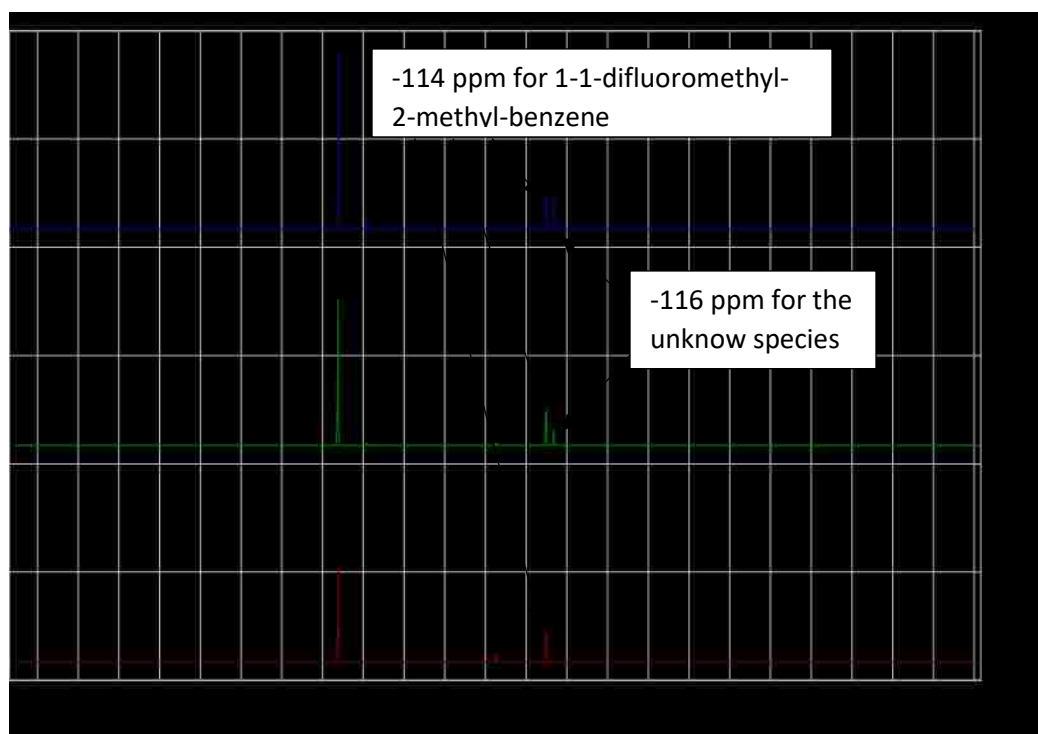
Figure 5b. Spectrums for monitoring the reaction using HCF_2I at different temperature,1 hour at room temperature (blue); 15 hours at room temperature (green); 15 hours at 40 °C (red).

Since the elemental step of reaction between (dtbpy)Ni(o-tol)Cl and HCF_2X (X=Cl, Br,I) has been proved feasible in our experiments, the next step is to reduce (dtbpy)NiX$_2$ to (dtbpy)Ni(0) by Zn or Mn to regenerate the catalyst as shown in Scheme 5a. Though (dtbpy)Ni(o-tol)Cl readily reacts with HCF_2I and HCF_2Br at room temperature, the possible insertion of Zn or Mn to HCF_2I and HCF_2Br to generate *in situ* nucleophiles precludes these two gases as reductive partner. To make sure HCF_2Cl would not react with Zn or Mn, we performed the experiments of heating HCF_2Cl with Zn or Mn in DMF even at 100 $^\circ$C. The starting material HCF_2Cl kept unreacted and no inserted product was observed via ^{19}F NMR spectroscopy, making it qualified to develop the final catalytic system.

5.2.2. Optimization of Catalytic System

Solvent effects. We started the optimization with the complexes used during our previous mechanistic study (Scheme 5d). Solvents turned out to be essential for the catalytic reaction. At first, DMF was the only solvent to give noticeable amount of desired product, though the NMR yield was as low as 7%. It is known that pyridine as additive will increase the yield in some cases of nickel-catalyzed reductive coupling by virtue of the fact that the pyridine-ligated nickel center was electronically enriched. Attempts to add one equivalent of pyridine in the system failed to increase yield but using pyridine as the solvent successfully promoted the yield to 20%. Other solvents shut down the reactivity totally and the results for solvent screen were summarized in Table 5a.

Reaction scheme:

HCF_2Cl + [biphenyl]–I → [biphenyl]–CF_2H

HCF_2Cl: 4 equiv
Aryl iodide: 0.05 mmol

Conditions: 10% dtbpy, 10% $NiBr_2$, solvent 0.5 ml, 80 °C, 4 equiv Zinc
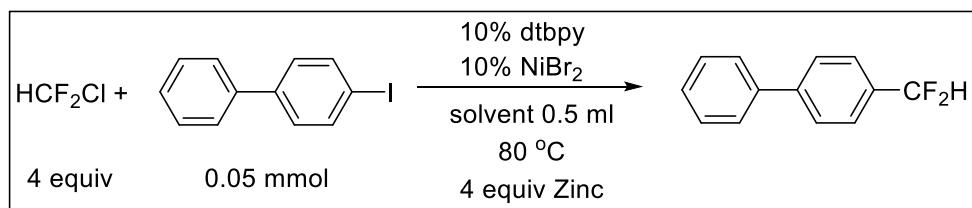
Entry	Ligand	Catalyst	Solvent	Temperature	Time	Aryl halide	Yield
1	dtbpy	$NiBr_2$	THF	80 °C	20h	4-iodobiphenyl	trace
2	dtbpy	$NiBr_2$	diglyme	80 °C	20h	4-iodobiphenyl	trace
3	dtbpy	$NiBr_2$	DMF	80 °C	20h	4-iodobiphenyl	7%
4	dtbpy	$NiBr_2$	DMA	80 °C	20h	4-iodobiphenyl	trace
5	dtbpy	$NiBr_2$	DMPU	80 °C	20h	4-iodobiphenyl	trace
6	dtbpy	$NiBr_2$	DMI	80 °C	20h	4-iodobiphenyl	None
7	dtbpy	$NiBr_2$	TBME	80 °C	20h	4-iodobiphenyl	None
8	dtbpy	$NiBr_2$	dioxane	80 °C	20h	4-iodobiphenyl	trace
9	dtbpy	$NiBr_2$	toluene	80 °C	20h	4-iodobiphenyl	None
10	dtbpy	$NiBr_2$	benzene	80 °C	20h	4-iodobiphenyl	None
11	dtbpy	$NiBr_2$	DME	80 °C	20h	4-iodobiphenyl	None
12	dtbpy	$NiBr_2$	PhCN	80 °C	20h	4-iodobiphenyl	trace
13	dtbpy	$NiBr_2$	MeCN	80 °C	20h	4-iodobiphenyl	trace
14	dtbpy	$NiBr_2$	DMSO	80 °C	20h	4-iodobiphenyl	trace
15	dtbpy	$NiBr_2$	pyridine	80 °C	20h	4-iodobiphenyl	20%

Table 5a. Solvent screen for the reductive coupling of HCF_2Cl and 4-iodobiphenyl.

However, one drawback of using pyridine as solvent was the observation of difluoromethylated pyridine byproducts. Three doublets at -113, -115 and -116 ppm represented meta-, ortho- and para-difluoromethyl pyridine respectively. The formation of these byproducts also indicated that difluoromethyl radical was generated in the reaction process which was coincident with the mechanism proposed in Scheme 5a. Further experiments using radical traps may provide more evidence of radical process for the reaction system developed here.

To suppress the formation of difluoromethylated pyridine byproducts, we tried to use 4-dimethylaminopyridine as additive along with other solvents. In 1,4-dioxane, 1 equivalent of 4-dimethylaminopyridine slightly increased the yield from none to 5% while 10 equivalents of 4-dimethylaminopyridine pushed it further to 16%, indicating that the coordination of extra nitrogen-donor ligand is beneficial for this reductive coupling reaction. However, in DMF or DMPU, 4-dimethylaminopyridine was not as efficient as it in 1,4-dioxane. We reasoned that the coordination of 4-dimethylaminopyridine was competed by DMF or DMPU because they had stronger coordination ability than 1,4-dioxane. Exploration of more electron-rich pyridine derivatives as additives in different solvents is undertaken in our lab to improve the yield.

GC-MS analysis of reaction carried out in pyridine revealed that the starting material 4-iodobiphenyl was 100% converted, and desired product 4-difluoromethyl biphenyl was present along with biphenyl as byproduct. This byproduct was also observed in the case of reductive coupling between aryl halides and alkyl halides. The 4-iodobiphenyl might be reduced to biphenyl either by reductant zinc or the in-situ generated Ni(0). Strategy to suppress the formation of Ar-H is under investigation to increase the yield.

Ligand effects. We used pyridine as the solvent medium to perform further screens. We have learned that enrichment of electron density on nickel could increase the yield, and this was confirmed by the ligand screen as well. In our case, all the phosphine ligands failed to give desired product as shown in Table 5b. DPPF worked very well for the nickel-catalyzed conventional cross-coupling of aryl halides and $(DMPU)_2Zn(CF_2H)_2$,[1] but in this case it didn't give any product in the end.
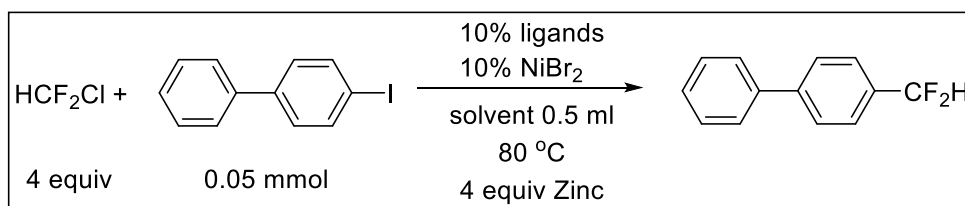
Entry	Ligand	Catalyst	Solvent	Temperature	Time	Aryl halide	Yield
1	PPh$_3$	NiBr$_2$	pyridine	80 °C	20h	4-iodobiphenyl	None
2	dppm	NiBr$_2$	pyridine	80 °C	20h	4-iodobiphenyl	None
3	dppe	NiBr$_2$	pyridine	80 °C	20h	4-iodobiphenyl	None
4	dppp	NiBr$_2$	pyridine	80 °C	20h	4-iodobiphenyl	None
5	dppf	NiBr$_2$	pyridine	80 °C	20h	4-iodobiphenyl	None
6	dippf	NiBr$_2$	pyridine	80 °C	20h	4-iodobiphenyl	None
7	xantphos	NiBr$_2$	pyridine	80 °C	20h	4-iodobiphenyl	None
8	segphos	NiBr$_2$	pyridine	80 °C	20h	4-iodobiphenyl	None
9	P(n-Bu)$_3$	NiBr$_2$	toluene	80 °C	20h	4-iodobiphenyl	None
10	Qphos	NiBr$_2$	benzene	80 °C	20h	4-iodobiphenyl	None

Table 5b. Phosphine ligands screen for the reductive coupling of HCF$_2$Cl and 4-iodobiphenyl.

Nitrogen-donor ligands are known to be more electron-rich than phosphine ligands, which is coincident with our observation as the ligands shown in Table 5c performed better than phosphine ligand. For the bipyridine derivatives, the yield of desired product was increased with more electron-donating group: OMe > $C(CH_3)_3$ > $CH(C_8H_{17})_2$ > Me. Terpyridine derivatives were not as efficient as bipyridine ligands. For diimine ligand L1 and L2, the yield was lowered to 8%. A control experiment without any ligand failed to provide any product, indicating the necessity of coordination of nitrogen-donor ligands onto nickel center.
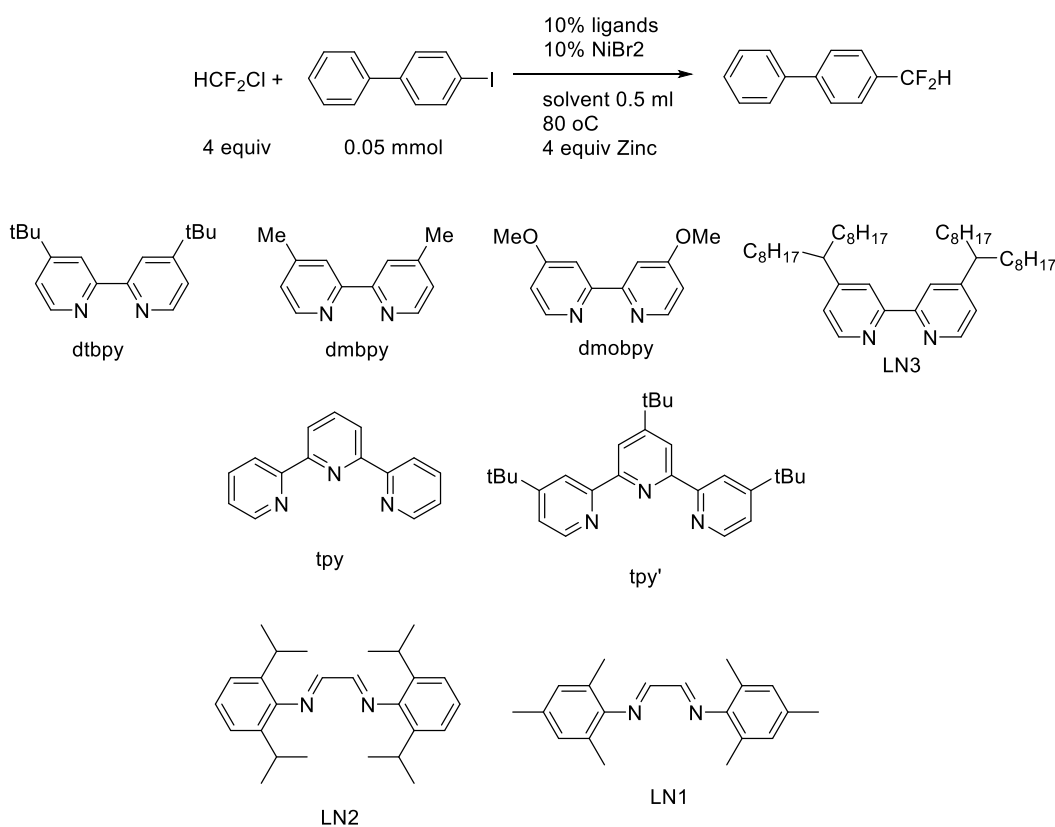
Entry	Ligand	Catalyst	Solvent	Temperature	Time	Aryl halide	Yield
1	dtbpy	NiBr$_2$	pyridine	80 °C	20h	4-iodobiphenyl	28%
2	dmbpy	NiBr$_2$	pyridine	80 °C	20h	4-iodobiphenyl	8%

3	dmobpy	NiBr$_2$	pyridine	80 °C	20h	4-iodobiphenyl	34%
4	tpy	NiBr$_2$	pyridine	80 °C	20h	4-iodobiphenyl	8%
5	tpy'	NiBr$_2$	pyridine	80 °C	20h	4-iodobiphenyl	10%
6	L1	NiBr$_2$	pyridine	80 °C	20h	4-iodobiphenyl	8%
7	L2	NiBr$_2$	pyridine	80 °C	20h	4-iodobiphenyl	9%
8	L3	NiBr$_2$	pyridine	80 °C	20h	4-iodobiphenyl	12%
9	tmeda	NiBr$_2$	pyridine	80 °C	20h	4-iodobiphenyl	11%
10	none	NiBr$_2$	pyridine	80 °C	20h	4-iodobiphenyl	None

Table 5c. Ligands used in the screen (top), results for nitrogen ligand screen (bottom) for the

reductive coupling of HCF$_2$Cl and 4-iodobiphenyl

It is interesting to notice that though 4 4'-dimethoxy-2 2'-bipyridine gave the best result out of all the ligand tested, it led to more formation of difluoromethylated pyridine byproducts with even more yield than the desired product (40%). This side reaction had the potential to be optimized for developing a radical difluoromethylation of arenes and heteroarenes. However, in this work, the suppression of this side reaction is one of our aims to improve the yield of desired products.

Reductant effect. One of the major differences between cross-electrophile coupling and conventional cross-coupling is the requirement of reductive agents. A variety of reductants have been utilized for reductive reactions in the literature, including electrochemical reduction, organic reductants, and metal powders, but zinc is particularly attractive. On a

cost/electron basis (~1$/mole of e-) or mass/electron basis (~33 g/mole of e-), zinc dust is very economical. Because zinc dust is a readily available and easy-to-handle reagent, the reactions require no specialized techniques or equipment to run.

In our case, zinc has the best performance compared with Mn or TDAE as shown in Table 5d. Activating zinc with chlorotrimethylsilane in situ or washing the zinc with HCl did not help the reaction, so we directly used the commercial-available zinc powder from Sigma-Aldrich with a larger particle size (-325 mesh, 44 μm diameter). Four equivalents of zinc were sufficient to run the reaction, and more amounts of zinc had no beneficial effect on the result. Two equivalents of zinc decreased the yield.

It was surprising to see no product formed in the case of Mn and TDAE because these two reducing agents worked for reductive coupling of aryl halides and alkyl halides. Using Mn along with TMSCl was slightly better than Mn alone, as TMSCl activated the Mn surface by removing MnO. This revealed that induction time of reducing Ni(II) to Ni(0) was influential for the efficiency of reaction system.
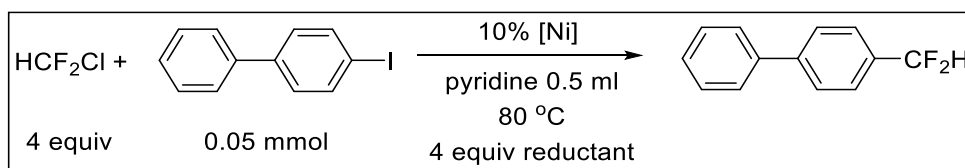
Entry	Ligand	Catalyst	Reductant	Aryl halide	Yield
1	dmobpy	NiBr$_2$	Zn	4-iodobiphenyl	34%
2	dmobpy	NiBr$_2$	Zn and TMSCl	4-iodobiphenyl	35%
3	dmobpy	NiBr$_2$	Zn activated by HCl	4-iodobiphenyl	33%

4	dmobpy	NiBr$_2$	Mn	4-iodobiphenyl	none
5	dmobpy	NiBr$_2$	Mn and TMSCl	4-iodobiphenyl	5%
6	dmobpy	NiBr$_2$	TDAE	4-iodobiphenyl	trace

Table 5d. Reducing agents effect for the reductive coupling of HCF$_2$Cl and 4-iodobiphenyl .

Temperature effect. We initially performed the reaction at 80 °C, but further optimization of temperature showed that lower temperature at 65 °C would suppress the formation of difluoromethylated pyridine byproducts and increased the yield of desired product. Continuing to lower the temperature to 50 °C decreased the yield, though no difluoromethylated pyridine byproducts were generated. The reaction shut down at 40 °C. This trend was observed in two sets of experiments using (dtbpy)NiBr$_2$ and (dmobpy)NiBr$_2$ respectively. We reasoned that the activation of HCF$_2$Cl had certain energy barrier so that heating was necessary, but high temperature will accelerate side reactions as well. The optimized result was summarized in Table 5e.
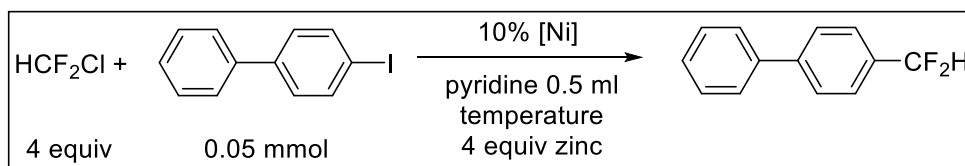
Entry	Ligand	Catalyst	Temperature	Aryl halide	Yield
1		(dtbpy)NiBr$_2$	40 °C	4-iodobiphenyl	0%
2		(dtbpy)NiBr$_2$	50 °C	4-iodobiphenyl	22%
3		(dtbpy)NiBr$_2$	65 °C	4-iodobiphenyl	35%
4		(dtbpy)NiBr$_2$	80 °C	4-iodobiphenyl	26%

5	(dtbpy)NiBr$_2$	90 °C	4-iodobiphenyl	21%
6	(dmobpy)NiBr$_2$	50 °C	4-iodobiphenyl	12%
7	(dmobpy)NiBr$_2$	65 °C	4-iodobiphenyl	42%
8	(dmobpy)NiBr$_2$	80 °C	4-iodobiphenyl	35%

Table 5e. Temperature effect for the reductive coupling of HCF$_2$Cl and 4-iodobiphenyl

Nickel catalysts. It is known that the rate of initial reduction of Ni(II) to Ni(0) was different for different Ni(II) sources. As we demonstrate previously, the induction time influenced on the results shown in Table 5d. We also found that the pre-synthesized nickel catalysts worked better than the ones generated in *situ*. This might due to the insolubility of some Ni(II) salts, for example, NiI$_2$ was almost insoluble in pyridine at room temperature, but (dtbpy)NiI$_2$ and (dmobpy)NiI$_2$ dissolved very well. From the Table 5f, we recognize that the current best result was given by (dtbpy)NiI$_2$.
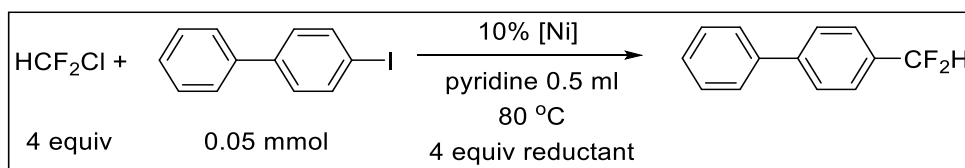
Entry	Ligand	Catalyst	Solvent	Aryl halide	Yield
1	dtbpy	NiCl$_2$	pyridine	4-iodobiphenyl	25%
2	dtbpy	NiBr$_2$	pyridine	4-iodobiphenyl	28%
3	dtbpy	NiI$_2$	pyridine	4-iodobiphenyl	40%
4	dtbpy	Ni(acac)$_2$	pyridine	4-iodobiphenyl	12%

5	dtbpy	Ni(COD)$_2$	pyridine	4-iodobiphenyl	10%
6	(dtbpy)NiBr$_2$		pyridine	4-iodobiphenyl	35%
7	(dtbpy)NiI$_2$		pyridine	4-iodobiphenyl	45%
8	(dmobpy)NiBr$_2$		pyridine	4-iodobiphenyl	34%
9	(dmobpy)NiI$_2$		pyridine	4-iodobiphenyl	43%

Table 5f. Nickel(II) salt screen for the reductive coupling of HCF$_2$Cl and 4-iodobiphenyl.

Concentration effect. In contrast to our previous difluoromethylation strategy using (DMPU)$_2$Zn(CF$_2$H)$_2$, this protocol favored diluted reaction mixtures. The benefit of dilution stopped at certain level, as shown in Table 5g. We also noticed that using more volume of pyridine increased the amount of difluoromethylated pyridine byproducts.
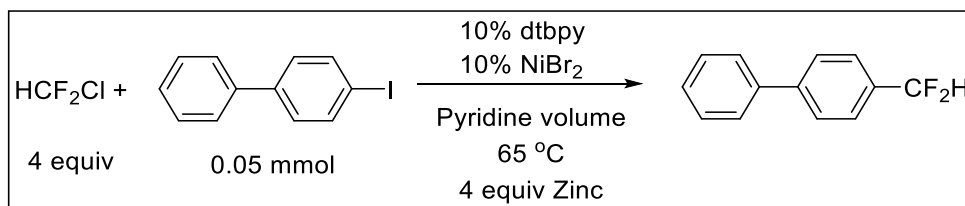
Entry	Ligand	Catalyst	Volume of solvent	Temperature	Aryl halide	Yield
1		(dmobpy)NiBr$_2$	0.25 ml	65 °C	4-iodobiphenyl	18%
2		(dmobpy)NiBr$_2$	0.5 ml	65 °C	4-iodobiphenyl	34%
3		(dmobpy)NiBr$_2$	1.0 ml	65 °C	4-iodobiphenyl	40%
4		(dmobpy)NiBr$_2$	1.5 ml	65 °C	4-iodobiphenyl	41%
5		(dmobpy)NiBr$_2$	2.0 ml	65 °C	4-iodobiphenyl	40%

Table 5g. Concentration effect for the reductive coupling of HCF$_2$Cl and 4-iodobiphenyl.

Iodide additives. It is known that addition of catalytic amounts of sodium iodide provided higher yields of nickel-catalyzed reductive coupling. The role of the iodide may be to (1) help facilitate reduction of the nickel catalyst by acting as a bridging ligand with zinc;[18] (2) promote formation of more reactive nickelate complexes;[19] (3) generate a small amount of the more reactive alkyl iodide *in situ*.[20]

In contrast to the previous work, the addition of sodium iodide was not beneficial for reactions conducted in our lab. Reactions conducted with different sources of iodide (tetrabutylammonium iodide and potassium iodide) all showed the same detrimental effect as shown in Table 5h. To rule out the difluorocarbene pathway, we tested two bases in the system, however, the addition of bases lowered the yield a lot (Table 5h, entry 4 and 5).
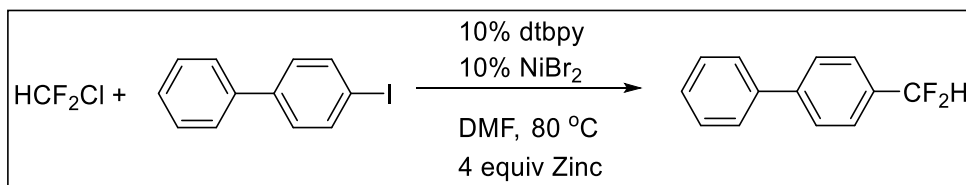
Entry	Ligand	Catalyst	Additives	Temperature	Aryl halide	Yield
1		(dtbpy)NiI$_2$	NaI	65 °C	4-iodobiphenyl	12%
2		(dtbpy)NiI$_2$	TABI	65 °C	4-iodobiphenyl	10%
3		(dtbpy)NiI$_2$	KI	65 °C	4-iodobiphenyl	13%
4		(dtbpy)NiI$_2$	Cs$_2$CO$_3$	65 °C	4-iodobiphenyl	11%
5		(dtbpy)NiI$_2$	*t*-BuOK	65 °C	4-iodobiphenyl	15%

Table 5h. Iodine additives effect for the reductive coupling of HCF$_2$Cl and 4-iodobiphenyl.

Substrate scope. With the current optimized condition in hand, we started to explore the substrate scope of this catalytic reaction. Interestingly, unlike our previous work, electron-rich aryl halides had better performance than electron-deficient ones. Alkylated aryl iodides were well-tolerated here while they gave none to very low yield in the case of conventional cross-coupling using $(DMPU)Zn(CF_2H)_2$. Electron-deficient ones like 4-iodobenzonitrile gave lower yield than phenyl iodide. This trend was coincident with our previous investigation that enrichment of electron-density on nickel would facilitate the activation of HCF_2Cl as the intermediates of Ni(EDG)X is more electron-dense than Ni(EWG)X. Aryl bromides worked similarly as aryl iodides, but aryl chlorides gave poor yields at current conditions. Further modification of the reaction system to utilize aryl chlorides will be of great value to make the reaction more economical. The preliminary screen of substrates is shown in Table 5i.
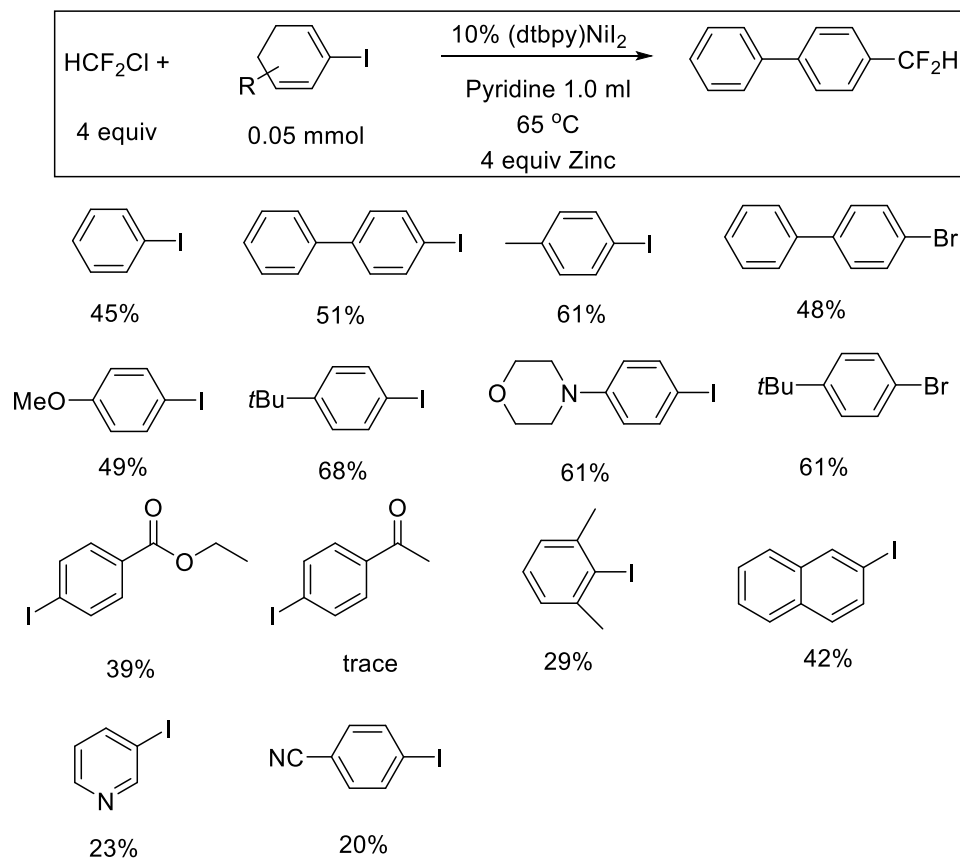
Table 5i. Substrate scope for the reductive coupling of HCF$_2$Cl and 4-iodobiphenyl.

5.3. Summary

This chapter has presented preliminary catalyst and reaction conditions developed for the nickel-catalyzed reductive cross-coupling of aryl iodides and bromides with HCF$_2$Cl. Such a reductive cross-coupling using this inexpensive source of CF$_2$H has never been demonstrated before. Additionally, early investigations into the mechanism of this new method were undertaken. Based on our work and prior literature, we proposed a tentative mechanism shown in Scheme 5e. The results, while promising, show that several improvements are needed to suppress some side reactions and increase the yield of difluoromethylated arenes. Isolation of possible intermediate [Ni(Ar)(CF$_2$H)] during this

process is desired to provide more evidence for the proposed mechanism. Bubbling the gaseous HCF_2Cl into polar solvents and storing the mixture in the freezer makes it a readily available source of HCF_2Cl. Hopefully, the catalytic reaction developed in this chapter will provide a convenient and cheap strategy to dilfuoromethylate aryl and heteroaryl halides with potentials to be applied in industry as well.
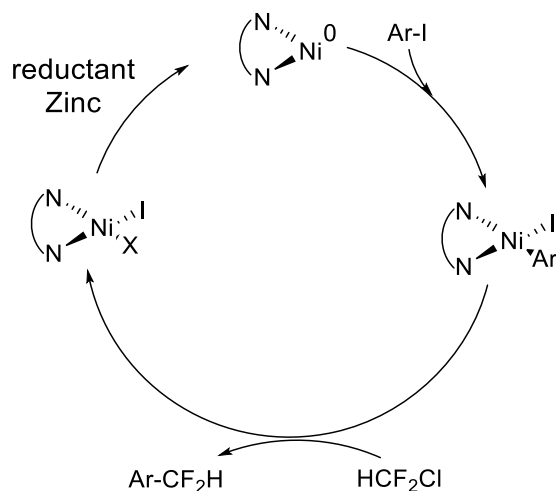
Scheme 5e. Proposed mechanism for the developed catalytic reaction

5.4. Experimental

5.4.1. General Information

All manipulations were performed in a nitrogen filled glovebox. Anhydrous solvents were purified by passing through activated alumina and/or copper in a solvent purification system supplied by Pure Process Technology or were purchased from Aldrich. chlorodifluoromethane was purchased from SynQuest Labs. Ni(II) salts, ligands, aryl iodides, aryl bromides and aryl triflates were purchased from Aldrich or Strem. All the

purchased reagents were used without further purificationSolution. [(dtbpy)NiX$_2$] was synthesized according to the literature.[6] ^{1}H NMR spectra were recorded at ambient temperature on a Bruker DRX 500 MHz spectrometer and referenced to residual proton solvent signals: CDCl$_3$ 7.26 ppm for ^{1}H and CD$_2$Cl$_2$ 5.30 ppm for ^{1}H. ^{19}F NMR spectra were recorded on the Bruker NMR spectrometer operating at 470 MHz and referenced to α,α,α-trifluorotoluene as an internal standard (δ = -63.7). Coupling constants (*J*) are reported in Hz and coupling patterns are described as br = broad, s = singlet, d = doublet, t = triplet, q = quartet, m = multiplet. A Bruker D8 Quest diffractometer was used for X-ray crystal structure determinations. GC-MS were recorded on a Shimadzu with positive ion mode.

5.4.2. General Procedure for the Reductive Coupling between ArX (X=I, Br) and HCF$_2$Cl
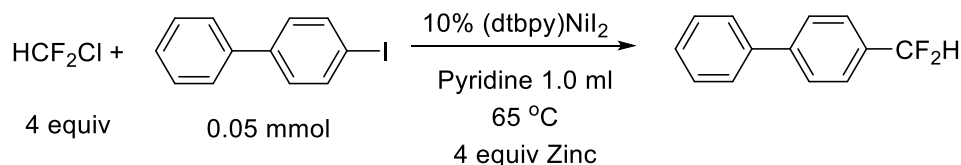
In a nitrogen-filled glove box, ArX (0.05 mmol, 1.0 equiv) and (dtbpy)NiI$_2$ (3.0 mg, 0.005 mmol, 0.1 equiv) were combined in a 5mL vial. To this vial was added 13 mg commercial-available zinc powder (0.2 mmol, 4 equiv) and 0.2 ml refrigerated 1M pyridine solution of HCF$_2$Cl (0.2 mmol, 4 equiv). The vial was sealed and stirred at 65 °C for 20 hours. The solution was then diluted with CH$_2$Cl$_2$ (15 mL). The mixture was filtered through a short plug of Celite, washed with H$_2$O (20 mL). The organic layer was combined, dried over NaSO$_4$, filtered, and concentrated under vacuum. The crude product was purified by column chromatography on silica gel with hexane or hexane/Et$_2$O mixture as the eluent to give the product.

5.4.3. Analytical data for two isolated organic products on a 0.2 mmol scale
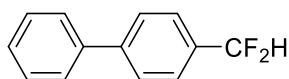
4-(difluoromethyl)-1,1'-biphenyl: The title compound was prepared following the standard procedure. After purification, it was isolated as white solid (16 mg, 40% yield). ^{1}H NMR (500 MHz, CDCl$_3$): δ= 7.69 (d, J = 8.0 Hz, 2H), 7.63 – 7.55 (m, 4H), 7.52 – 7.45 (m, 2H), 7.43 – 7.37 (m, 1H), 6.71 ppm(t, J = 56.5 Hz, 1H); ^{19}F NMR (470 MHz, CDCl$_3$): δ= -111.47 ppm (d, J = 56.1 Hz); ^{13}C NMR (126 MHz, CDCl$_3$) δ= 143.82 (t, J = 2.5 Hz)), 140.30, 133.34 (t, J = 22.7 Hz), 129.04, 128.03, 127.55, 127.37, 126.15 (t, J = 5.0 Hz), 114.89 ppm (t, J =239.4 Hz, CF$_2$H).
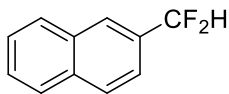
2-(difluoromethyl)naphthalene: The title compound was prepared following the standard procedure. After purification, it was isolated as white solid (13mg, 38% yield). ^{1}H NMR (400 MHz, CDCl3): δ= 8.10 – 7.80 (m, 4H), 7.77 – 7.40 (m, 3H), 6.82 ppm (t, J = 56.4 Hz, 1H); ^{19}F NMR (470 MHz, CDCl$_3$): δ= -111.66 ppm (d, J = 56.4 Hz). ^{13}C NMR (126 MHz, CDCl$_3$): δ= 134.33 (t, J = 1.4 Hz), 132.57, 131.64 (t, J = 22.3 Hz), 128.91, 128.54, 127.98, 127.50, 126.91,126.00 (t, J = 7.6 Hz), 122.12 (t, J = 4.8 Hz), 115.20 ppm (t, J = 238.5 Hz, CF$_2$H).

5.5. Reference

1. Xu, L.; Vicic, D. A. *J. Am. Chem. Soc.* **2016**, *138*, 2536.
2. Yu, X.;Yang, T.; Wang, S. L.;Xu, H; Gong, H. G. *Org. Lett.* **2011**, *13*, 2138.
3. M. R. Prinsell, D. A. Everson and D. J. Weix, *Chem. Commun.* **2010**, *46*, 5743.
4. H. Xu, C. Zhao, Q. Qian, W. Deng and H. Gong, *Chem. Sci.* **2013**, *4*, 4022.
5. W. Xue, H. Xu, Z. Liang, Q. Qian and H. Gong, *Org. Lett.* **2014**, *16*, 4984.
6. Z. Liang, W. Xue, K. Lin and H. Gong, *Org. Lett.* **2014**, *16*, 5620.
7. L. L. Anka-Lufford, M. R. Prinsell and D. J. Weix, *J. Org. Chem.* **2012**, *77*, 9989.
8. S. Biswas and D. J. Weix, *J. Am. Chem. Soc.* **2013**, *135*, 16192.
9. C. Yan, Y. Peng, X. Xu and Y. Wang, *Chem. – Eur. J.* **2012**, *18*, 6039.
10. A. C. Wotal and D. J. Weix, *Org. Lett.* **2012**, *14*, 1476.
11. Y. Zhao and D. J. Weix, *J. Am. Chem. Soc.* **2014**, *136*, 48.
12. L. K. G. Ackerman, L. L. Anka-Lufford, M. Naodovic; D. J. Weix, *Chem. Sci.* **2014**, *6*, 1115.
13. S. Wang; Q. Qian; H. Gong, *Org. Lett.* **2012**, *14*, 3352.
14. Everson, D. A.; Jones, B. A.; Weix, D. J. *J. Am. Chem. Soc.* **2012**, *134*, 6146.
15. Burton, D. J.; Hartgraves, G. A. *J. Fluorine Chem.* **2007**, *128*, 1198-1215.
16. Miller T. G.; Thanassi J. W. *J. Org. Chem.* **1960**, *25*, 2009.
17. Morimoto, K.; Makino,K.; Sakata, G. *J. Fluorine Chem.* **1992**, *59*, 417.
18. Terao, J.; Watanabe, H.; Ikumi, A.; Kuniyasu, H.; Kambe, N. *J. Am. Chem. Soc.* **2002**, *124,* 4222.
19. Takahashi, H.; Inagaki, S.; Nishihara, Y.; Shibata, T.; Takagi, K. *Org. Lett.* **2006**, *8,* 3037.
20. Klein, A.; Kaiser, A.; Wielandt, W.; Belaj, F.; Wendel, E.; Bertagnolli, H.; Zális, S. *Inorg. Chem.* **2008**, *47,* 11324.

Appendix

NMR Spectra

Figure A1: ^{19}F NMR: (DMPU)$_2$Zn(CF$_2$H)$_2$ in CD$_2$Cl$_2$.
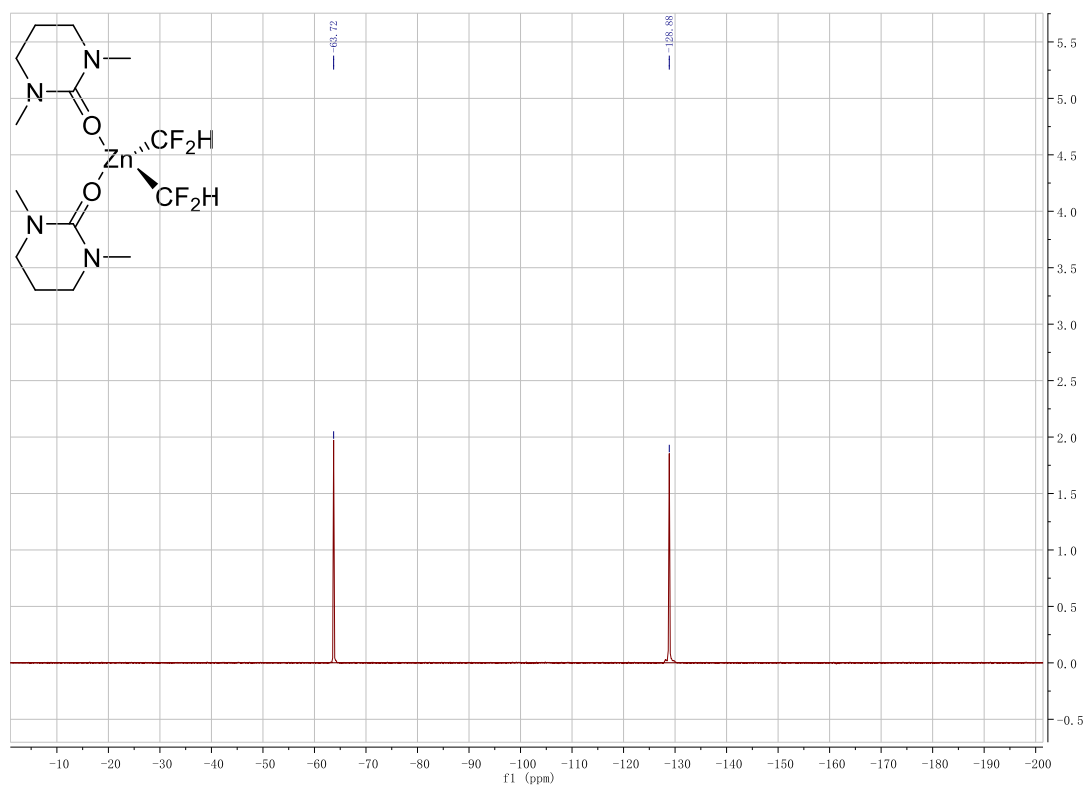
Figure A2: ^{1}H NMR (top) and 13C NMR (bottom): (DMPU)$_2$Zn(CF$_2$H)$_2$ in CD$_2$Cl$_2$.
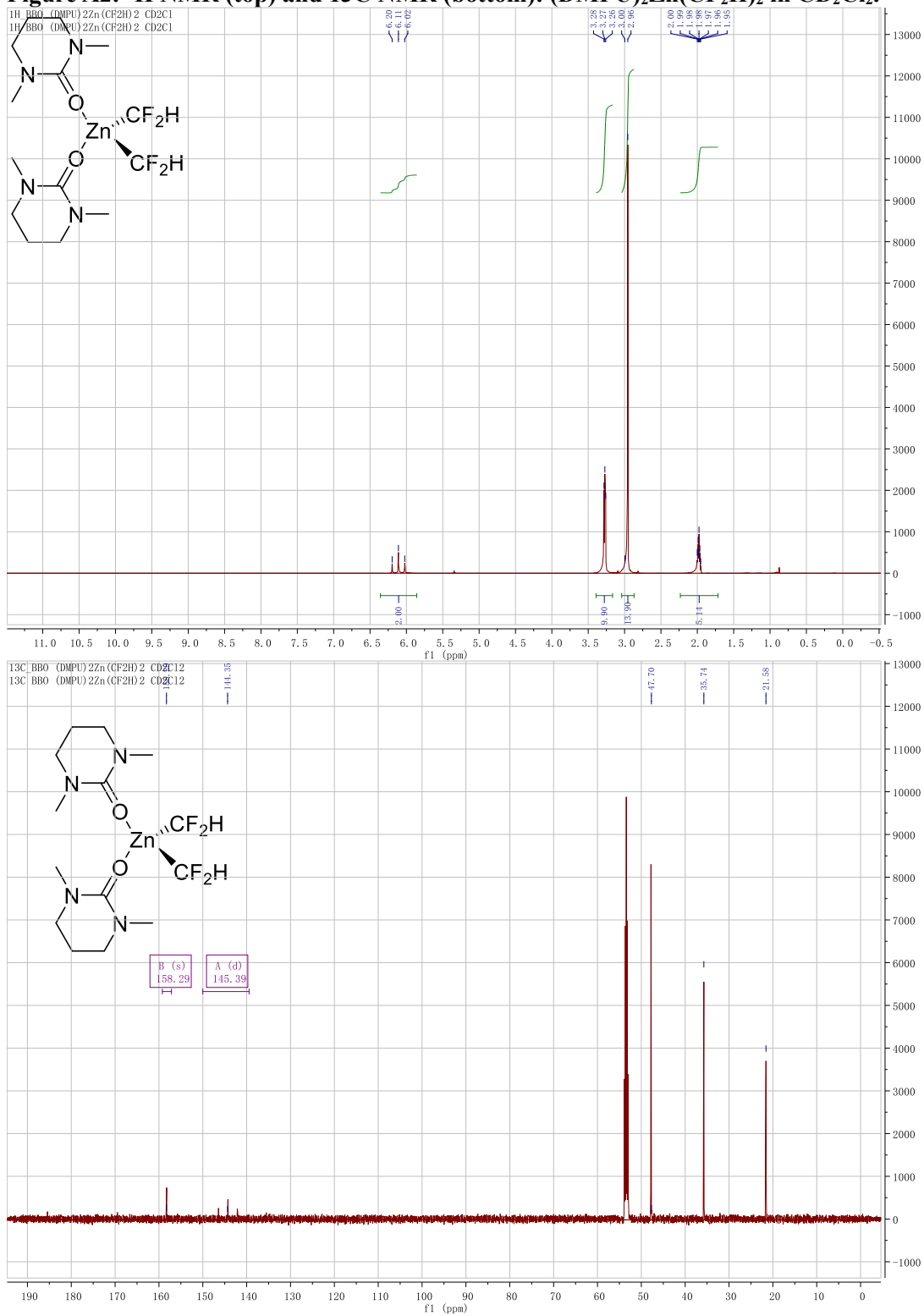
Figure A3: ^{19}F NMR (top), ^{1}H NMR (middle), and ^{13}C NMR (bottom) of 2-(difluoromethyl)dibenzofuran in CDCl$_3$.
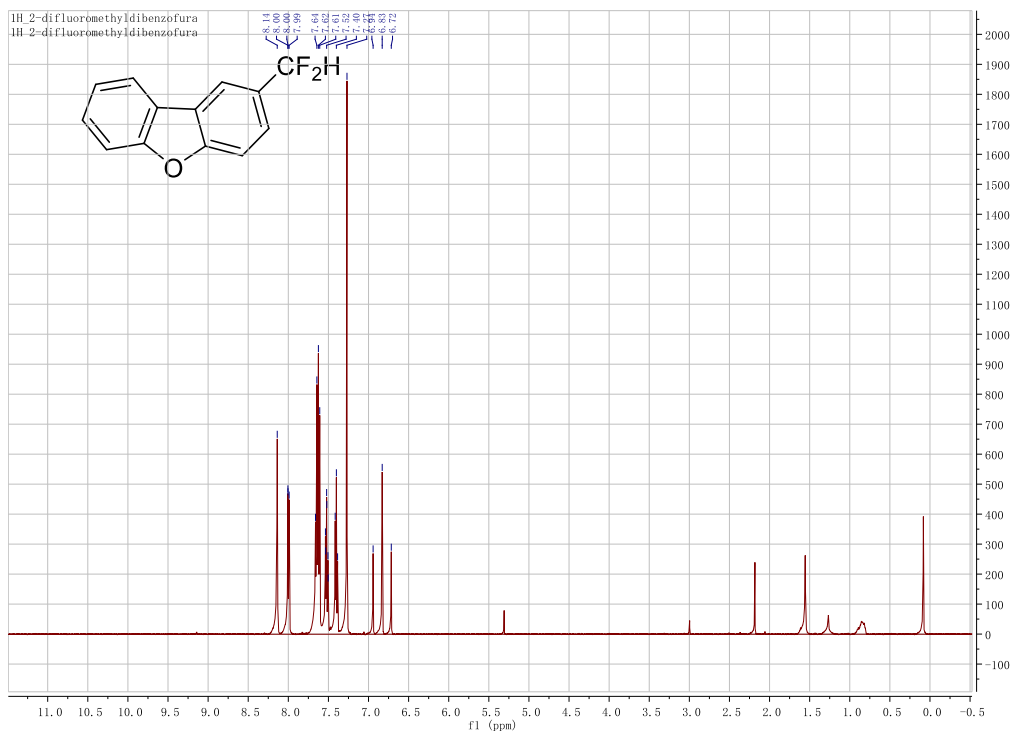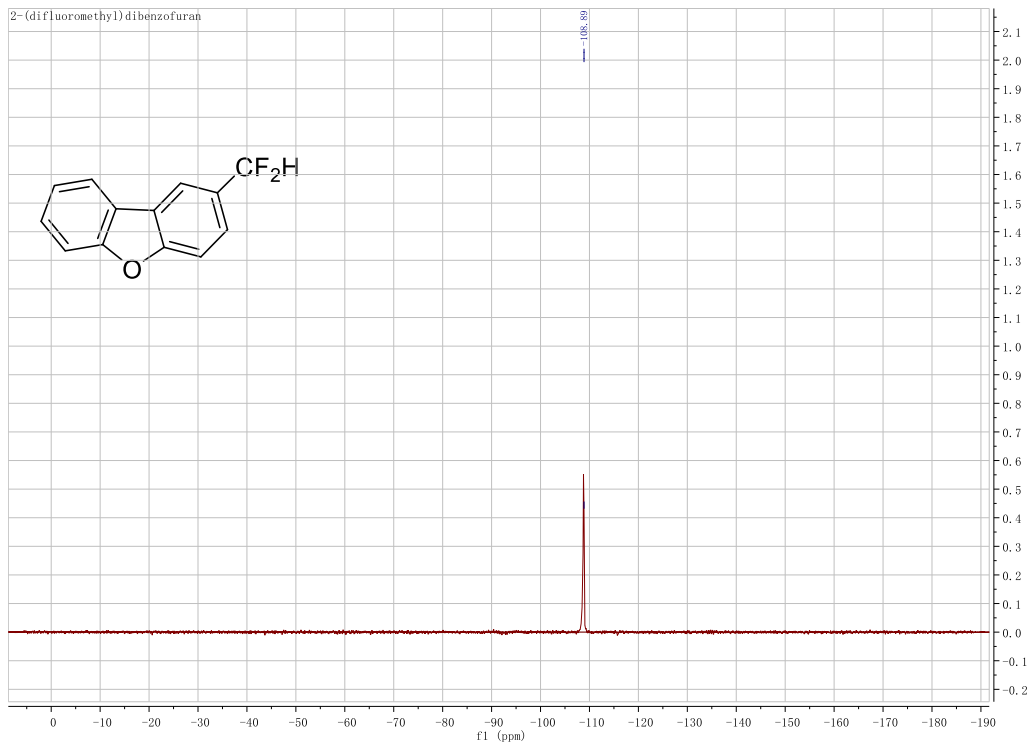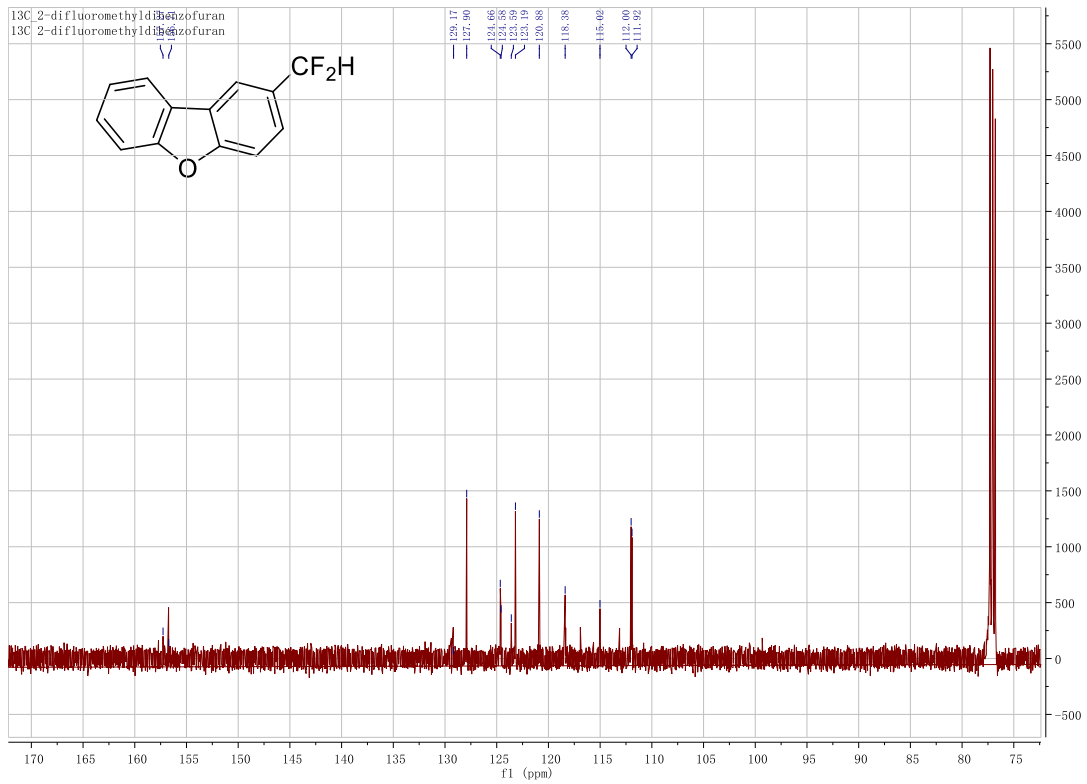
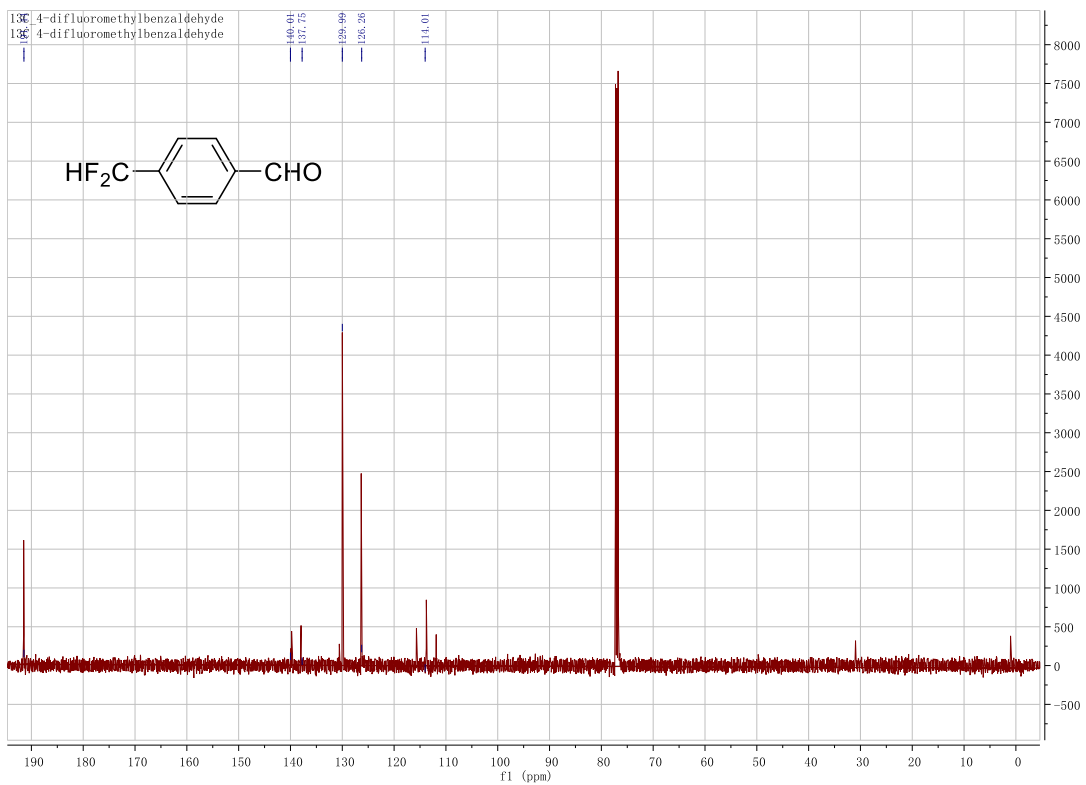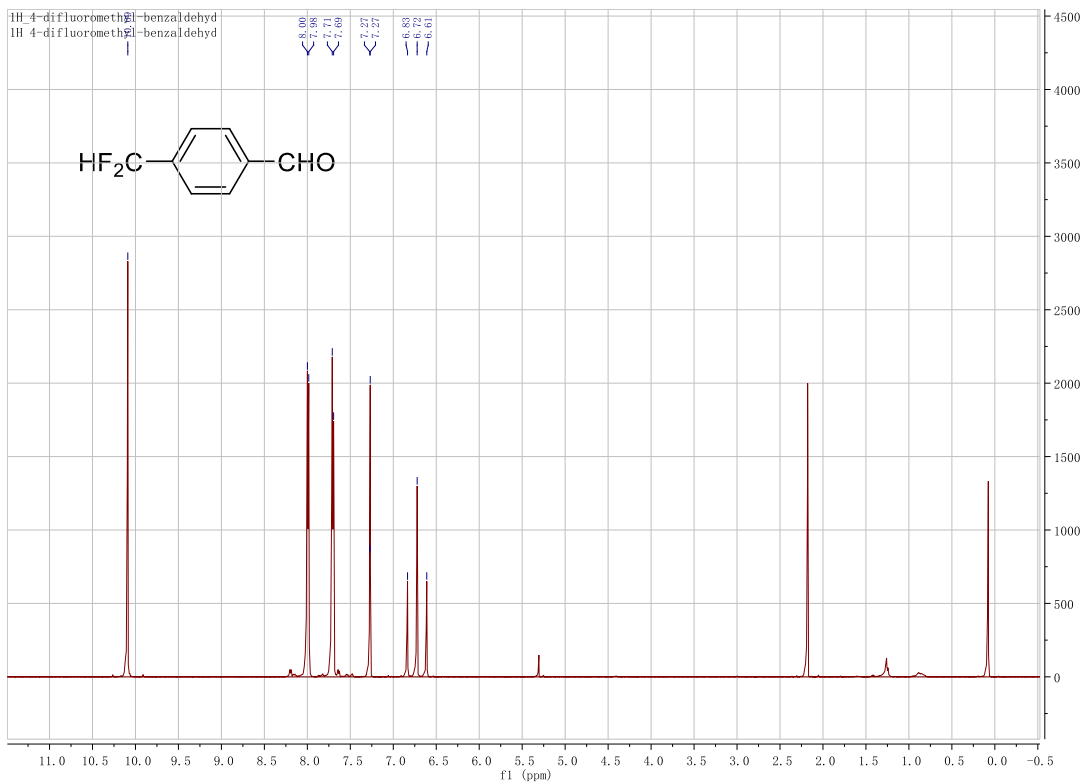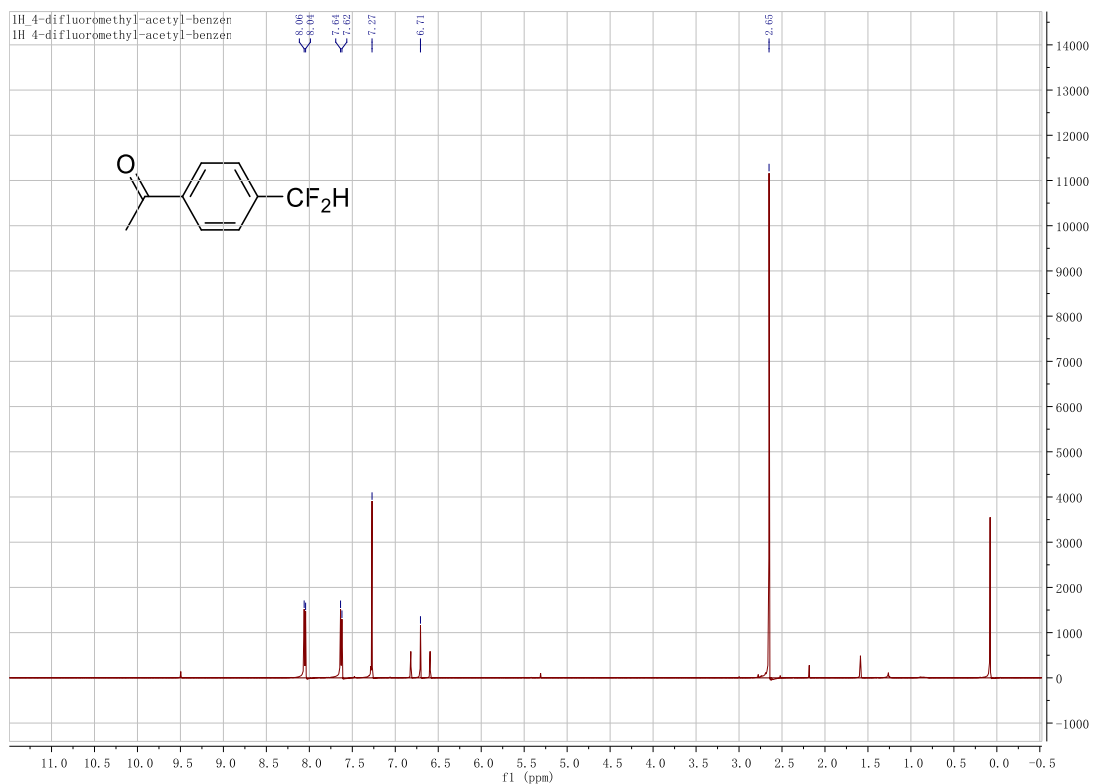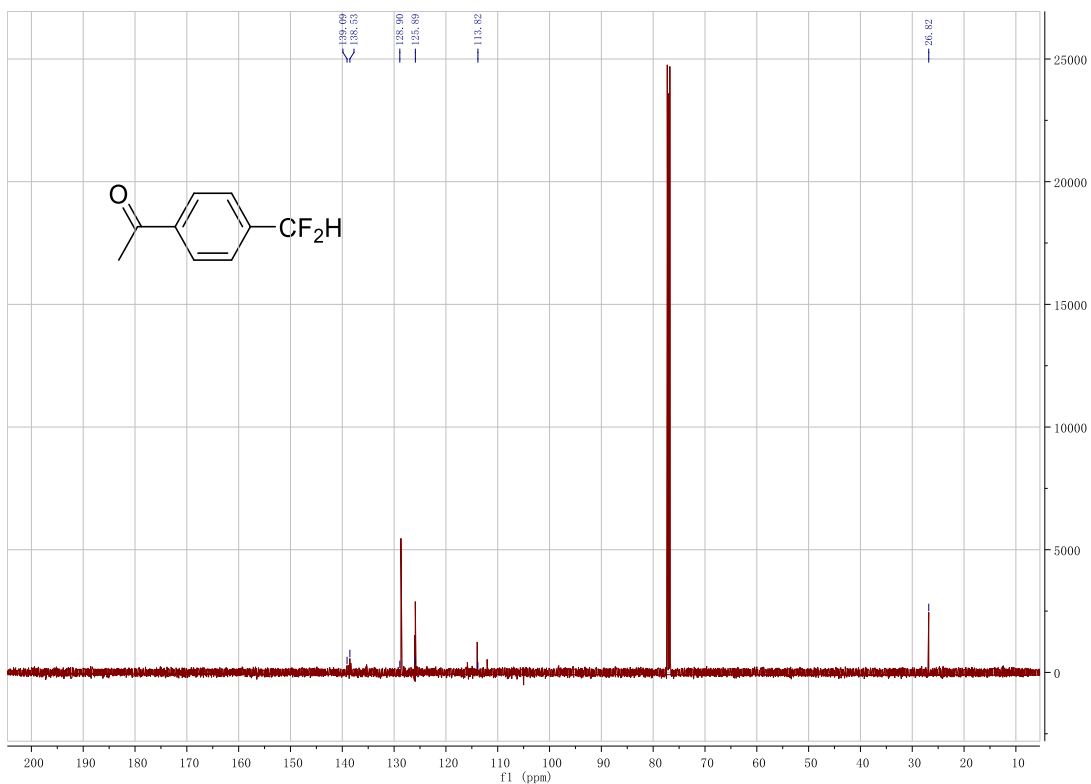**Figure A4: ^{19}F NMR (top), ^1H NMR (middle), and ^{13}C NMR (bottom) of 5-(difluoromethyl)-2-furaldehyde in CDCl$_3$.**

HF$_2$C —[O]— CHO

7.28
6.87
6.69

1.00
1.59
0.87
1.13

11.0 10.5 10.0 9.5 9.0 8.5 8.0 7.5 7.0 6.5 6.0 5.5 5.0 4.5 4.0 3.5 3.0 2.5 2.0 1.5 1.0 0.5 0.0 -0.5
f1 (ppm)

153.29
151.14

120.06
120.05

111.94
107.80
105.17

HF$_2$C —[O]— CHO

200 190 180 170 160 150 140 130 120 110 100 90 80 70 60 50 40 30 20 10
f1 (ppm)

109

Figure A5: ¹⁹F NMR (top), ¹H NMR (middle), and ¹³C NMR (bottom) of 4-(Difluoromethyl)-1,1'-biphenyl in CDCl₃.

13C 4-difluoromethyl-biphenyl in CD3Cl
13C 4-difluoromethyl-biphenyl in CD3Cl

Figure A6: ¹⁹F NMR (top), ¹H NMR (middle), and ¹³C NMR (bottom) of 2-(Difluoromethyl)naphthalene in CDCl₃.
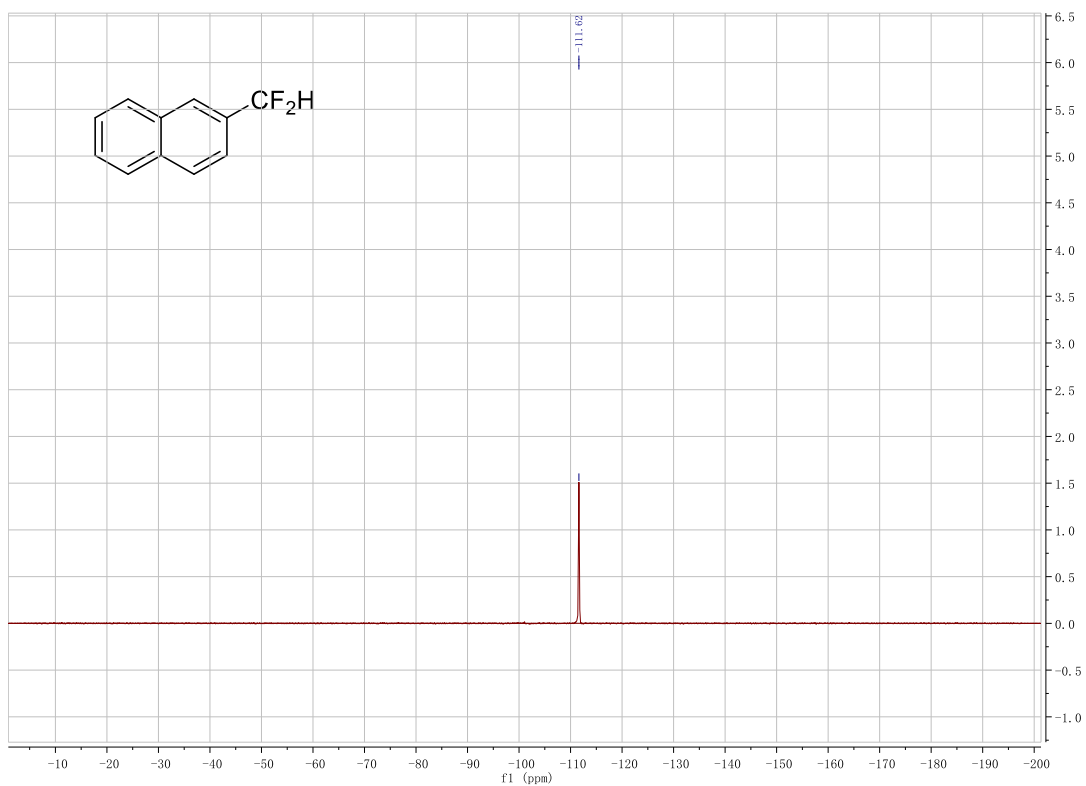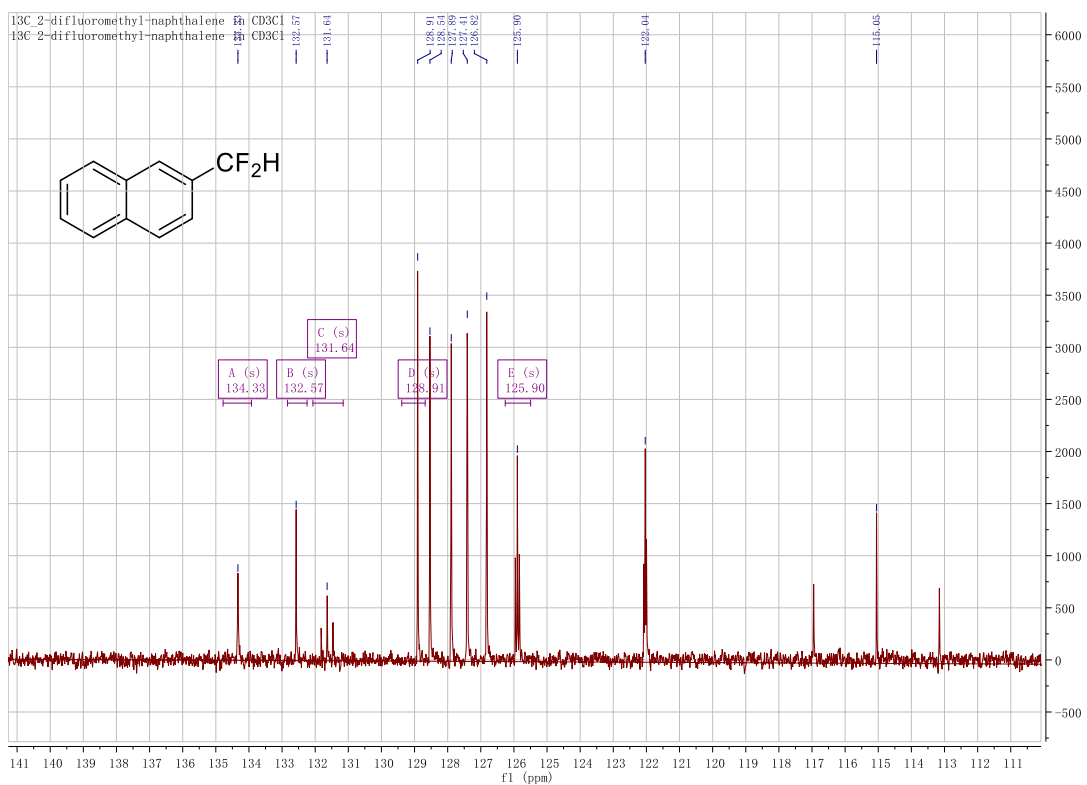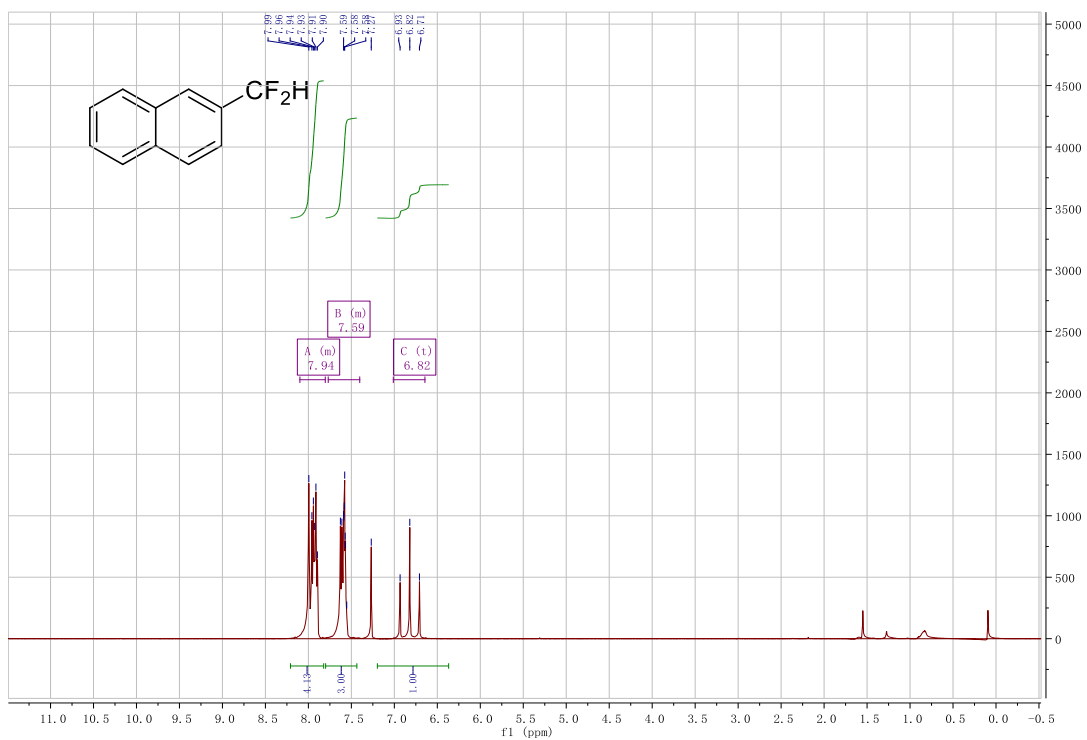
Figure A7: ^{19}F NMR (top), ^1H NMR (middle), and ^{13}C NMR (bottom) of (2-(difluoromethyl)phenyl)(phenyl)methanone in CDCl₃.
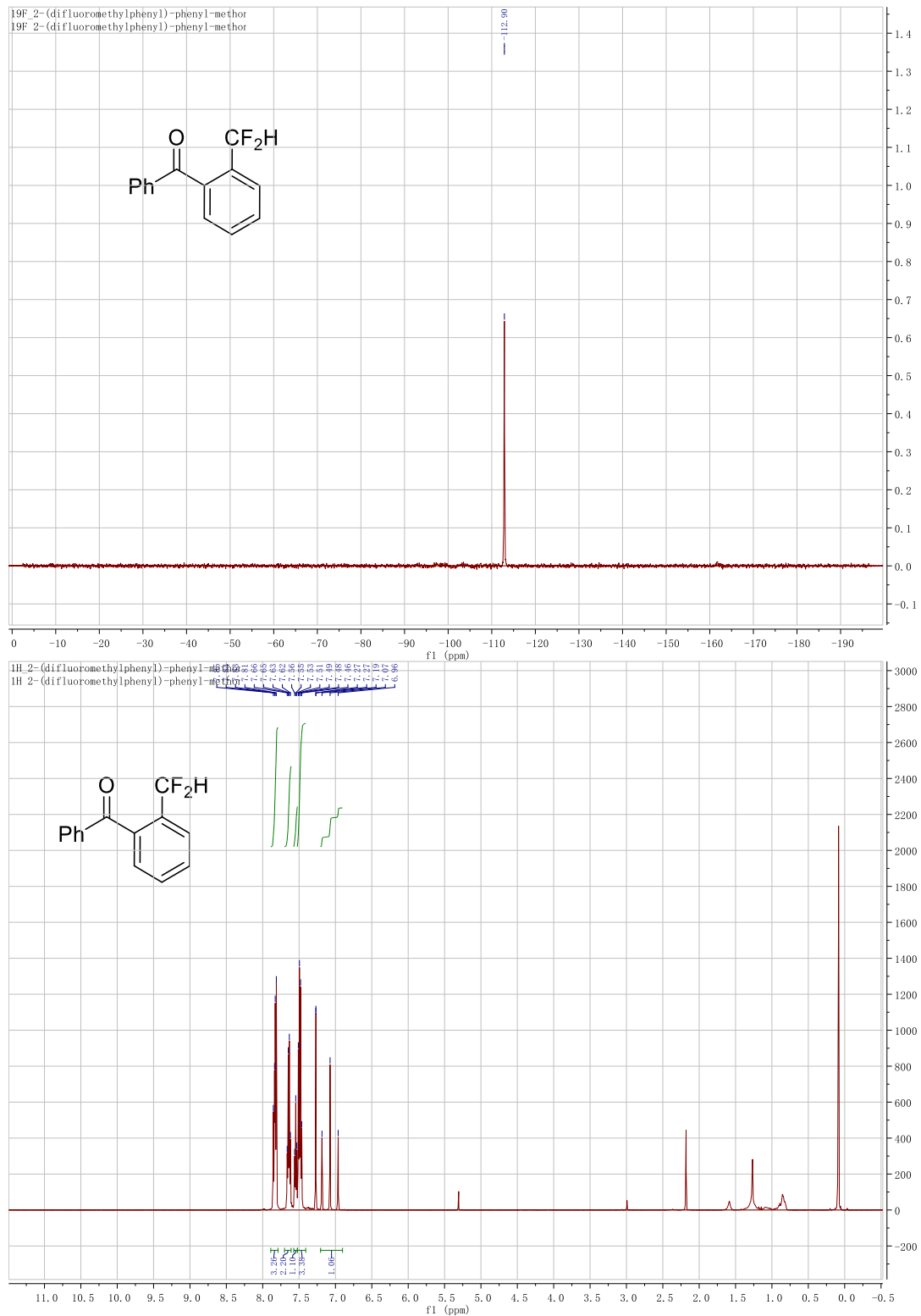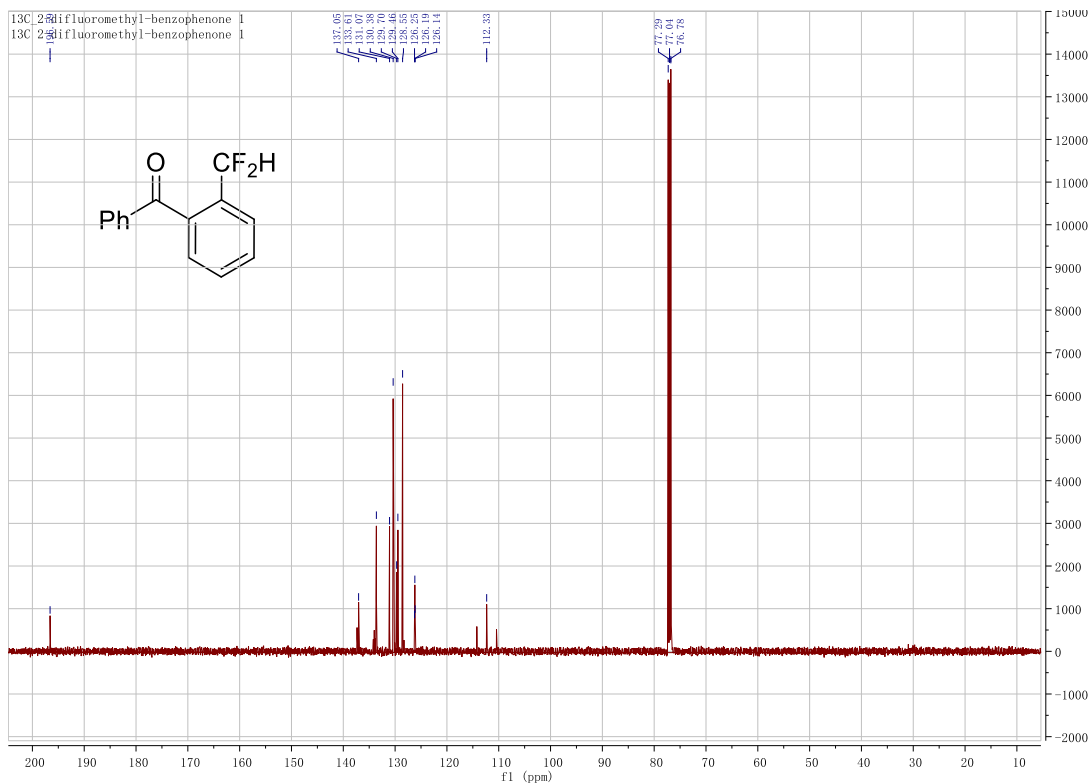
Figure A8: ^{19}F NMR (top), ^{1}H NMR (middle), and ^{13}C NMR (bottom) of methyl 4-(difluoromethyl)benzoate in CDCl₃.

1H_4-difluoromethyl methyl benzoat
1H 4-difluoromethyl methyl benzoat

8.14
8.13
7.61
7.59
7.27
6.81
6.70
6.59
3.96
3.94

HF₂C—⬡—C(=O)OMe

13C_4-difluoromethyl-methyl benzoate
13C 4-difluoromethyl-methyl benzoate

138.31
132.10
129.85
125.50
113.82
52.41

HF₂C—⬡—C(=O)OMe

115
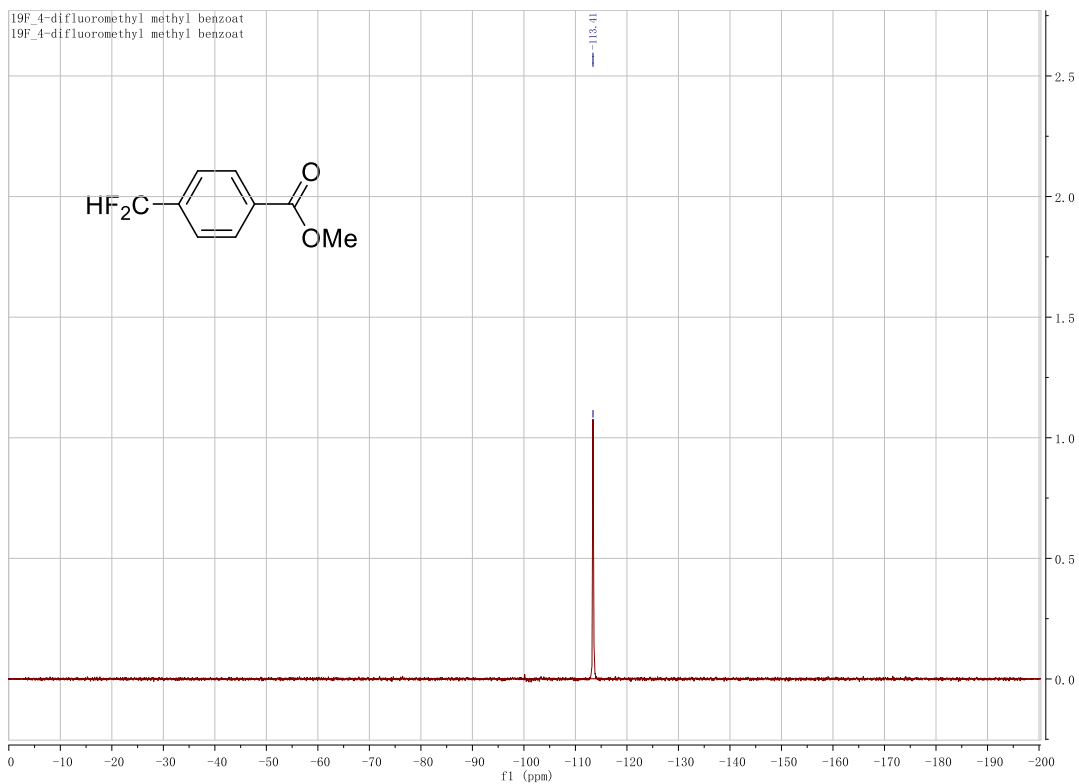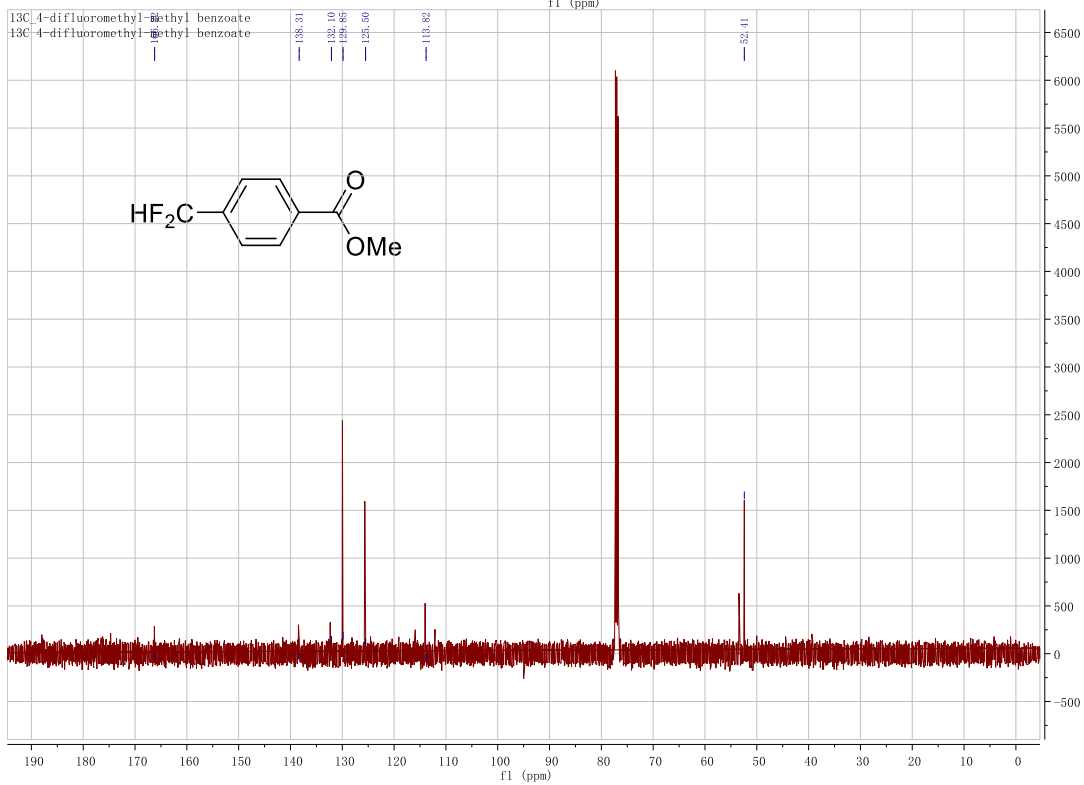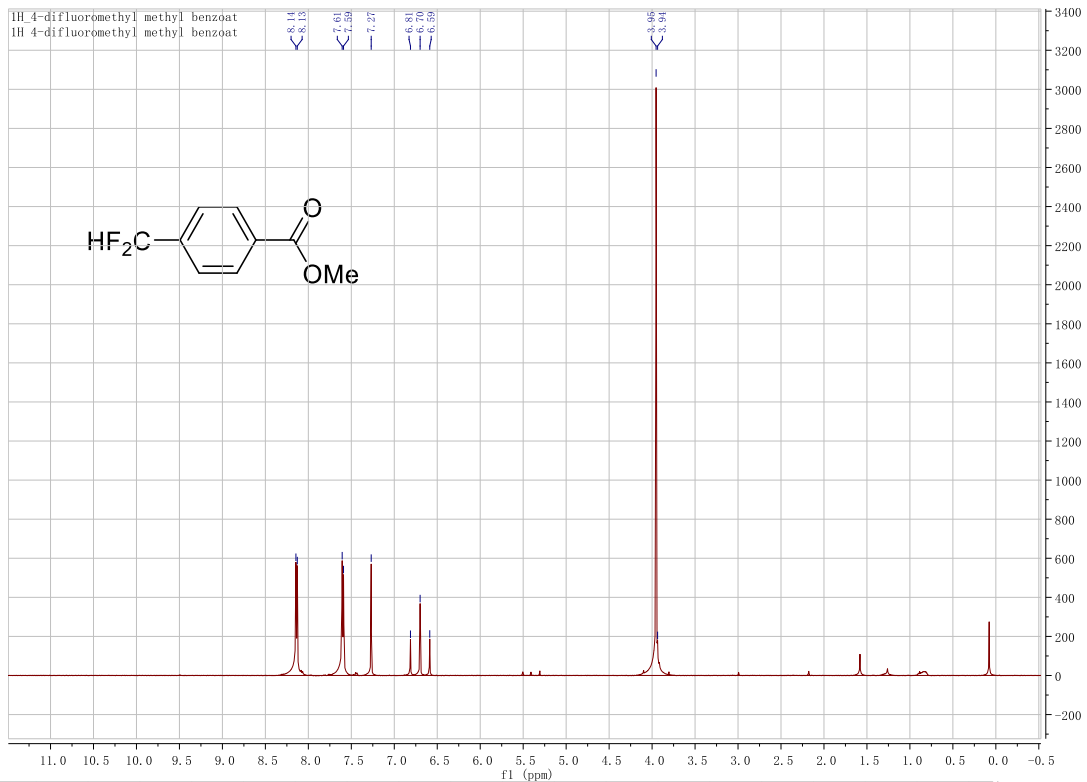
Figure A9: ^{19}F NMR (top), ^{1}H NMR (middle), and ^{13}C NMR (bottom) of ethyl 4-(difluoromethyl)benzoate in CDCl$_3$.
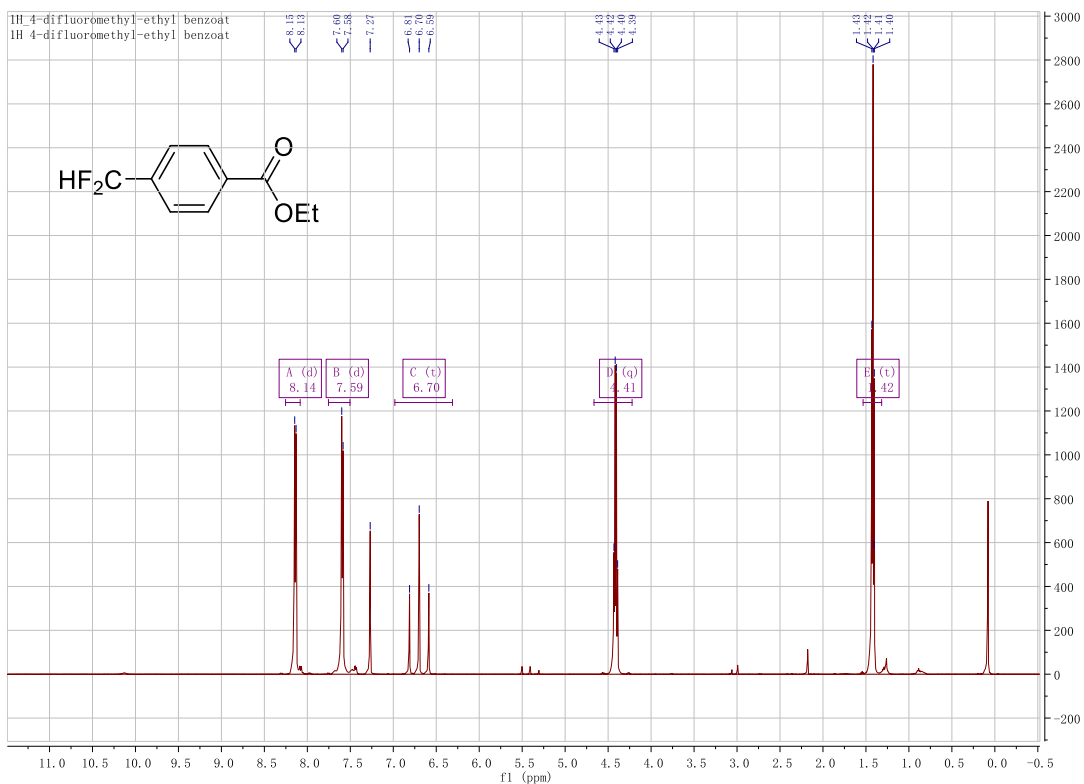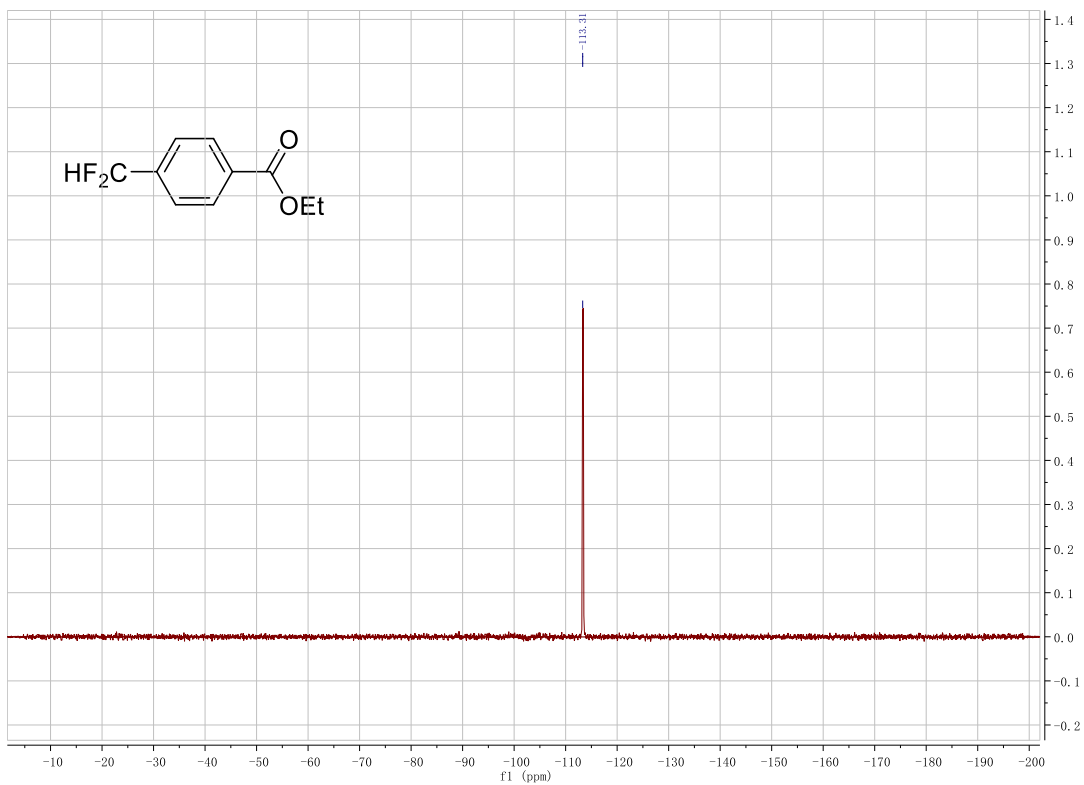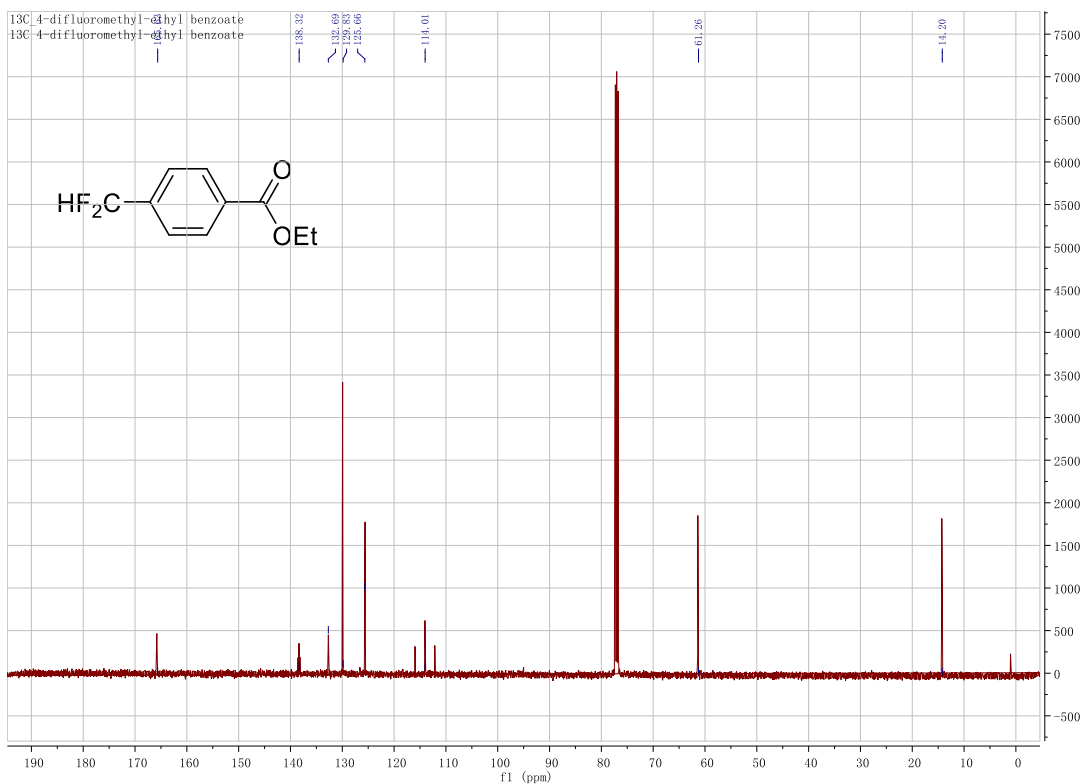
Figure A10: ¹⁹F NMR (top), ¹H NMR (middle), and ¹³C NMR (bottom) of 4-(Difluoromethyl)benzaldehyde in CDCl₃.

HF$_2$C——⟨benzene ring⟩——CHO

8.00
7.98
7.71
7.69
7.27
7.27
6.83
6.72
6.61

f1 (ppm)

HF$_2$C——⟨benzene ring⟩——CHO

140.01
137.75
129.99
126.26
114.01

f1 (ppm)

118
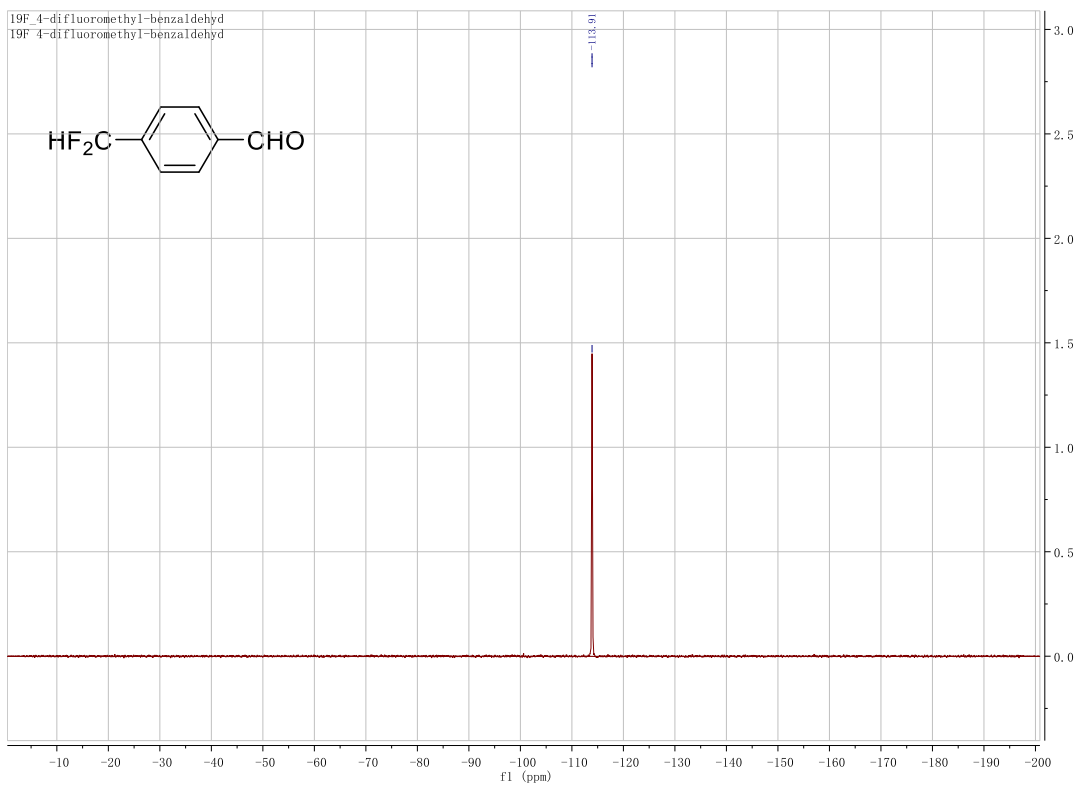
Figure A11: ^{19}F NMR (top), ^{1}H NMR (middle), and ^{13}C NMR (bottom) of 1-(4-(Difluoromethyl)phenyl)ethanone in CDCl₃.
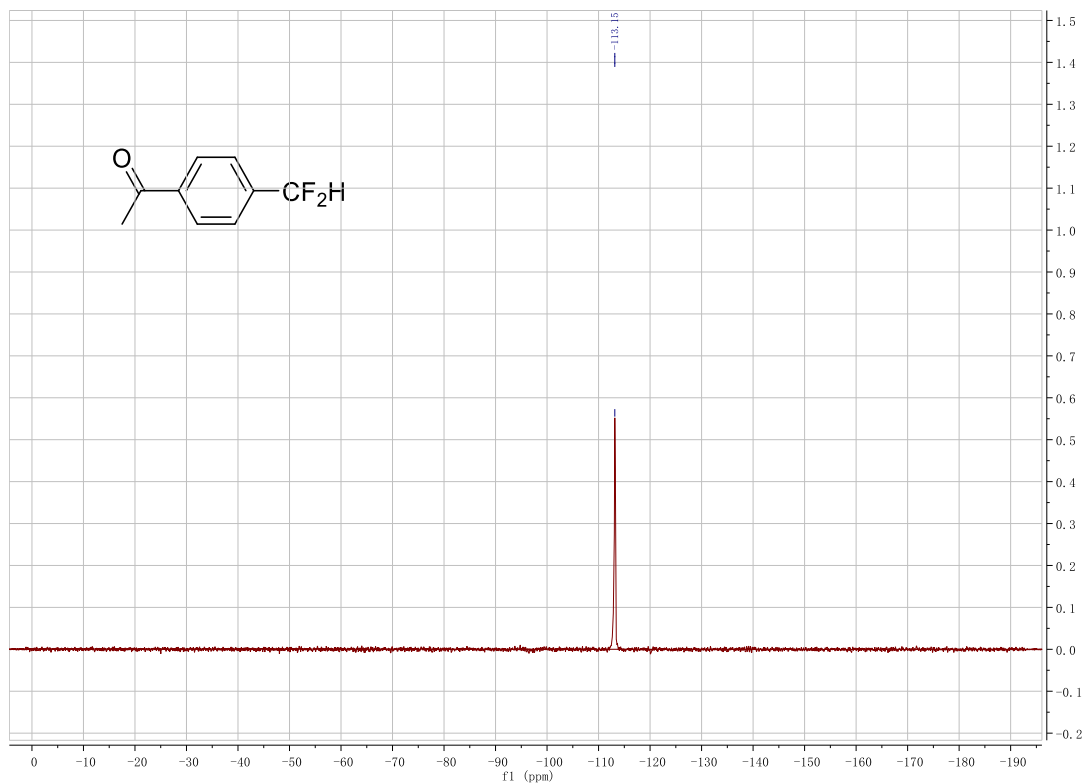
Figure A12: ^{19}F NMR (top), ^{1}H NMR (middle), and ^{13}C NMR (bottom) of 1-(3-(Difluoromethyl)phenyl)ethanone in CDCl$_3$.

1H_3-difluoromethyl-acetylbenzen
1H_3-difluoromethyl-acetylbenzen

8.10
8.09
8.07
7.74
7.72
7.60
7.59
7.27
7.27
6.71
2.65

2.00
0.99
0.98
1.00
3.31

13C_3-difluoromethyl-acetylbenzene 1
13C_3-difluoromethyl-acetylbenzene 1

137.49
130.49
129.99
129.21
125.52
114.13
77.31
77.06
76.80
67.98
42.71
30.94
26.67
25.61
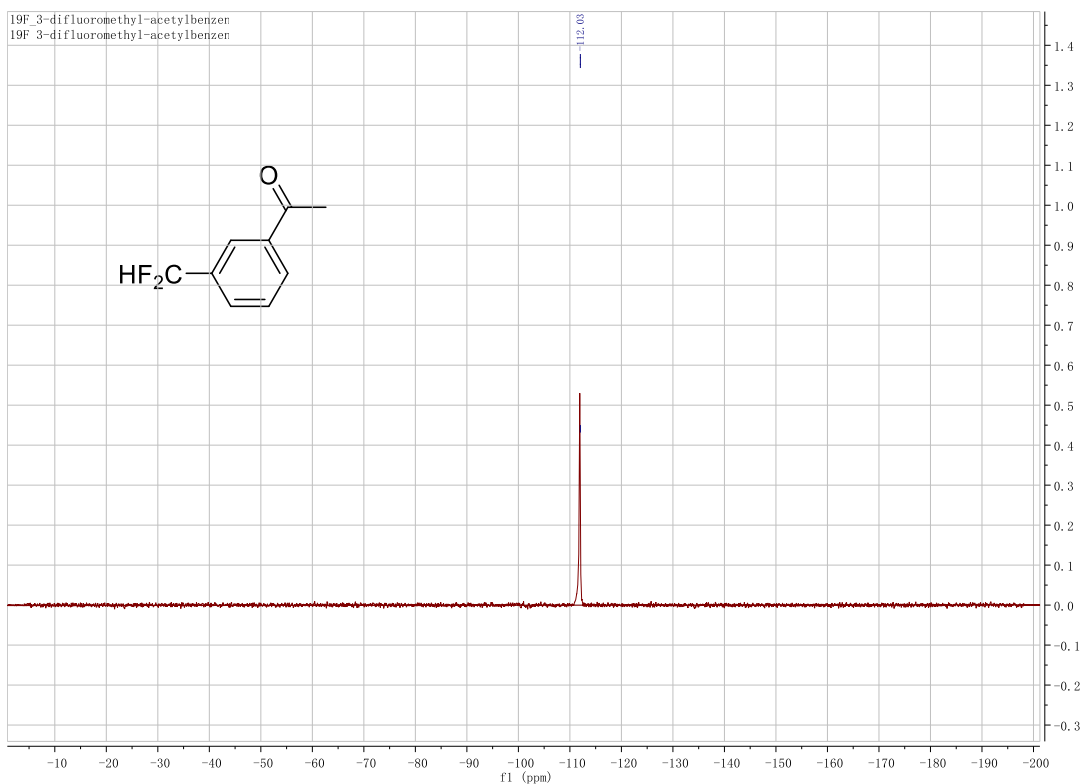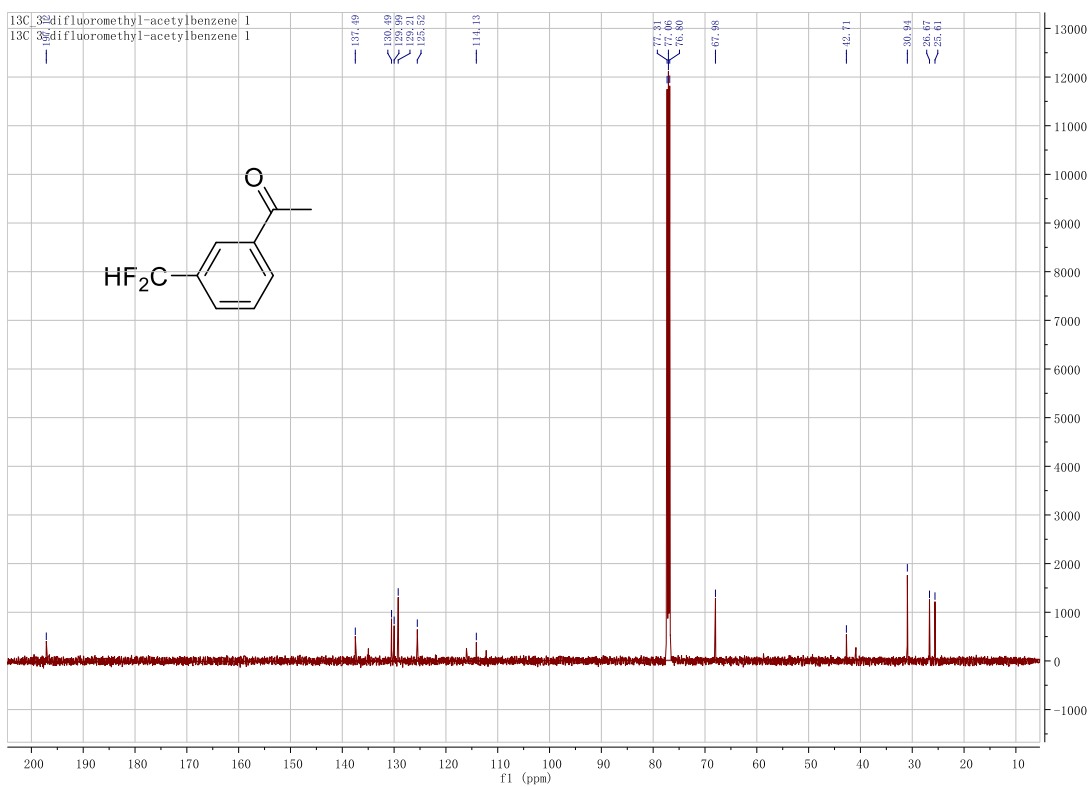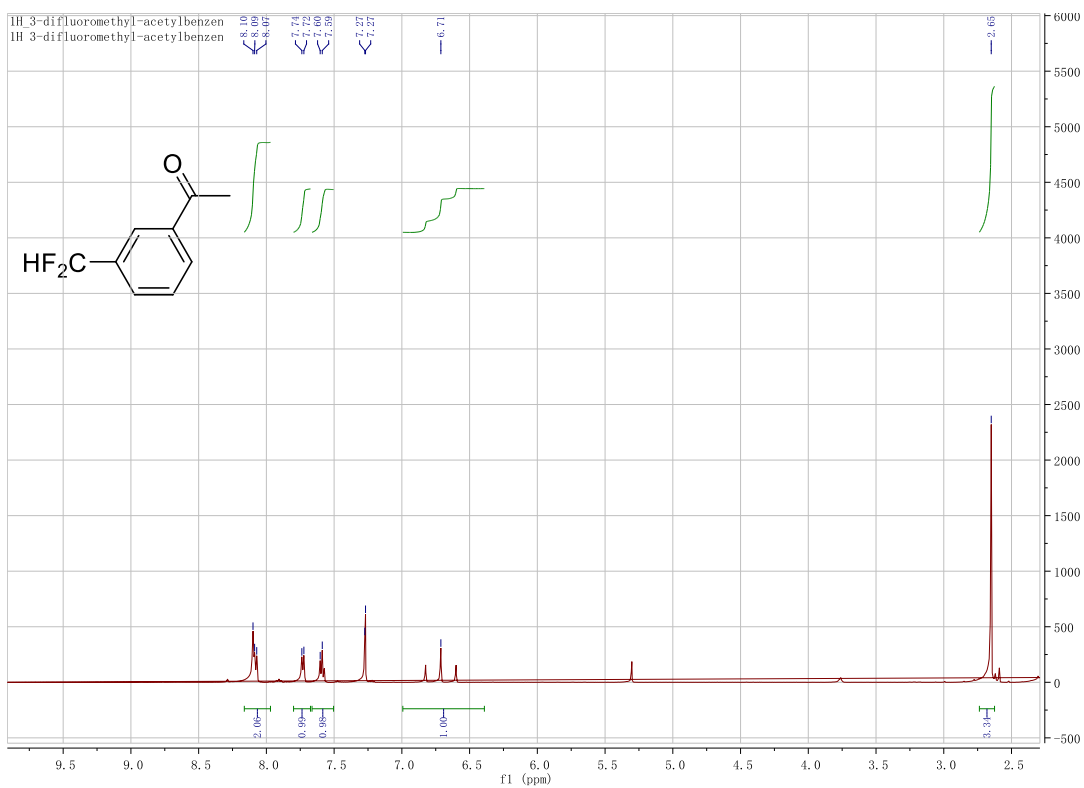
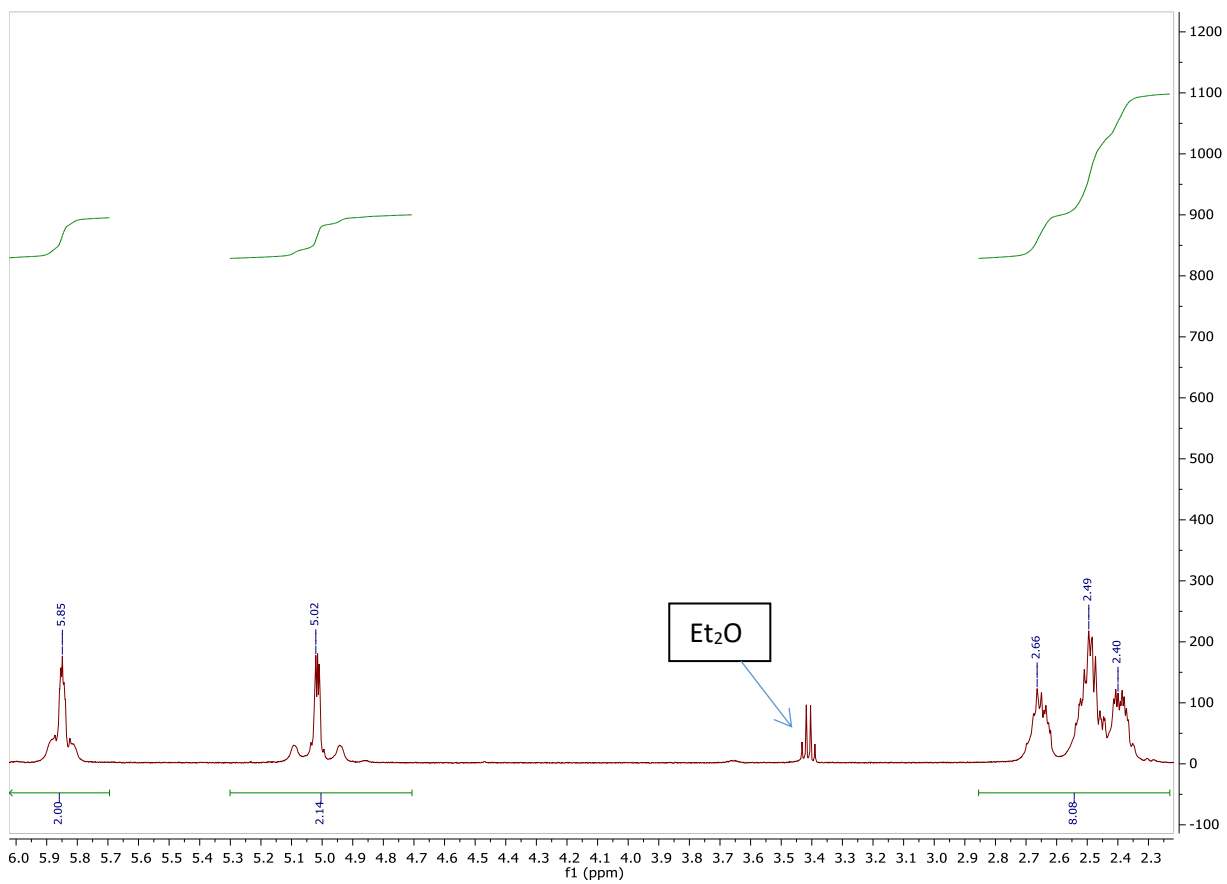**Figure A13:** ^{195}Pt NMR of **10** in CD_2Cl_2 with external [(COD)PtMe$_2$] standard.
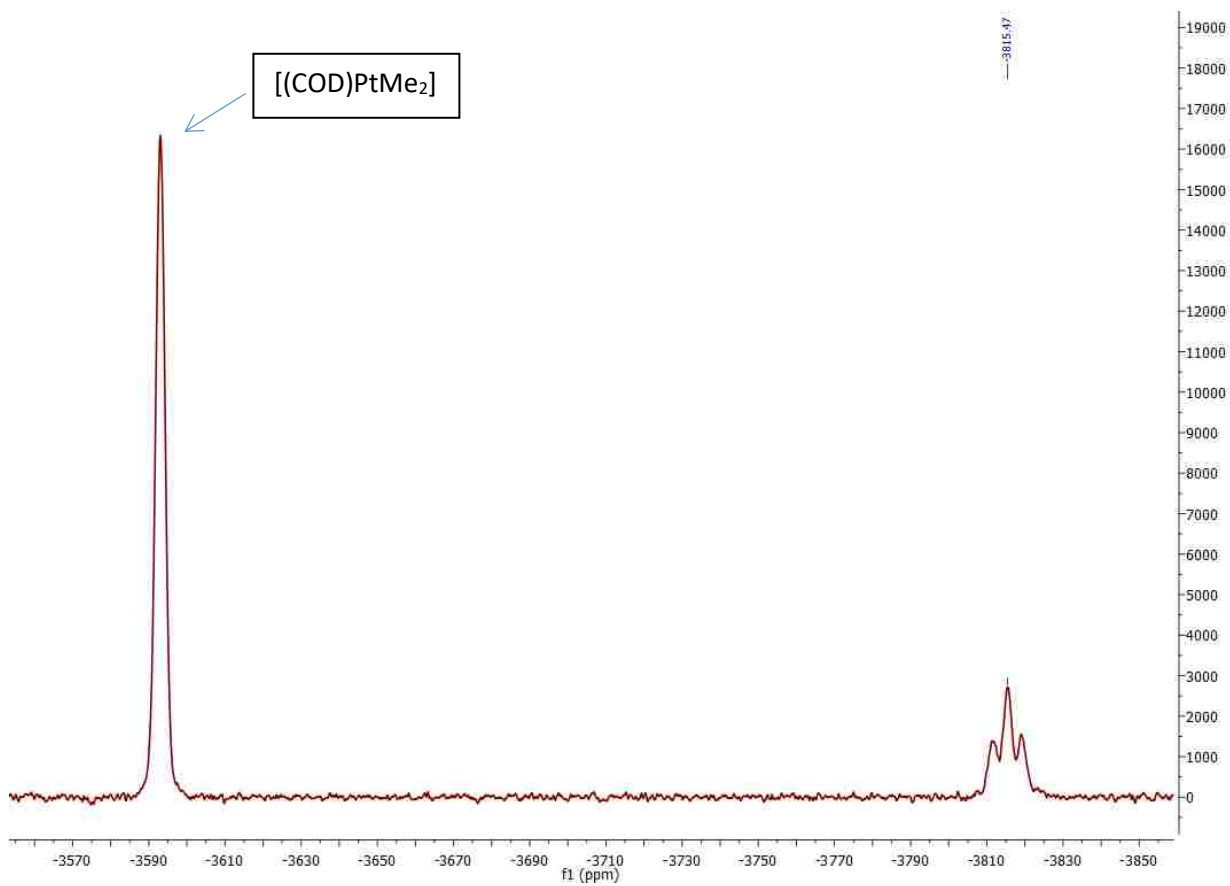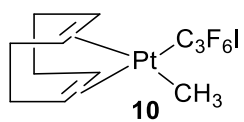
Figure A14: ^{19}F NMR of **10** in CDCl$_3$.
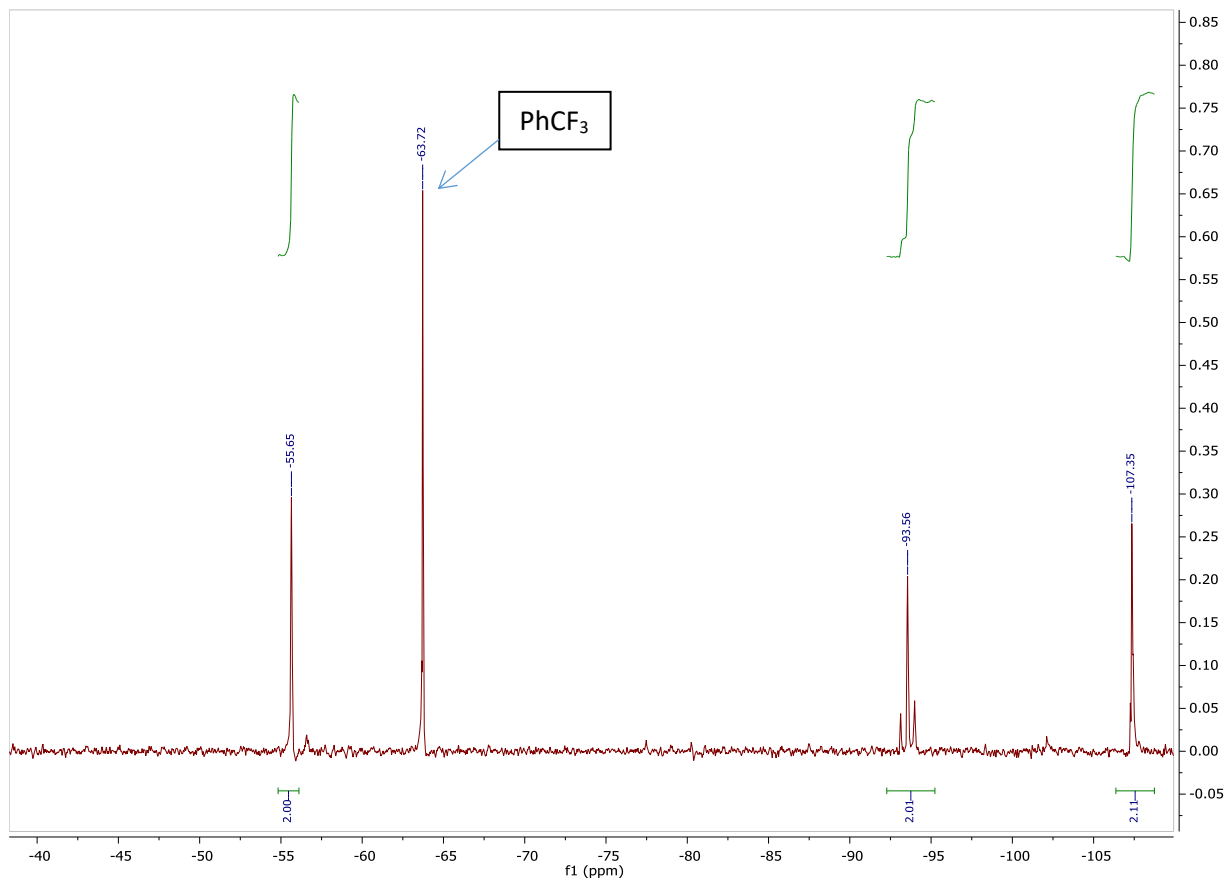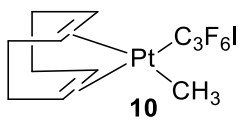
Figure A15: ^{1}H NMR of **10** in CDCl$_3$.
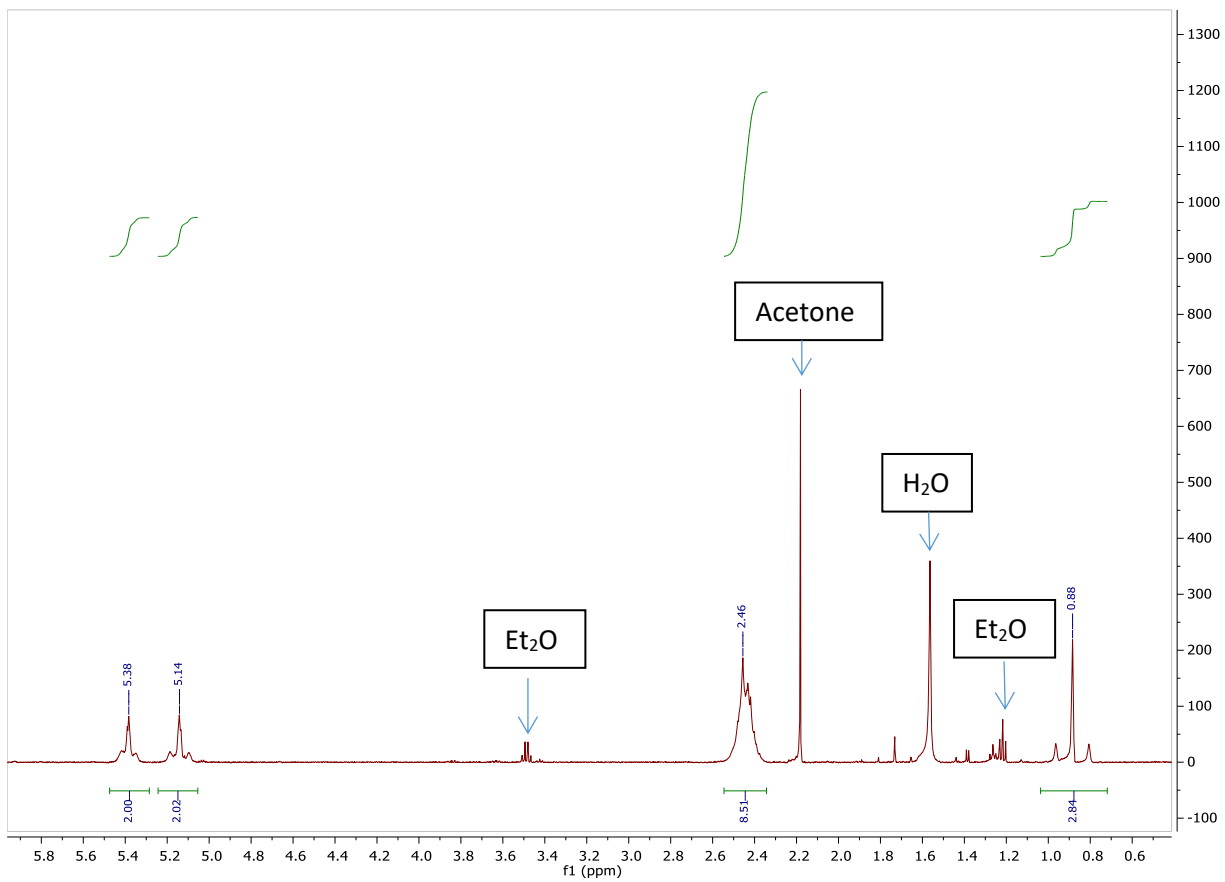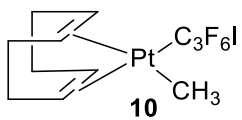
Figure A16: ^{19}F NMR of **11** in THF-d_8.
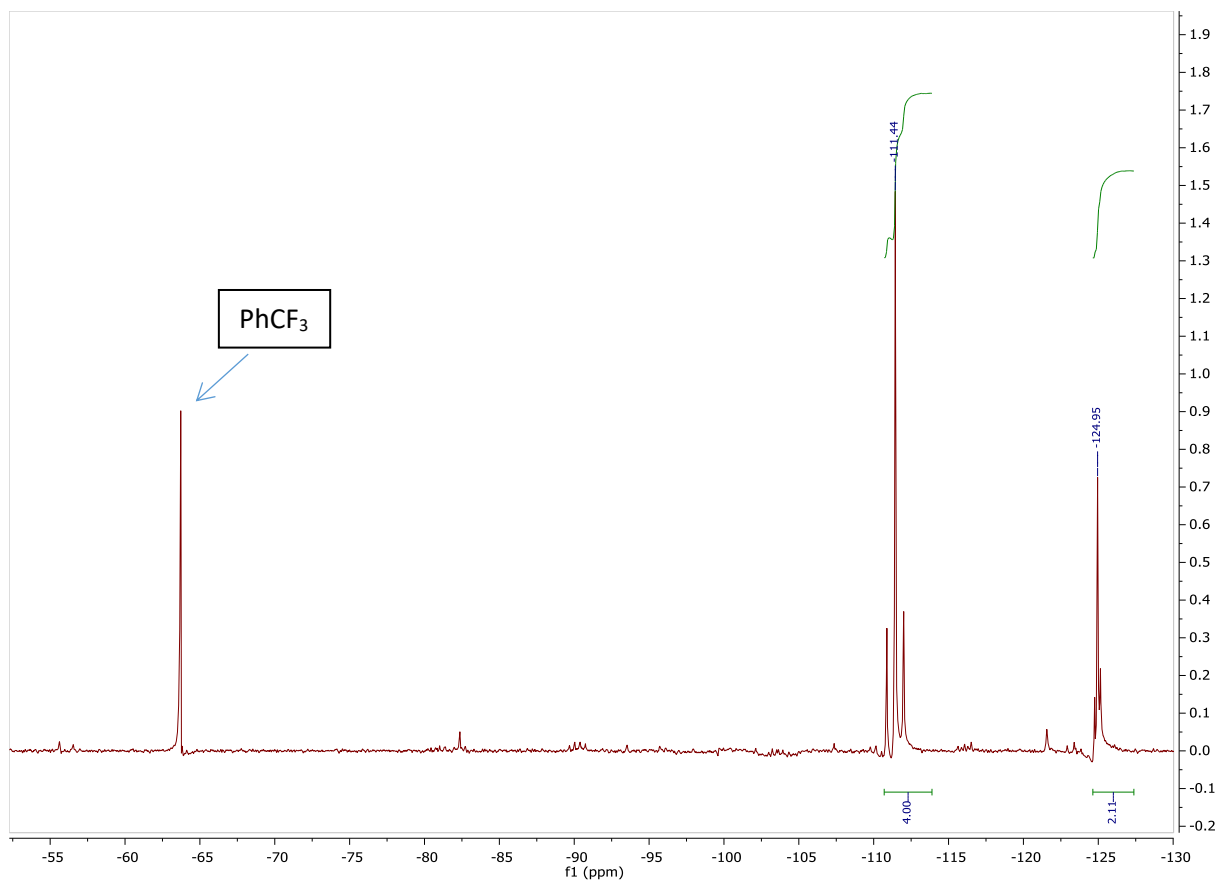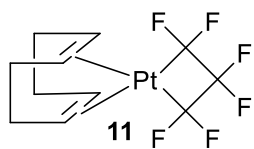
Figure A17: ^{1}H NMR of **11** in THF-d_8.
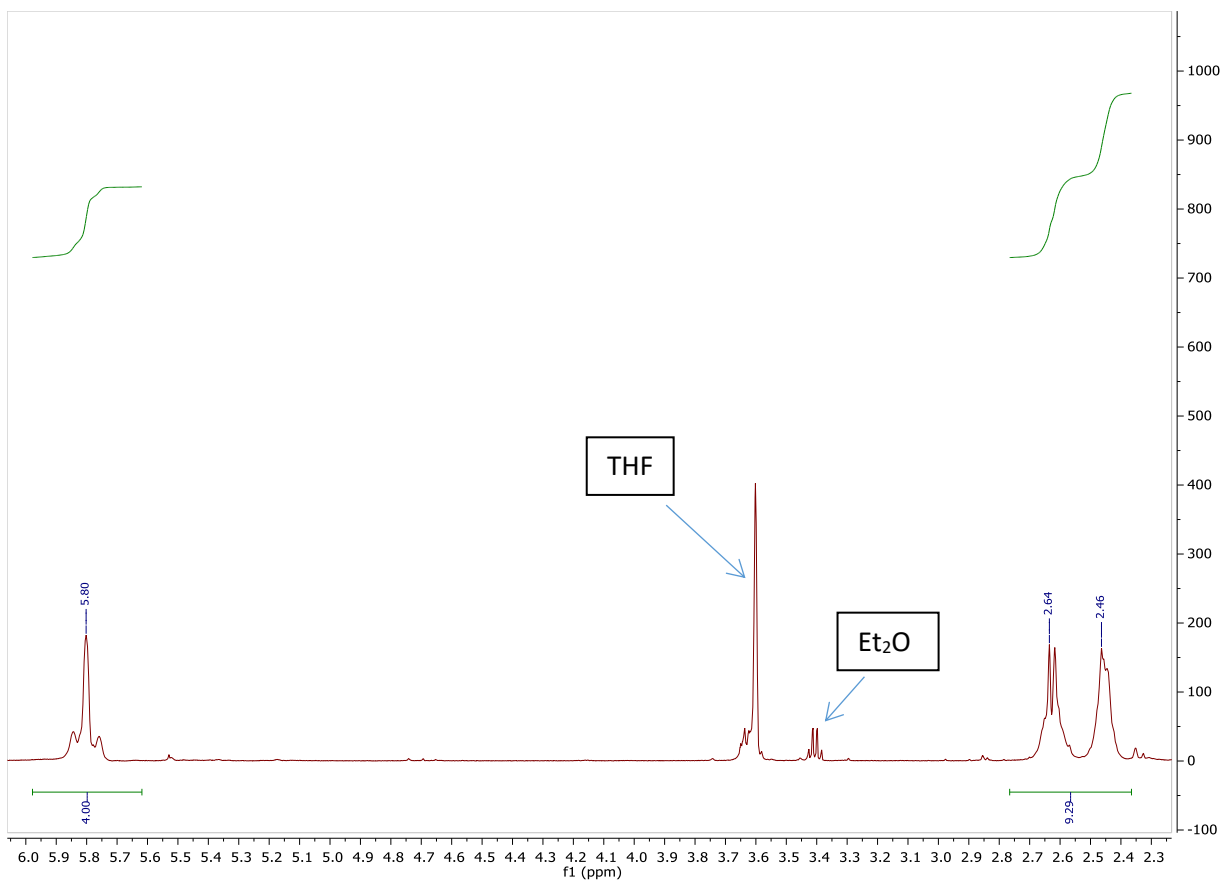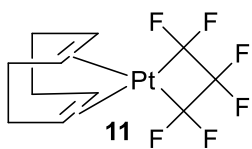
Figure A18: ^{195}Pt NMR of **11** in CD_2Cl_2 with external [(COD)PtMe$_2$] standard.
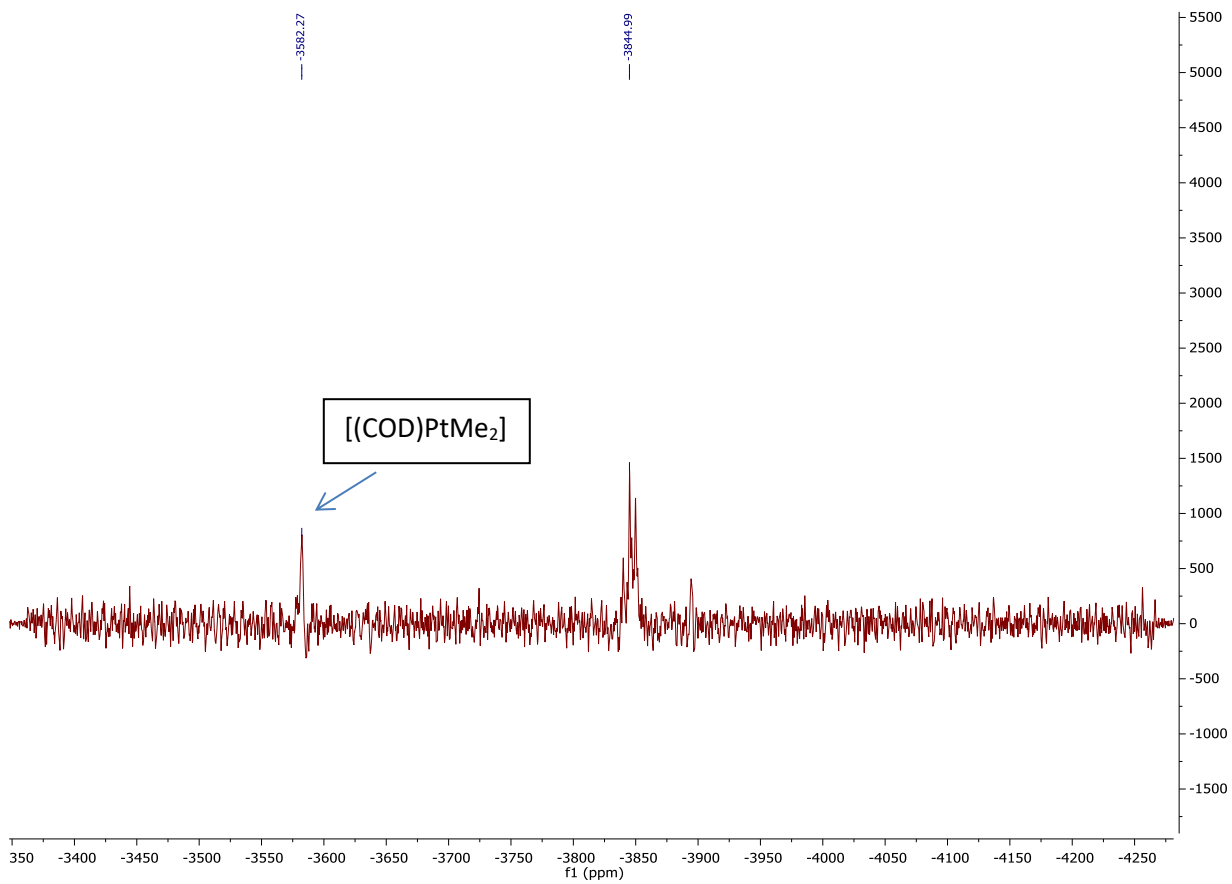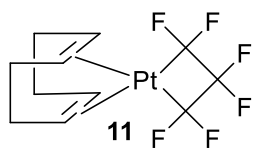
Figure A19: ^{19}F NMR of **12** in CDCl$_3$.
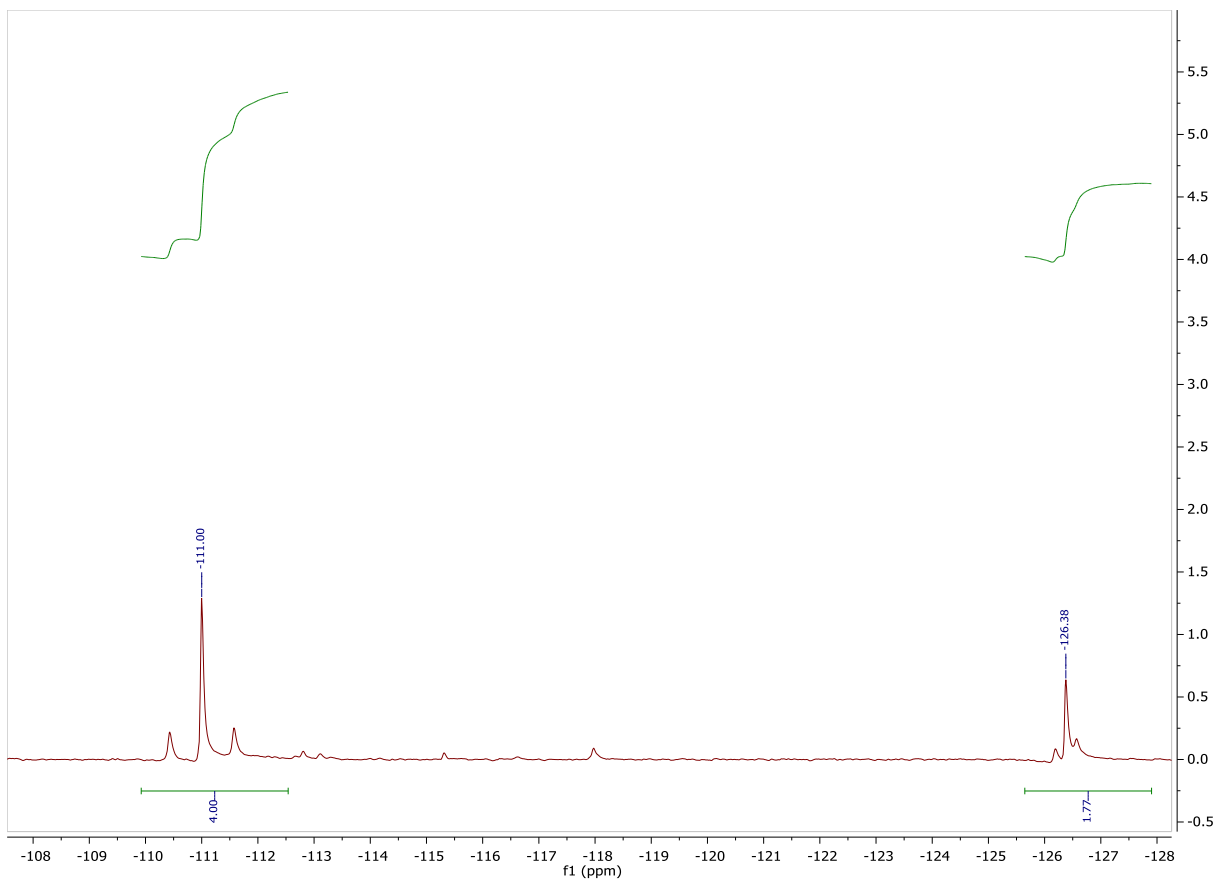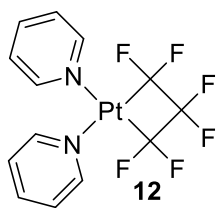
Figure A20: ^{1}H NMR of **12** in CDCl$_3$.
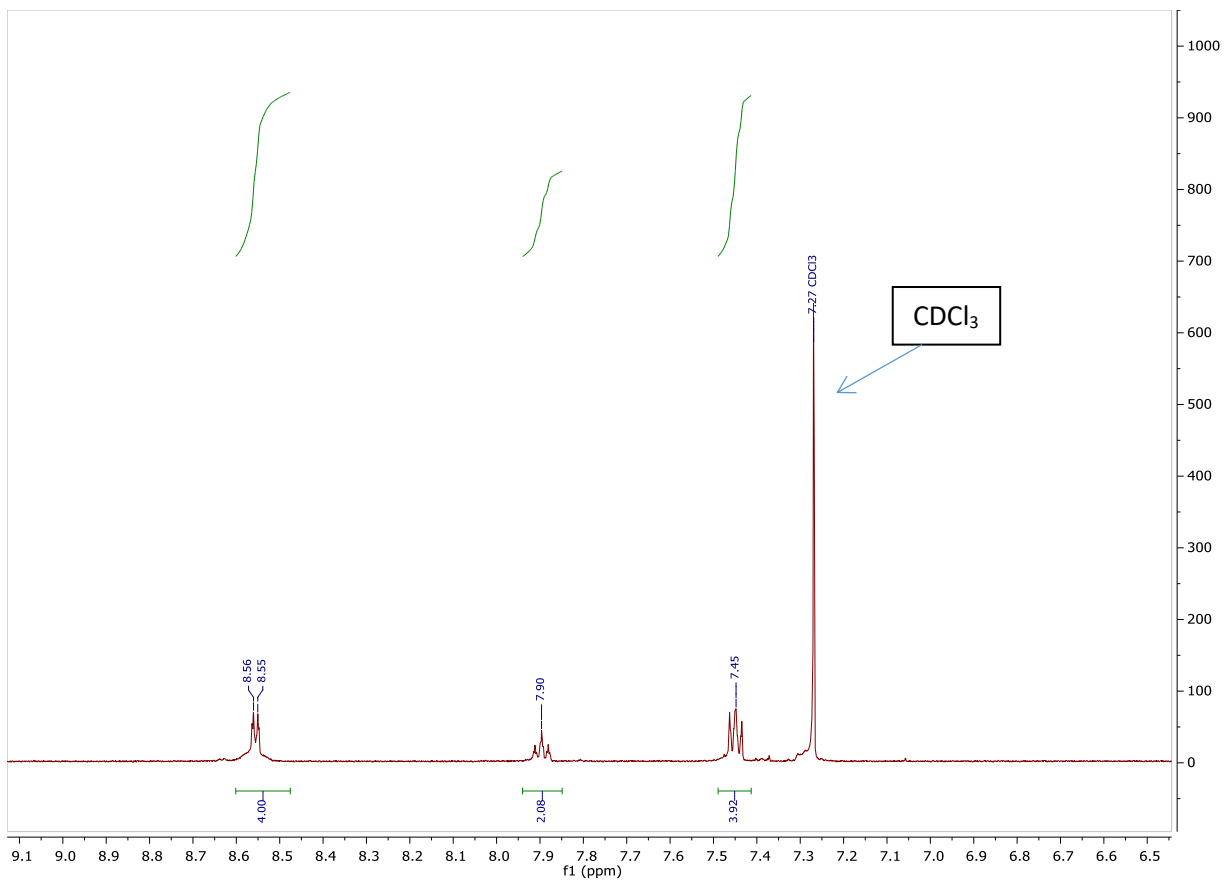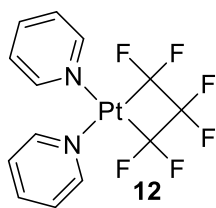
Figure A21: ^{19}F NMR of **13** in CDCl$_3$.
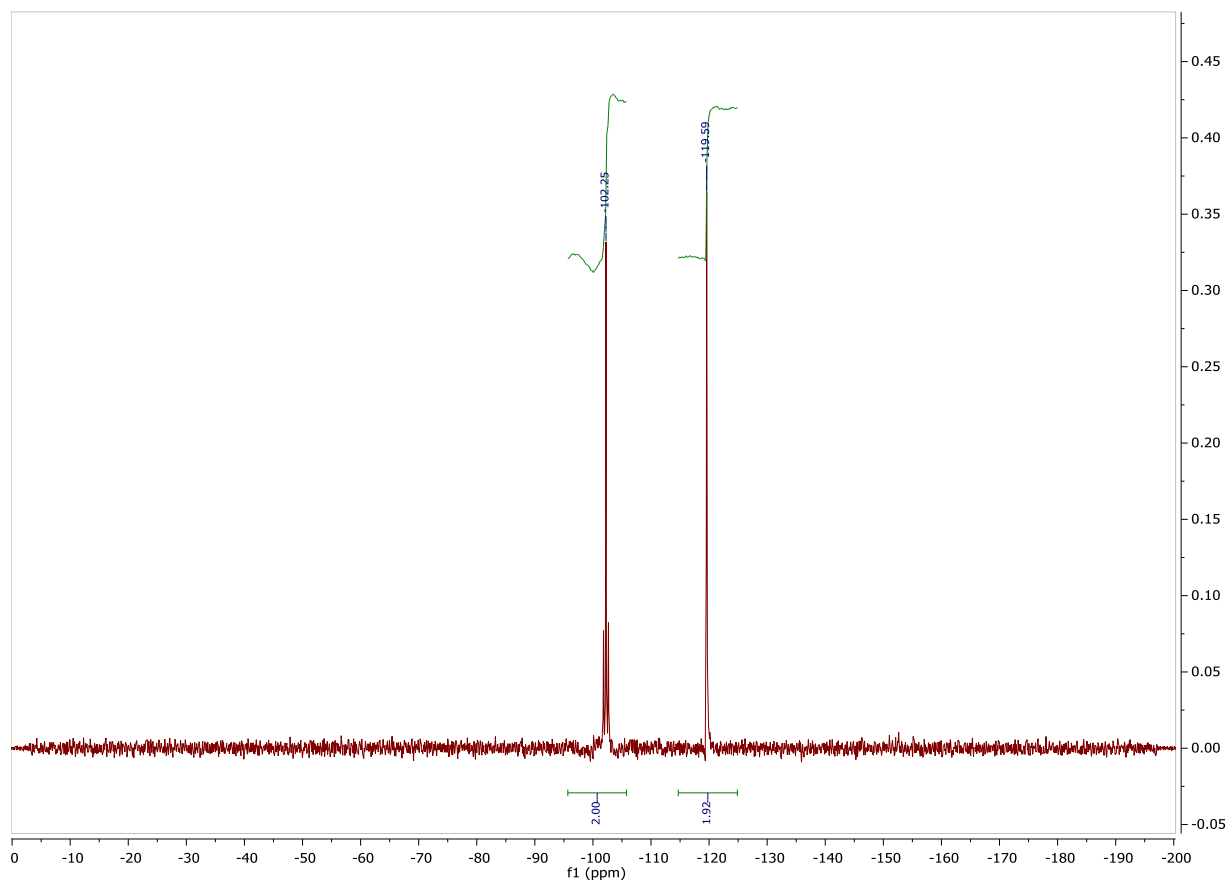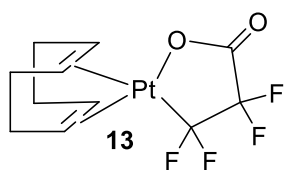
Figure A22: ^{1}H NMR of **13** in CDCl$_3$.
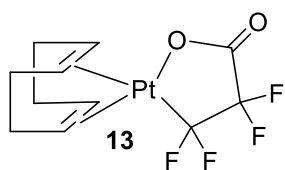
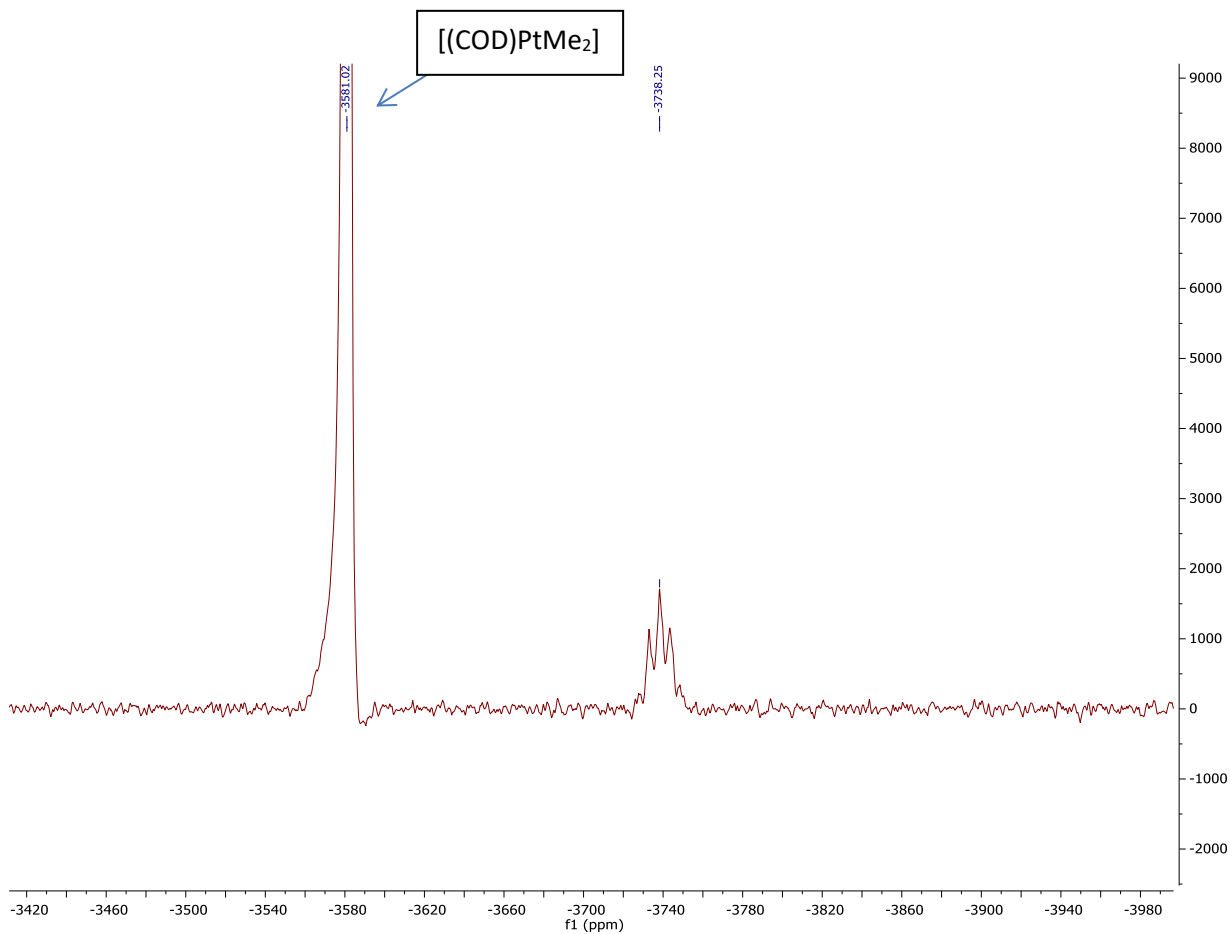**Figure A23:** ^{195}Pt NMR of **14** in CD_2Cl_2 with external [(COD)PtMe$_2$] standard.
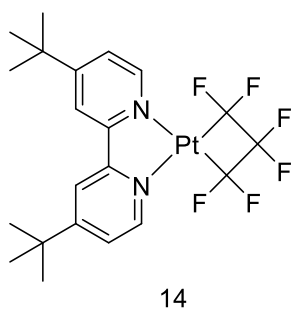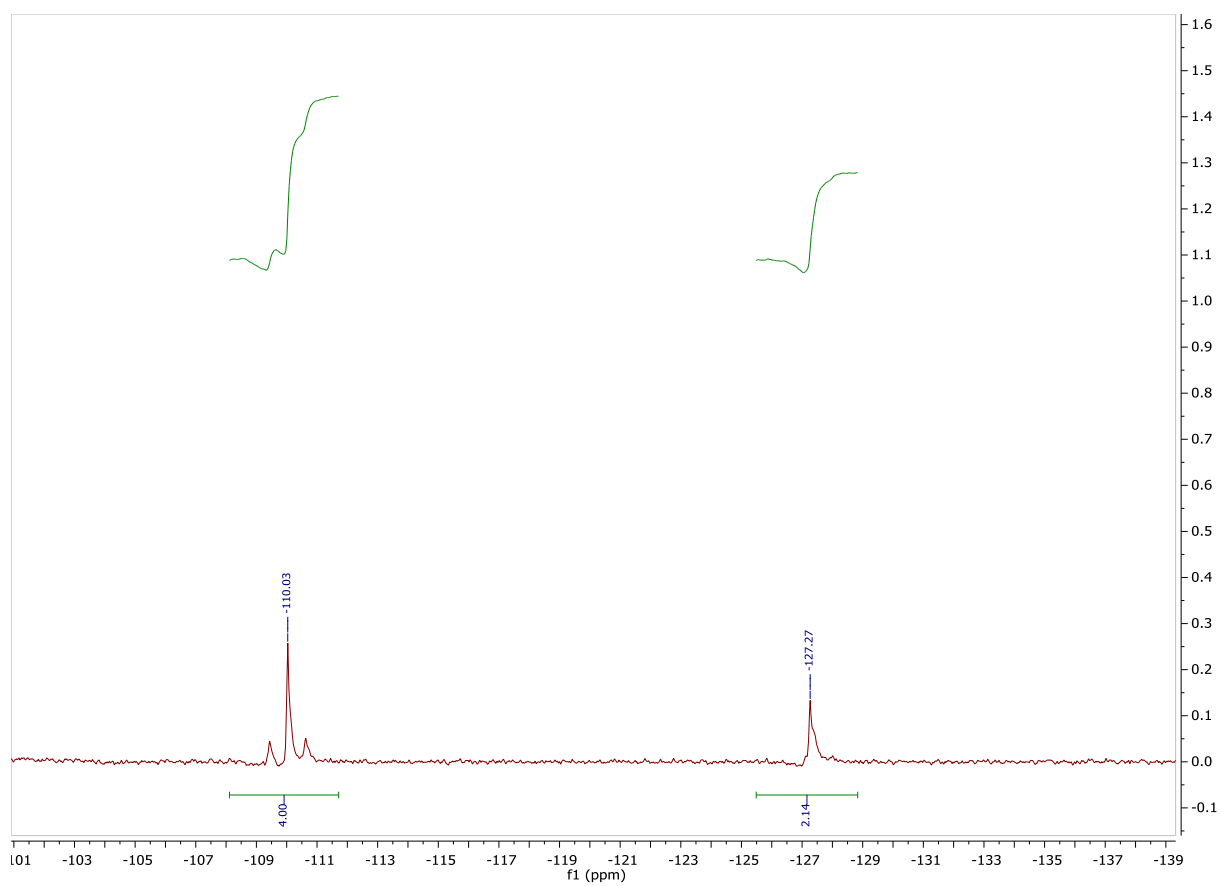
Figure A24: ^{19}F NMR of **14** in CD_2Cl_2.
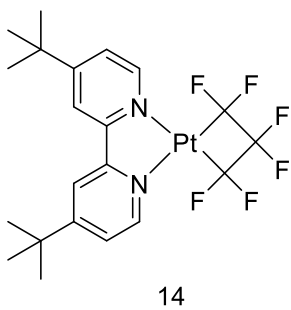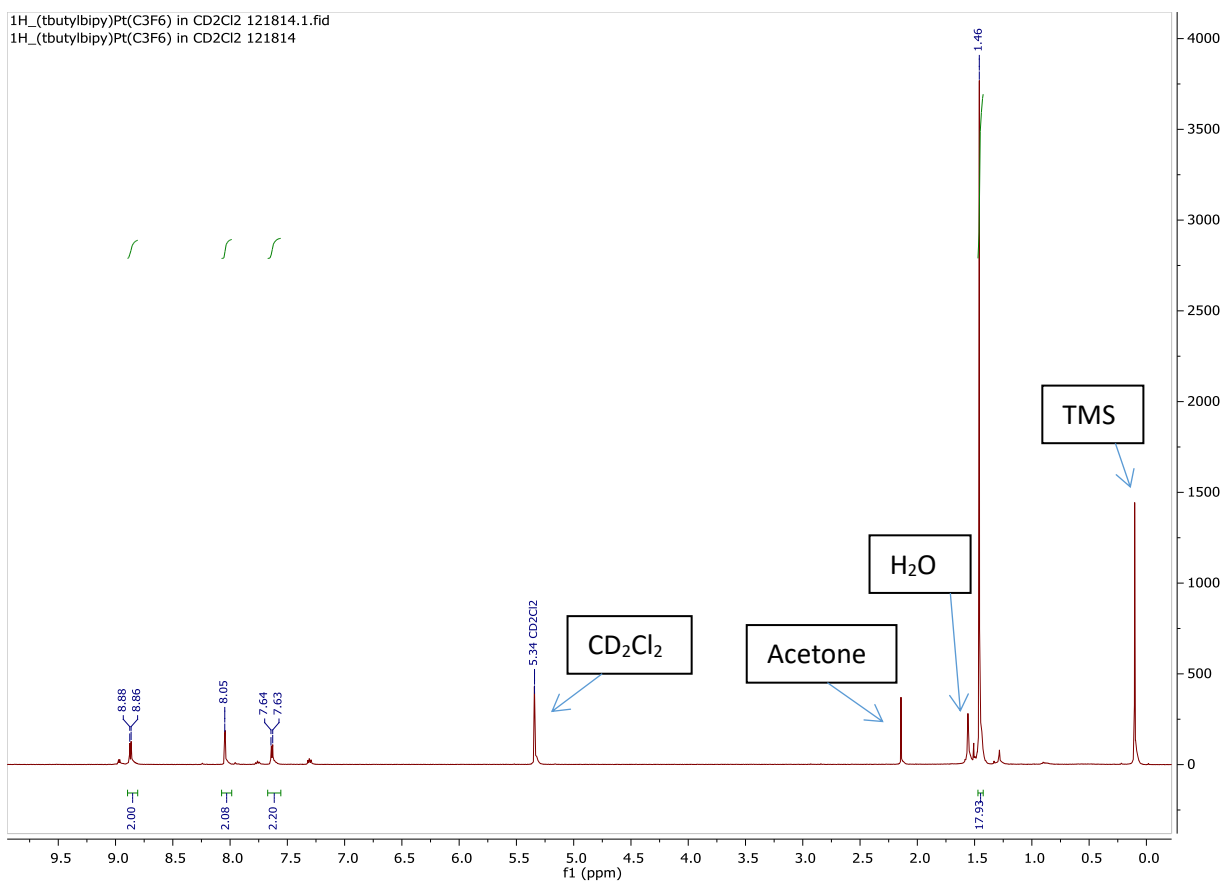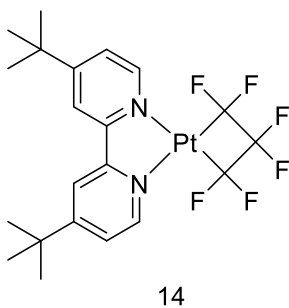

14

Figure A25: ^{1}H NMR of **14** in CD$_2$Cl$_2$.
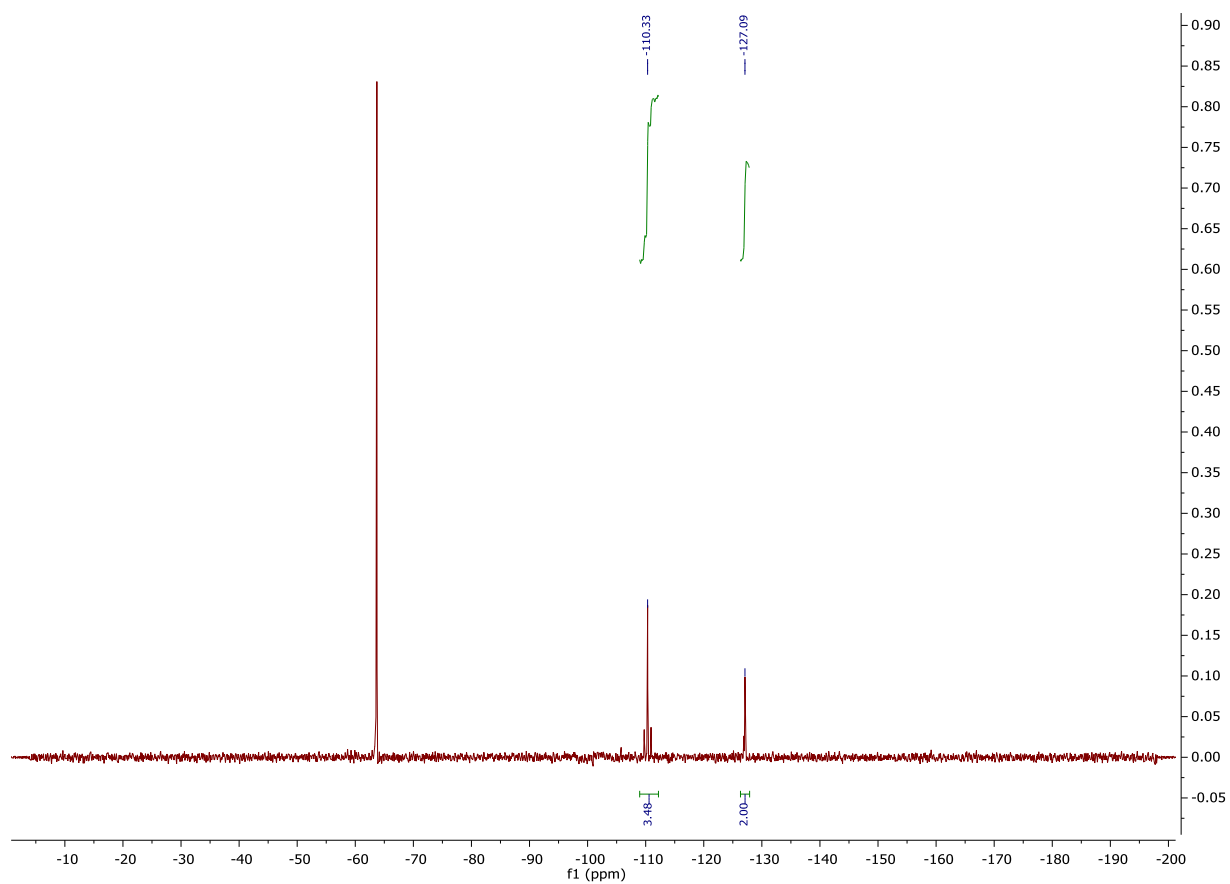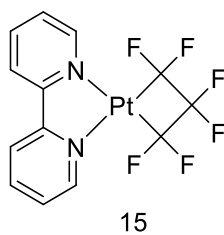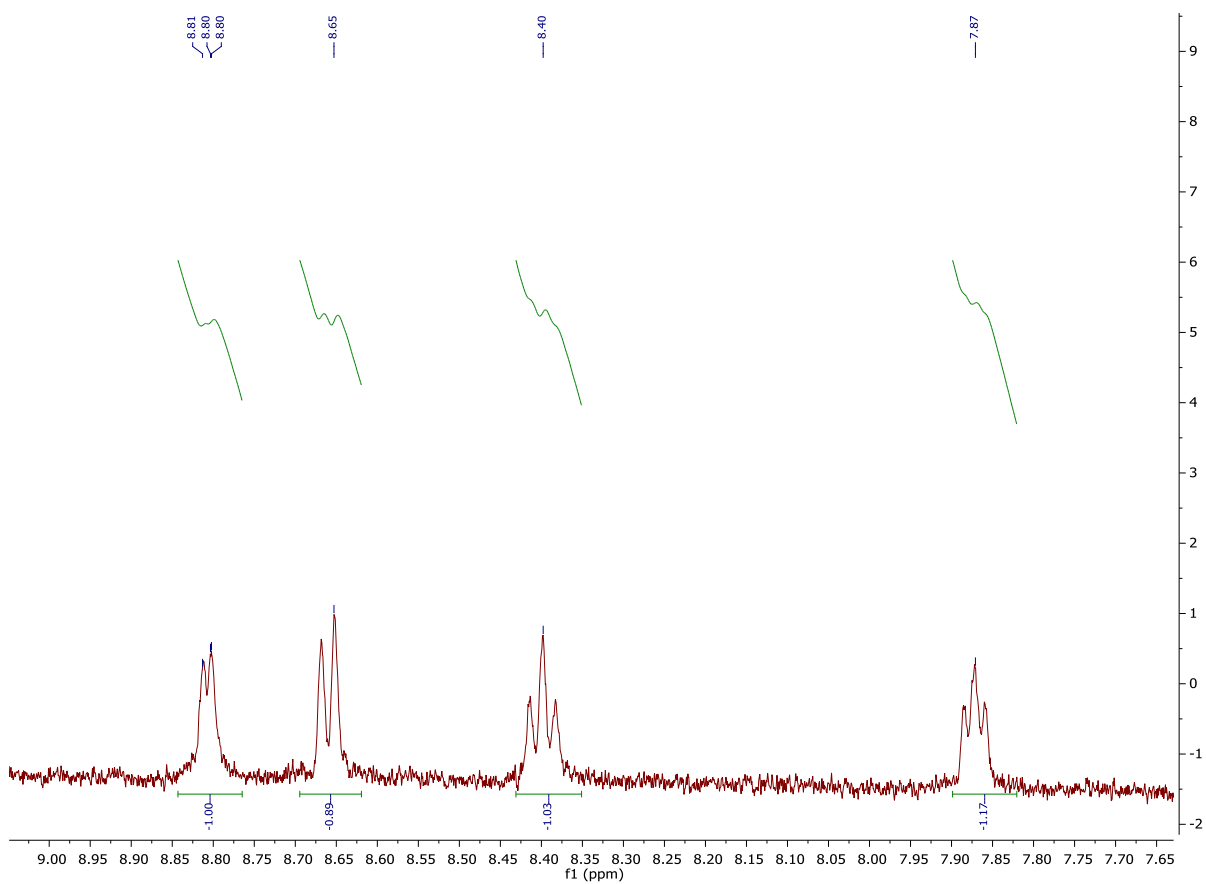
Figure A26: ^{19}F NMR of **15** in DMF-d7.

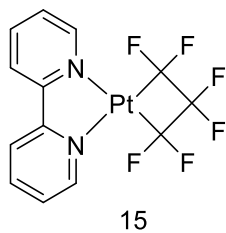**Figure A27:** ^{1}H NMR of **15** in DMSO-d_6.

Long Xu

31 W MORTON ST   CELL: (484) 725-1118
BETHLEHEM, PA 18015   EMAIL: lox212@lehigh.edu

Profile

- Expertise in development and characterization of fluoroalky organometallic compounds.
- 3-year of experience in design and synthesis of novel fluoroalkyl zinc reagents and their applications in coupling reactions.
- Hands-on experiences in various modern spectroscopies techniques (NMR, GC-MS, Single Crystal X-ray Diffraction).
- Skilled in organic synthesis and handling air- and moisture-sensitive materials (glove box, schlenk line, high-vac line).
- English and Chinese Proficiency

Education

- **Ph.D**   Lehigh University, *USA*   Chemistry,   **2012.09-2017.04**

- **B.S.** Dalian University of Technology.*, China*   Chemistry,   **June 2011**

Research Experiences

Project 1: Mild, Safe, and Versatile Zinc Reagents for (CF$_2$)n Transfer 2013-2014
- Synthesized, purified and characterized new dizinc reagents $(MeCN)_2Zn((CF_2)n)_2Zn(MeCN)_2$.
- Transmetalation from Zinc reagents to Nickel(II) center to form a perfluoronickelacycle.
- Coupling reaction using copper chloride as the catalyst to incorporate (CF$_2$)n onto various aryl or heroaryl substrates to prepare novel fluoroorganics containing either perfluoroalkyl
  ring systems or perfluoroalkyl linked arenes.

Project 2: Synthesis of Perfluorometallacyclobutane Derivative 2014-2015
- Synthesis of perfluorometallacyclobutanes via halogen exchange using $C_3F_6I_2$ and $(COD)PtMe_2$.
- Characterization of these new perfluorometallacyclobutanes by $^1H, ^{19}F, ^{195}Pt$ NMR and Single Crystal X-ray Diffraction.
- Unique transformation whereby one $Pt(C_3F_6)$ functionality was converted to $Pt(C_3F_4O_2)$.

Project 3: Direct Difluoromethylation of Aryl Halides via Nickel Catalysis 2015-2016

- Synthesis and characterization of a novel difluoromethyl reagent $(DMPU)_2Zn(CF_2H)_2$.
- Application of this novel zinc reagent in coupling reaction using $(dppf)Ni(COD)$ as catalyst to difluoromethylate aryl iodides, bromides and triflates at room temperature.

Project 4: Reductive coupling of Aryl Halides and HCF_2Cl via Nickel Catalysis 2016-present
- Preliminary mechanistic study of this reductive coupling system
- Stoichiometric reaction between $LNi(Ar)X$ and HCF_2Cl
- Ligand, nickel salt and solvent identification

Publications

9) **Xu, L**.; Vicic, D. A. "Direct Difluoromethylation of Aryl Halides via Base Metal Catalysis at Room Temperature" *J. Am. Chem. Soc*. **2016**, *138*, 2536-2539. This article was highlighted in *SynFacts* **2016**, *12*, 0515.

8) Yang, Y.; **Xu, L**.; Yu, S.; Liu, X.; Zhang, Y.; Vicic, D. A. "Triphenylphosphine-Mediated Deoxygenative Reduction of CF_3SO_2Na and its Application for Trifluoromethylthiolation of Aryl Iodides" *Chem. Eur. J.* **2016**, *22*, 858-863. This article received the frontispiece for the journal.

7) Khrizanforov, M.; Strekalova, S.; Khrizanforova, V.; Grinenko, V.; Kholin, K.; Gryaznova, T.; Sinyashin, O.; **Xu,** L.; Vicic, D. A.; Budnikova, Y. "Iron-Catalyzed Electrochemical C-H Perfluoroalkylation of Arenes" *Dalton Trans*. **2015**, *44*, 19674-19681.

6) **Xu, L**.; Cramer, R. E.; Vicic, D. A. "An Unusual Example of Halogen Bonding to Potassium t-Butoxide" *J. Fluorine Chem*. **2015**, *179*, 53-55.

5) **Xu, L**.; Solowey, D. P.; Vicic, D. A. "Stepwise Conversion of a Platinum Dimethyl Complex to a Perfluorometallacyclobutane Derivative" *Organometallics* **2015**, *34*, 3474-3479. This article made the cover of the journal.

4) Kaplan, P. T.; **Xu. L**.; Chen, B.; McGarry, K. R.; Yu, S.; Wang, H.; Vicic, D. A. "Mild, Safe, and Versatile Reagents for $(CF_2)n$ Transfer and the Construction of Fluoroalkyl-Containing Rings" *Organometallic*s **2013**, *32,* 7552-7558. This article was

highlighted in *C&E News* **2014**, *92*, 28-29.

3) Zhang, C. P.; Wang, H.; Klein, A.; Biewer, C.; Stirnat, K.; Yamaguchi, Y.; **Xu, L**.; Gomez-Benitez, V.; Vicic, D. A. "A Five-Coordinate Nickel(II) Fluoroalkyl Complex as a Precursor to a Spectroscopically Detectable Ni(III) Species"*J. Am. Chem. Soc*. **2013**, *135*, 8141-8144.

2) Li, Z. Y.; Huang, H. Q.; **Xu, L.**; Liu, R. B.; Zhang, J. J.; Liu, S. Q.; Duan, C. Y. "3d–4d–4f Heterotrimetallic 3D Chiral Frameworks Based on Octahedral $\{Ni_6Ag_8S_{12}Cl\}$ or Trigonal Dipyramidal $\{Co_2Ag_3S_6\}$ Clusters: Synthesis, Crystal Structures, and Characterization" *Cryst. Growth Des*. **2013**, *13*, 918-925.

1) Wang, X. Y., **Xu, L.**, Liu, R. B., Liu, S. Q., Yang, W. B. and Zhang, J. J. "Two 2D Metal-organic Networks Based on a Rigid Imidazolate/Sulfonate Functionalized Ligand – Effect of the Coordination Modes of the Ligand on Crystal Structures" *Z. anorg. allg. Chem*., **2012**, *638*, 1006–1011.

Teaching Experiences

- Teaching assistant for Chm 30, Chm 111, Chm 110, Chm 343, Chm 341 in department of chemistry at Lehigh University.

Honors and Awards

- Horner Fellowship at Lehigh University   2016
- Outstanding Graduate of Dalian City (top 2%).   2011
- National Scholarship at Dalian University of Technology (top 2%).   2008